Kairos Power

KP-NRC-1903-001

March 6, 2019

Project No. 99902069

US Nuclear Regulatory Commission
ATTN: Document Control Desk
Washington, DC 20555-0001

Subject: Kairos Power LLC
Topical Report Submittal
Scaling Methodology for the Kairos Power Testing Program

This letter submits the subject topical report which provides the scaling methodology for the Kairos Power Fluoride Salt-Cooled, High Temperature Reactor (KP-FHR) testing program. This topical report is provided for NRC review and approval and is expected to be referenced by future license applicants using the KP-FHR. The scope and schedule for submittal of this report was discussed in a closed meeting with NRC staff January 16, 2019. Kairos Power respectfully requests NRC acceptance review be completed and a review schedule be provided within 60 days of the receipt of this letter. In recognition of an aggressive deployment schedule and substantial pre-application engagement, Kairos Power has established a generic assumption of a 12-month review for topical reports.

Portions of the attached report are considered proprietary, and Kairos Power requests it be withheld from public disclosure in accordance with the provisions of 10 CFR 2.390. Enclosure 1 provides the proprietary version of the report and Enclosure 2 provides the non-proprietary report. An affidavit supporting the withholding request is provided in Enclosure 3.

Additionally, the information indicated as proprietary has also been determined to contain Export Controlled Information. This information must be protected from disclosure pursuant to the requirements of 10 CFR 810.

If you have any questions or need any additional information, please contact Drew Peebles at peebles@kairospower.com or (214) 783-3276, or Darrell Gardner at gardner@kairospower.com or (704) 769-1226.

Sincerely,

Peter Hastings, PE
Vice President, Regulatory Affairs and Quality

707 W Tower Ave
Alameda, CA 94501

Kairos Power LLC
www.kairospower.com

121 W Trade St, Ste 1010
Charlotte, NC 28202

Enclosures:

1) Scaling Methodology for the Kairos Power Testing Program (Proprietary)
2) Scaling Methodology for the Kairos Power Testing Program (Non-Proprietary)
3) Affidavit Supporting Request for Withholding from Public Disclosure (10 CFR 2.390)

xc (w/enclosure):

J. P. Segala, Chief, NRO Advanced Reactor and Policy Branch
S. L. Magruder, Project Manager, NRO Advanced Reactor and Policy Branch

Enclosure 2

Scaling Methodology for the Kairos Power Testing Program (Non-Proprietary)

KP-TR-006-NP

Kairos Power LLC
707 W. Tower Ave
Alameda, CA 94501

Scaling Methodology for the Kairos Power Testing Program

Topical Report

Revision No. 0
Document Date: March 2019

Non-Proprietary

COPYRIGHT NOTICE

Rev	Description of Change	Date
0	Initial Issuance	March 2019

Executive Summary

This topical report summarizes the scaling methodology used by the Kairos Power testing program to design scaled experiments that predict behavior in the prototypical Kairos Power fluoride-salt-cooled, high-temperature reactor (KP-FHR). This methodology will be used to perform scaling analyses as part of the Evaluation Model Development and Assessment Process (EMDAP) described in Regulatory Guide 1.203.

The Hierarchical Two-Tiered Scaling (H2TS) methodology was selected for Kairos Power scaling efforts that will be applied to Integral Effects Tests (IETs) for system level testing, and Separate Effects Tests (SETs) for phenomenon and component level testing. This report details the H2TS methodology, and how it is used by Kairos Power. The scaling methodology is presented for thermal-fluids IETs that will model the KP-FHR primary heat transport system under normal operations and transient conditions. The methodology is also presented for a comprehensive set of SETs for phenomena and component level tests.

This topical report provides a basis for using surrogate fluids for testing that requires the thermal-fluids performance of the KP-FHR primary coolant Flibe ($2LiF:BeF_2$) to be replicated. The high operating temperatures, power requirements, and toxicity hazards of working with Flibe make the use of surrogate fluids beneficial for testing. The use of surrogate fluids enables direct and comprehensive measurements of the phenomena under investigation due to the higher compatibility of available, highly accurate instrumentation (e.g., temperature, flow velocity, pressure) in surrogate fluids vs. prototypical molten salts at high temperatures. Kairos Power intends to use heat transfer oil and water as surrogate fluids for Flibe in some thermal-fluids tests. This report demonstrates that these surrogate fluids provide acceptable substitutes for Flibe for some types of scaled IETs and SETs, and that the important thermal-fluids properties can be properly scaled. This enables Kairos Power to perform scaled experiments with these surrogate fluids before testing with Flibe, enabling the realization of Kairos Power's rapid analysis, prototyping and iterative design cycle while providing high-quality data for safety analysis code validation.

Kairos Power is requesting NRC review and approval to use the scaling methodology with surrogate fluids (heat transfer oil and water) for Flibe as described in this report for testing included in the assessment base of evaluation models supporting KP-FHR safety analysis required by 10 CFR 50.34 (a)(4), 10 CFR 50.34(b)(4), 10 CFR 52.47(a)(4), 10 CFR 52.79(a)(5), 10 CFR 52.137(a)(4), or 10 CFR 52.157(f)(1).

Table of Contents

ABBREVIATIONS

Abbreviation or Acronym	Definition
AOO	Anticipated Operational Occurrence
CFR	Code of Federal Regulations
EMDAP	Evaluation Model Development and Assessment Process
Flibe	$2\text{-}^{7}LiF:BeF_2$
FRC	Fractional Rate of Change
H2TS	Hierarchical Two-Tiered Scaling
IET	Integral Effects Test
IHX	Intermediate Heat Exchanger
KP-FHR	Kairos Power Fluoride-Salt-Cooled, High-Temperature Reactor
LOCA	Loss of Coolant Accident
LWR	Light Water Reactor
MHR	Modular Helium Reactor
MHTGR	Modular High Temperature Gas-Cooled Reactor
Mk1 PB-FHR	Mark 1 Pebble-Bed Fluoride-Salt-Cooled, High-Temperature Reactor
NRC	U.S. Nuclear Regulatory Commission
PHTS	Primary Heat Transport System
PWR	Pressurized Water Reactor
RG	Regulatory Guide
SASM	Severe Accident Scaling Methodology
SET	Separate Effects Test
TRISO	Tristructural Isotropic

1 INTRODUCTION

Kairos Power LLC (Kairos Power) is pursuing the design, licensing, and deployment of a Fluoride-Salt-Cooled, High-Temperature Reactor (KP-FHR). To enable these objectives, a scaling methodology is needed to properly scale tests in support of developing an adequate evaluation model. This process is in line with the Evaluation Model Development and Assessment Process (EMDAP) detailed in Regulatory Guide (RG) 1.203. Scaling analyses are an integral part of the EMDAP and used to scale non-prototypical tests that are performed to develop an assessment base for the evaluation model. This report has been prepared to document the methodology for development of scaling analyses to be used for testing that supports the assessment base of the KP-FHR evaluation model. The scaling methodology detailed in this report is applicable to the types of tests described in Section 1.3 of this report. This report also documents the acceptable use of surrogate fluids in scaled tests.

Kairos Power is requesting U.S. Nuclear Regulatory Commission (NRC) review and approval to use the scaling methodology along with the use of heat transfer oil (e.g., DOWTHERM™ A, Therminol® VP-1 or XCELTHERM® MK1, all commercial names for a eutectic mixture of two organic compounds, biphenyl ($C_{12}H_{10}$) and diphenyl oxide ($C_{12}H_{10}O$), referred to as 'heat transfer oil' in the rest of this report) and water as surrogate fluids for $2\text{-}^{7}LiF:BeF_2$ (Flibe) as described in this report for testing included in the assessment base of evaluation models supporting KP-FHR safety analysis required by 10 CFR 50.34 (a)(4), 10 CFR 50.34(b)(4), 10 CFR 52.47(a)(4), 10 CFR 52.79(a)(5), 10 CFR 52.137(a)(4), or 10 CFR 52.157(f)(1).

1.1 DESIGN FEATURES

1.1.1 Design Background

To facilitate NRC review of this topical report, key design features are described in Section 1.1.2, which are considered inherent to the KP-FHR technology. These features are not expected to change during the design development by Kairos Power and provide the basis to support the safety review of the scaling methodology provided in this report. Should fundamental changes occur regarding these key design features or revised regulations be promulgated, such changes would be reconciled and addressed in future license application submittals.

The KP-FHR is a U.S. developed Generation IV advanced reactor technology. In the last decade, U.S. national laboratories and universities have developed pre-conceptual FHR designs with different fuel geometries, core configurations, heat transport system configurations, power cycles, and power levels. More recently, the University of California at Berkeley developed the Mark 1 pebble-bed FHR (Mk1 PB-FHR), incorporating lessons learned from the previous decade of FHR pre-conceptual designs (Reference 1). Kairos Power has built on the foundation laid by U.S. Department of Energy sponsored university Integrated Research Projects to develop the KP-FHR.

Although not intended to support the findings necessary to approve this topical report, additional design and testing concept information is provided in the "Design Overview of the Kairos Power Fluoride Salt Cooled, High Temperature Reactor (KP-FHR)" Technical Report (Reference 2) and the "Testing and Development Program Overview for the Kairos Power Fluoride Salt Cooled, High Temperature Reactor" Technical Report (Reference 3).

1.1.2 Key Design Features of the KP-FHR

The KP-FHR is a high-temperature reactor with molten fluoride salt coolant operating at near-atmospheric pressure. The fuel in the KP-FHR is based on the tristructural isotropic (TRISO) high-temperature carbonaceous-matrix coated particle fuel developed for high-temperature gas-cooled reactors, in a pebble fuel element. Coatings on the particle fuel provide retention of fission products. The reactor coolant is a chemically stable molten fluoride salt mixture, $2\text{-}^{7}LiF:BeF_2$ (Flibe with [[ ]]), which also provides retention of fission products that escape from fuel defects. A primary coolant loop circulates the reactor coolant using pumps and transfers the heat to an intermediate coolant loop via a heat exchanger. The pumped flow intermediate coolant loop utilizes a nitrate salt, compatible with reactor coolant, and transfers heat from the reactor coolant to the power conversion system through a steam generator. The design includes two decay heat removal systems. A normal decay heat removal system is used following normal shutdowns and anticipated operational occurrences (AOOs). The design also includes a separate passive decay heat removal system, which along with natural circulation in the reactor vessel, is used to remove decay heat in response to a design basis accident and does not rely on electrical power.

The KP-FHR design relies on a functional containment approach similar to the Modular High Temperature Gas-Cooled Reactor (MHTGR) instead of the typical light water reactor (LWR) low-leakage, pressure retaining containment structure. The KP-FHR functional containment safety design objective is to meet 10 CFR 50.34 (10 CFR 52.79) offsite dose requirements at the plant's exclusion area boundary with margin. A functional containment is defined in RG 1.232 as a "barrier, or set of barriers taken together, that effectively limit the physical transport and release of radionuclides to the environment across a full range of normal operating conditions, AOOs, and accident conditions." RG 1.232 includes an example design criterion for the functional containment (MHTGR Criterion 16). As also stated in RG 1.232, the NRC has reviewed the functional containment concept and found it “generally acceptable,” provided that “appropriate performance requirements and criteria” are developed. The NRC staff has developed a proposed methodology for establishing functional containment performance criteria for non-LWRs, which is presented in SECY-18-0096. This SECY document has been approved by the Commission.

The functional containment approach for the KP-FHR is to control radionuclides primarily at their source within the coated fuel particle under normal operations and accident conditions without requiring active design features or operator actions. The KP-FHR design relies primarily on the multiple barriers within the TRISO fuel particles and fuel pebbles to ensure that the dose at the site boundary as a consequence of postulated accidents meets regulatory limits. However, in the KP-FHR as opposed to the MHTGR, the molten salt coolant serves as a distinct barrier providing retention of fission products that escape the fuel particle and fuel pebble barriers. This additional retention is a key feature of the enhanced safety and reduced source term in the KP-FHR.

1.2 REGULATORY BACKGROUND

Kairos Power intends to license the KP-FHR under Title 10 of the Code of Federal Regulations (10 CFR) using a licensing pathway provided in Part 50 or Part 52. Regardless of the licensing path, there is an associated requirement to provide a safety analysis of the design. 10 CFR 50.34(a)(4) provides the requirement for an applicant submitting a preliminary safety analysis report:

> *A preliminary analysis and evaluation of the design and performance of structures, systems, and components of the facility with the objective of assessing the risk to public health and safety resulting from operation of the facility and including determination of the margins of safety during normal operations and transient conditions anticipated during the life of the facility, and the adequacy of structures, systems, and components provided for the prevention of accidents and the mitigation of the consequences of accidents. Analysis and evaluation of ECCS cooling performance and the need for high point vents following postulated loss-of-coolant accidents must be performed in accordance with the requirements of § 50.46 and § 50.46a of this part for facilities for which construction permits may be issued after December 28, 1974.*

This requirement is echoed for the final safety analysis report in 10 CFR 50.34(b)(4) and for Part 52 licensing paths in 10 CFR 52.47(a)(4), 10 CFR 52.79(a)(5), 10 CFR 52.137(a)(4), and 10 CFR 52.157(f)(1). The first sentence of the requirement (requiring a safety analysis of the design) applies to the KP-FHR. Kairos Power will [[

]]

To perform a safety analysis, an evaluation model must be developed to analyze transient and accident behavior. The concept of an evaluation model is presented in 10 CFR 50.46 for evaluating emergency core cooling systems for light-water nuclear power reactors. Although 10 CFR 50.46 does not apply to the KP-FHR (Reference 4), the need for an acceptable evaluation model is relevant. The NRC produced RG 1.203, "Transient and Accident Analysis Methods" to describe a process that the staff considers acceptable for use in developing and assessing evaluation models that may be used to analyze transient and accident behavior within the design basis of a nuclear power plant. In RG 1.203, the NRC endorses the EMDAP, demonstrated in Figure 1. The scaling methodology detailed in this report will be used to perform the scaling analyses shown in Element 2 of the EMDAP shown in Figure 1.

Kairos Power intends to use the Hierarchical Two-Tiered Scaling (H2TS) methodology developed by the NRC-initiated Severe Accident Scaling Methodology (SASM) program. The NRC Severe Accident Research Program identified the need for a scaling methodology to guide the formation of experimental programs and analytical methods (Reference 5), and initiated the SASM program (Reference 6). Kairos Power is requesting NRC review and approval of the documented methodology for this purpose as well as the use of surrogate fluids in some of these tests.

1.3 SCOPE

This report documents the scaling methodology that will be used to scale thermal-fluids tests that support the licensing basis for the KP-FHR. Kairos Power is requesting NRC review and approval of this methodology to be applied to the scaling of thermal-fluids integral effects tests (IETs) and separate effects tests (SETs). Kairos Power is also asking for NRC concurrence on the acceptable use of heat transfer oil and water as acceptable surrogate fluids for Flibe in IETs and SETs.

Kairos Power has adopted the H2TS methodology, developed by the NRC, to scale thermal-fluids tests. A general overview of H2TS methodology, including the scaling methods as well as the method used to quantify distortions, is provided in Section 2.

This methodology is applicable to the scaling of thermal-fluids IETs using heat transfer oil for the KP-FHR Primary Heat Transport System (PHTS). Section 3 documents the similarity criteria for an IET of the PHTS using top-down and bottom-up scaling methods. Section 3 presents the IET scaling for the PHTS at

normal operation conditions (forced flow) and transients involving natural circulation. The use of heat transfer oil is demonstrated as a scalable surrogate fluid that would be acceptable to use in an IET. The use of this methodology to scale IETs outside of these applications would be reconciled and addressed in future license application submittals.

The scaling methodology for SETs documented in Section 4 is applicable to the scaling of specific phenomena and component level tests. If the phenomena and process identification step of the EMDAP (see Figure 1) reveals a phenomenon that requires testing, and that test is not captured by the types of SETs covered in this report, the methodology used to scale that SET would be reconciled and addressed in future license application submittals.

2 HIERARCHICAL TWO-TIERED SCALING (H2TS) METHODOLOGY

The H2TS methodology was proposed by Zuber and colleagues to provide a clear yet simple scaling methodology for complex systems such as nuclear reactors (Reference 7). Its original development was motivated by the NRC SASM program to resolve validation issues for modeling and simulation of severe accidents in LWRs. The basis of H2TS is that the methodology and information have to be practical, traceable, and comprehensive in the approach to provide a technically justified basis for resolving issues in a cost-effective manner (Reference 7). The methodology has been used for the development of previous and current experimental programs of Westinghouse Electric Company's Advanced Passive Pressurized Water Reactor (AP600 and AP1000) (Reference 8), (Reference 9), General Atomics' Energy Multiplier Module and Modular Helium Reactor (MHR) (Reference 10), (Reference 11), and TerraPower's Traveling Wave Reactor (TWR) (Reference 12). Some specific examples include analysis of passive containment for advanced LWRs (Reference 13), analysis of the depressurization loss of forced convective events in an EM2, and transient/steady-state operations in the TWR. Due to the pedigree, applicability, and flexibility of H2TS, Kairos Power has adopted the methodology as the basis of its experimental program.

The H2TS methodology (Figure 2) is used to scale experimental efforts using both system (top-down) and process (bottom-up) approaches while retaining information in a way that is technically justifiable. The use of both approaches ensures that characteristic behavior occurring within the system is not missed in the scaling activity and that distortions are properly accounted for. The H2TS methodology consists of system decomposition into a hierarchical structure with a physically meaningful basis, identifying the characteristic scales at each level of the hierarchy, conducting the top-down scaling analysis, and conducting the bottom-up scaling analysis.

2.1 HIERARCHY AND IDENTIFICATION OF CHARACTERISTIC MASS/VOLUME, TEMPORAL AND SPATIAL SCALES

The establishment of the hierarchy of a complex system is undertaken using a physically meaningful decomposition as seen in Figure 3. The complex system is decomposed fully from the highest level of the entire system down to individual transfer processes. The transfer processes are processes, such as thermal energy transfer in a pipe, that occur across a transfer area at a given rate, and whose importance may be determined by the magnitude of the rate and transfer area.

The system hierarchy may be decomposed in the following order (Reference 7):

1. The system (e.g., KP-FHR plant) is split into subsystems that interact with each other.
2. Each subsystem (e.g., PHTS) is split into modules that interact with each other. Because modules are commonly also components, this report uses the term module/component.
3. Each module/component (e.g., reactor vessel, core) is split into constituents.
4. Each constituent (e.g., working fluids, solid structures) is split into phases that interact with each other.
5. Each phase (e.g., liquid, solid, gas) is characterized using one or more geometric features.
6. Each geometric feature (e.g., solid heat conducting structure, liquid-filled volume, frozen zones, boundary layers, jets, films, droplets) is characterized by different fields.

7. Each field (e.g., mass (M), momentum (MM), energy (E)) involves potentially several transfer processes.

By defining a transfer process, transfer area, and a rate at which the transfer process occurs, the entire complex system may be described by characteristic spatial, temporal, and concentration (volumetric or mass) scales of varying magnitudes, depending on the level in the hierarchy, as seen in Figure 4. The characteristic scales are then utilized for determining scaling from the prototype down to the model experiment or simulation. Normally for IETs, scaling similitude is sought at the subsystem and module/component levels so that system transient response can be reproduced, and distortions are accepted and managed at lower levels.

At the process level, only spatial and temporal characteristic scales may be used. When progressing upwards in the hierarchy, the characteristic scale of concentration (e.g., ratio of cover gas volume to volume of a molten salt pool in the reactor vessel, ratio of solid structure volume to molten salt volume, etc.) may be used. The characteristic scales also lose information or are averaged when progressing from a lower level to a higher level of the hierarchy. For example, the temperature distribution of a fluid in a pipe is known at a low level in the hierarchy, while at a higher level, only the average or bulk temperature is known. The spatial, temporal, and concentration scales that define a transfer process may be combined to include a characteristic time or frequency that characterizes the process in its entirety.

2.1.1 Characteristic Time Ratios

To identify and assess the importance of the different phenomena occurring in a system, the temporal scale for each applicable hierarchical level must be characterized and compared. The two classes of characteristic time scales involve either the system response or transfer processes (several of which may exist for a given system). For system response characteristic time scale, the temporal scale is defined using a control volume viewpoint. A system with a nominal control volume has a volumetric rate of a process occurring within it, and the nominal amount of time needed for the process to change in the entire volume is the residence time for the specific process. The reciprocal of the residence time is the frequency, which may be viewed as the number of times the control volume changes per unit time.

$$\tau_{system} = \frac{V_{system}}{\dot{V}_{system}} = \frac{1}{\omega_{system}} \tag{1}$$

where τ_{system} is the system's characteristic time scale, V_{system} the control volume for the system, $\dot{V}_{system}$ the volumetric rate of the process occurring in the system, and ω_{system} the characteristic frequency associated with the system and process.

An example for the characteristic time scale of a system would be the residence time of the reactor coolant in the PHTS of a KP-FHR. The coolant volumetric flow rate, Q_{system}, and the coolant volume, V_{system}, would yield a $\tau_{system} = \frac{V_{system}}{Q_{system}}$. This is the average residence time of the reactor coolant to circulate around the PHTS once.

For an individual transfer process, the temporal scale of a transfer process may be defined as:

$$\tau_j = \frac{\varphi V}{j_j A_T} = \frac{1}{\omega_j} \tag{2}$$

where τ_j is the characteristic time scale of the transfer process, φ a quantity per unit volume within a volume, V that volume, j_j the flux associated with the transfer process, A_T the transfer area associated with the transfer process, and ω_j the characteristic frequency of the transfer process in volume V, or the fractional rate of change (FRC) as defined in Reference 14.

An example for a transfer process' temporal scale is heat transfer to or from a solid sphere of diameter D, with a heat flux q''. The temporal scale associated with the heat transfer process, τ_{HT}, is defined as:

$$\tau_{HT} = \frac{(\rho \Delta e)\left(\frac{1}{6}\pi D^3\right)}{(q'')(\pi D^2)} = \frac{\rho \Delta e D}{6q''} = \frac{1}{\omega_{HT}} \tag{3}$$

where ρ is the density of the sphere, Δe the characteristic change in the average internal energy of the sphere, and ω_{HT} the specific frequency (or FRC) of the heat transfer process. Note that the internal energy is an absolute quantity, based upon some reference condition where the energy is defined to be zero. An appropriately scaled change in internal energy Δe would be the product of specific heat multiplied by a characteristic temperature difference scale for the system (e.g., $T_H - T_C$ where T_H is the hot temperature of the system of interest and T_C the cold temperature).

Characteristic temporal scales and associated frequencies may be used to determine the impact or importance of the transfer processes throughout the hierarchical system. This is done by comparing each transfer process' characteristic time scale or specific frequency to the system's characteristic time scale to form a characteristic time ratio Π_j:

$$\Pi_j = \frac{\tau_{system}}{\tau_j} = \omega_j \tau_{system} \tag{4}$$

Continuing from the previous example, the characteristic time ratio between the heat transfer from a spherical pebble in the KP-FHR reactor core and the overall residence time of the reactor coolant in the PHTS would then be:

$$\Pi_{HT} = \omega_{HT} \tau_{system} = \frac{V_{system}}{Q_{system}} \frac{6q''}{\rho \Delta e D} \tag{5}$$

Qualitatively, when the characteristic time ratio is very large or very small, the slow process experiences the integrated effect of the fast process and the slow process is not sensitive to the details of the fast process. Conversely, when the characteristic time ratio is of order unity, the processes are tightly coupled. Two important conclusions may be drawn from this:

1. The characteristic time ratio may be used to determine the importance and resulting priority of phenomena to be characterized and quantified as a result of a scaling exercise.
2. To preserve the impact or effect of a transfer process in a scaled experiment, when the associated characteristic time ratio is close to unity, the process must be matched carefully between the prototype and scaled experiment.

In a practical system, some characteristic time ratios or scaling parameters may not be matched without distortions depending on the situation. Characteristic time ratios may be used to evaluate the

magnitude of distortions in a scaled experiment, as discussed in Sections 2.3 and 2.4, and to select scaling parameters and approaches that minimize distortions of dominant phenomena.

2.1.2 Power to Volume Scaling Example

The power to volume scaling criterion is an example of how characteristic time ratios may be used to ensure that system dynamic response behaviors are properly captured between two different facilities (prototype and model), potentially using different fluids and dimensions. This method has been used in the past for pressurized water reactor (PWR) loss of coolant accident (LOCA) IETs (Reference 7). For prototypical and scaled experimental facility representing the PHTS in a KP-FHR, the characteristic heat transfer time ratios for modules/components are set equal to each the model m and in the prototype p:

$$\left[\frac{q'' A_T}{\rho_f c_{pf}(T_{H0} - T_{C0}) V_{CV}} \tau_{CV}\right]_{j,fm} = \left[\frac{q'' A_T}{\rho_f c_{pf}(T_{H0} - T_{C0}) V_{CV}} \tau_{CV}\right]_{j,fp} \quad (6)$$

where j is the specific module/component, q'' the heat flux, A_T the heat transfer area of module/component j, V_{CV} the fluid control volume of module/component j, c_{pf} the specific heat of the fluid, T_{C0} and T_{H0} the characteristic cold and hot temperatures in the system (generally the normal core inlet and core bulk outlet temperatures, respectively), τ_{CV} the fluid residence time in the control volume of module/component j, and the subscripts m and p are used for the model and prototype, respectively.

The KP-FHR has a large thermal inertia, with the heat capacity of solid structures (fuel, reflector, coolant boundary) having similar magnitude to the coolant heat capacity (Reference 15). Therefore, in KP-FHRs, scaling to match the heat capacity of solid structures at the module/component level j is also important to properly capture transient response.

$$\left[\frac{q'' A_T}{m_s c_{ps}(T_{H0} - T_{C0})} \tau_{CV}\right]_{j,sm} = \left[\frac{q'' A_T}{m_s c_{ps}(T_{H0} - T_{C0})} \tau_{CV}\right]_{j,sp} \quad (7)$$

where m_s is the mass and c_{ps} the specific heat of the solid heat structures in module/component j. Matching the relative thermal capacity of fluid and solid structures at the module/component level is achieved by matching the ratios:

$$\left[\frac{m_s c_{ps}}{\rho_f c_{pf} V_{CV}}\right]_{j,m} = \left[\frac{m_s c_{ps}}{\rho_f c_{pf} V_{CV}}\right]_{j,p} \quad (8)$$

Matching the characteristic time ratios and the relative thermal capacity of fluid and solid structures between the model and prototype for each module/component allows for a reduced scale experimental facility with lower power and volume requirements while matching the prototypical steady state and transient behavior of the heat transfer processes associated with the system.

2.2 DIMENSIONLESS SCALING GROUPS

Dimensionless scaling groups are used to express similitude between different systems described by the same set of equations. A simple example is the turbulent behavior of single-phase molten salt in a cylindrical pipe having the same scaled behavior as the turbulent behavior of a different single-phase fluid

such as water or heat transfer oil. In this example, the dimensionless scaling group of interest is the Reynolds number,

$$\Pi_{Re} = \frac{\rho u d}{\mu} \tag{9}$$

where the ratio of inertial $(\rho u d)$ to viscous forces (μ) is desired to be maintained in order reproduce the turbulent characteristics of the fluid flow. In order for the Reynolds number to be conserved, the pipe must be of a different diameter (d) and/or the fluid must have a different velocity (u) if the associated dimensionless scaling group (Reynolds number) is to be the same in each respective fluid. Dimensionless groups may be derived through the non-dimensionalization of conservation equations or identified through characteristic time ratios. The additional physics of the studied behavior will increase the number of dimensionless groups, which may make matching each group between a prototype and scaled experiment more complex and introduce scaling distortions. This is evident when attempting to match the dimensionless groups between the modules/components of a prototypical reactor having several interacting and competing phenomena to a scaled experiment replicating the same phenomena.

2.3 SCALING DISTORTIONS

For IETs, scaled experimental efforts may result in distortions of phenomena between the modules/components of the prototype and the scaled experiment. Conversely, for SETs the scaling may result in distortions at the field, geometric configuration, phase, and constituent levels of the prototype and the scaled experiment.

For both IETs and SETs, an optimization exercise is required to minimize distortions of important phenomena, while less important phenomena may have more significant distortions. The importance of the phenomena to be replicated in a scaled experiment is determined qualitatively through a Phenomena Identification and Ranking Table (PIRT) process, or quantitatively using characteristic time ratios compared to the global time scale in the system for IETs, and for the module/component for SETs.

For system-scale IETs, the PIRT process involves listing key phenomena for each module/component and ranking them both in terms of importance and knowledge level. By identifying knowledge gaps for key phenomena, the process enables prioritization of experimental activities to close these gaps. It is important to note that PIRTs can also be developed at the module/component scale.

Significant distortions of less important phenomena need to be evaluated to determine the impact on the investigated complex behavior in a scaled experiment. This includes the impact on the evolution of a transient if time-dependent behavior is considered. Distortions may be characterized using characteristic time ratios (Section 2.1.1), comparing dimensionless numbers or scaling parameters between the prototype and model. The distortion factor $DF_{j,k}$, which characterizes the distortion for each module/component j, for each phenomenon of interest k, may be evaluated between prototype and model characteristic time ratios, dimensionless numbers or scaling parameters:

$$DF_{j,k} = \frac{\left[\Pi_{j,k}\right]_p - \left[\Pi_{j,k}\right]_m}{\left[\Pi_{j,k}\right]_p} \tag{10}$$

$DF_{j,k}$ physically represents the fractional difference in the amount of conserved property transferred through the evolution of a specific process in each module/component j of the prototype to the amount of conserved property transferred through the same process in the corresponding module/component of the model during their respective residence times. The significance of scaling distortions is determined by the analyst or test engineer and the importance of the behavior.

2.4 AS-BUILT DISTORTIONS

In addition to scaling distortions for specific phenomena in an 'ideal' scaled experiment, there exist additional distortions which result from the as-built scaled experiment. As-built distortions may result from the following factors:

- Physical constraints in terms of total size of the scaled experiment because of available space at location where experiment is set up (e.g., scaled experiment should be 16 ft tall to avoid too large distortions from reduced length, but only 15 ft are available at experimental facility);
- Budgetary constraints that limit the use of specific materials or complex geometries [[

]]
- Mismatch between ideal materials and sizes of components and commercially available components (e.g., piping inner diameter in scaled experiment should be 6.00 in, but the closest commercially available pipe size is 6 in Schedule 40, which has an inner diameter of 6.07 in);
- Mismatch between ideal thermophysical properties of working fluid and solid structures over parameter range of interest and properties of commercially available fluids and solid materials (e.g., Prandtl number for surrogate heat transfer oil matches that of Flibe salt at average KP-FHR operating temperature, but distortion is close to 3% at the lower end of the operating temperature range, as detailed in Section 5; likewise, the scaled thermal conductivity and heat capacity of solid heat structures may have significant mismatch).

2.5 TOP-DOWN SCALING ANALYSIS

Top-down scaling is an inductive process that considers the whole system. Top-down scaling is commonly conducted as a control volume analysis, using conservation equations. A key question in scaling involves the selection of the control volume size at which similitude is evaluated. Generally, similitude must be established at the subsystem scale (see Figure 3)and often similitude is also sought at the module/component scale. In particularly fortuitous cases, for some modules/components, similitude can be achieved at the geometrical configuration scale. Overall, top-down scaling establishes and provides the scaling hierarchy of the system in question and enables most processes of the system to be identified. The processes may then be ranked in order of importance on system behavior. This approach ensures that the experimental and analytical methods used are comprehensive, systematic, auditable, and traceable.

The top-down scaling hierarchy has five functions (References 7 and 16):

1. Identifies the important transfer processes to be investigated through experimental and modeling campaigns;

2. Enables the determination of appropriate scaling groups that need to be matched between the prototypical operating conditions and the scaled experiment/model, at the module/component level for IETs and at lower levels for SETs;
3. Serves as the basis for the priorities/emphasis of the experimental, modeling, verification and validation, and uncertainty quantification activities;
4. Provides the underlying technical basis of simplifying assumptions to reduce complexity of the problem while retaining the ability to investigate the key phenomena of interest;
5. Establishes a procedure to break up the complex system into slow and fast phenomena for use in transient analysis.

With the sole use of top-down scaling approach, analysts may not identify all important transfer processes, which may result in experiments where important phenomena are not properly captured. Examples where important, highly localized phenomena may not be properly captured include subcooled boiling in a cold leg break of a PWR, or distortions from parasitic heat losses in scaled experimental facilities (Reference 17). For KP-FHR, onset of localized overcooling in subsystems such as the tubes of an intermediate heat exchanger would not be appropriately accounted for in a top-down scaling analysis alone (Reference 18). This points to the importance of performing PIRTs for both prototypical systems and scaled facilities to capture key phenomena. In addition, iterative use of top-down and bottom-up scaling analysis provides the best approach to develop reasonable assurance that all important transfer processes have been identified and scaled for all modules/components for IETs, and at lower levels for SETs.

2.6 BOTTOM-UP SCALING ANALYSIS

Bottom-up system scaling is a deductive approach that considers all modules/components of a complex system. It is conducted after top-down scaling to focus on and capture all important phenomena and associated processes at every lower hierarchical level. After conducting a bottom-up scaling analysis, the scaling criteria and characteristic time scales of each important process for each module/component may be determined.

Bottom-up system scaling is performed using stepwise integral scaling, which consists of the following steps (Reference 7).

1. Identify the important and dominant phenomena and how the sequence of analysis occurs:
    a. Starting at one hierarchical level higher, identify any potential processes at one level lower. Because top-down scaling for IETs commonly focuses on modules/components, bottom-up scaling commonly starts at the hierarchical levels of fields, geometrical configurations, phases and constituents (see Figure 3);
    b. Rank the identified processes in terms of relative importance and potential sequence of events;
    c. Determine the most important or dominant processes and consider:
        i. Any mechanisms occurring in parallel;
        ii. Potential bifurcation phenomena (e.g., topological change in flow behavior) (Reference 19);
        iii. Feedback mechanisms that act as coupling between different processes;

d. Establish the sequence of analysis for the important processes;

2. Apply the stepwise integral scaling analysis:
    a. Deduce the highest hierarchical level and process and start from the boundary and an event upstream to;
    b. Select the most probable or important mechanism;
    c. Write out the integral rate process equations;
    d. Identify the transition criteria for the mechanisms;
    e. Determine the solution or integral response;
    f. Determine the characteristic time constant;
    g. Nondimensionalize the results;
    h. Determine the integral scaling parameters for mechanisms of interest;
    i. Select the next most probable or important mechanism and repeat sub-steps 2(c)-2(h) using results from the previous mechanism;
    j. Use the integral scaling parameters to evaluate the relative importance of the two mechanisms;
    k. If needed, combine the two mechanisms in the analysis;
    l. Repeat process with additional mechanisms to obtain the complete set of scaling and transitional criteria and the characteristic time constants;
3. Evaluate the relative importance of various effects and mechanisms between prototype and model system:
    a. Using initial and boundary conditions from both prototypical and model systems, quantify scaling parameters and characteristic time scales;
    b. Analyze similitude between prototype and model, and characterize distortions;
    c. If large uncertainties exist for dominant mechanisms or processes, then SETs should be identified and conducted to reduce the associated uncertainty.

3 APPLICATION OF SCALING METHODOLOGY TO IETS

Kairos Power will perform scaled IETs on the systems that manage fission heat to provide an adequate assessment base for the evaluation model that will ultimately perform the plant event analyses. A flow chart for the different steps of the general KP-FHR IET scaling methodology is presented in Figure 5. The steps related to PIRT in Figure 5 are optional in the development of scaled experiments. If used, PIRT results may help prioritize dominant, not well-characterized phenomena in the Kairos Power test program if they are important to plant performance, or exclude these phenomena from the KP-FHR design if an alternative approach exists that does not have a significant performance penalty. In particular, PIRT results may support identification and prioritization of dominant phenomena and associated structures, systems and components that will need to be captured in Kairos Power IETs and SETs, as well as acceptable distortions from these IETs and SETs, to reduce modeling uncertainties resulting from novel KP-FHR design aspects. The PIRT process may help identify representative events to be captured by Kairos Power IETs, as well as important figures of merit to be measured through testing in support of evaluation model validation.

This section provides the methods necessary to perform a scaling analysis for a surrogate fluid (heat transfer oil) IET of the KP-FHR PHTS under normal conditions as well as transients involving the loss of forced flow (i.e., natural circulation conditions). An IET of the PHTS must have the essential characteristics of the classes of systems present in the KP-FHR design. The idealized version of the PHTS is presented in Figure 6 along with associated scaling parameters. This idealized model of the PHTS comprises the five major components of the actual KP-FHR PHTS including: the reactor core, primary salt pump, intermediate heat exchanger (IHX), and interconnecting hot leg and cold leg piping. Properly scaled, this idealized scaled PHTS replicates the full scale KP-FHR PHTS under normal conditions and transient conditions involving natural circulation for passive decay heat removal.

3.1 DEFINE EXPERIMENTAL OBJECTIVES AND METRICS OF INTEREST

The scaling methodology laid out in this Section covers two main classes of scenarios: steady-state, normal forced-circulation operation of the idealized KP-FHR PHTS, as well as transients resulting in natural circulation in the PHTS (e.g., pump trip, loss of heat sink). The natural circulation class of scenarios is further broken down into two phases, namely initial onset of natural circulation, followed by long-term quasi-steady natural circulation in the PHTS. The experimental objectives for a scaled test facility resulting from this scaling effort would be to perform tests that cover normal operation as well as both phases of the natural circulation scenario in a single test facility. Sections 3.2 and 3.3 cover each scenario of interest. Section 3.4 covers test facility design specifications to address both scenarios simultaneously, including quantification of scaling distortions when attempting to use a single facility to cover both scenarios. While this report covers an idealized version of the PHTS with only five modules/components, it presents the full methodology needed to perform system scaling for high-fidelity models for the KP-FHR, which will resolve transient response at the level of all individual modules/components in future analyses.

Because the KP-FHR PHTS is a high-temperature, near-atmospheric-pressure, single-phase system, principal figures of merit (metrics) investigated through thermal-fluids IETs have differences from those investigated for other classes of reactors – LWRs in particular – and comprise primary coolant boundary conditions that can lead to temperature-induced degradation of structural materials:

- Time-varying temperature under normal operation, because of risk of thermal striping and ratcheting damage to structures

- Time at elevated temperature and magnitude of temperature during transients, in particular:
    - Fuel temperature, as it influences fuel failure and radionuclide release, although this is very unlikely to govern KP-FHR safety case due to high temperature margin to fuel failure
    - Structural components temperature, for creep deformation and degradation of metallic structural materials
- Peak temperature gradients in structural components during transients, which may result in thermal stress and thermal creep damage
- Peak bulk coolant outlet temperature, which is indirectly related to structural integrity of the system.

3.2 NORMAL OPERATION SCALING ANALYSIS

During normal operation of the idealized PHTS, the primary salt pumps provide the driving force to circulate the primary coolant. Normal operation covers the power range for the KP-FHR plant for steady-state power production, where the temperature across the core is maintained at the same values as 100% nominal power.

A flow diagram for normal operation scaling analysis, building on the steps laid out through the generic scaling methodology in Figure 5, is shown in Figure 7. During load change transients between 40% and 100% power, the KP-FHR core inlet and outlet temperatures would be maintained constant by varying the primary salt pump speeds and the idealized PHTS would not need to undergo any substantive thermal transients. For application of the H2TS methodology, it is assumed that all boundary conditions are kept constant for this operation mode. Furthermore, the following assumptions are made to simplify the scaling analysis:

1. The flow is assumed to be incompressible and the Boussinesq approximation is applied
2. The flow is treated as 1-D around a single loop
    a. The fluid properties are considered constant across every cross-section in the two loops, which are modeled as a single effective loop
    b. The effects of non-uniform flow distribution in the core and IHXs are treated using a heat transfer effectiveness correction which is a conventional constitutive model used to simulate heat exchangers as 1-D components;
3. Parasitic heat losses from the coolant boundary and thermal inertia of the hot and cold leg structures are neglected
    a. Adiabatic boundary conditions are assumed outside of the core and IHX.

3.2.1 Normal Operation Phenomena and Figures of Merit

Thermal-fluids phenomena of interest during normal operation of the idealized PHTS, addressed in this section, include:

- Core friction losses (porous media flow);
- Core and reflector heat transfer (packed bed convective and conduction heat transfer, flow distribution and heat transfer effectiveness);

- Convective heat transfer to core support structures, including graphite reflectors;
- Friction and form losses in IHX and PHTS piping system;
- Primary salt free surface levels.

For simplification, the scaling methodology applied here focuses on a single loop PHTS, however the methodology may be extended to flow networks with branches and allow for investigation of bypass flows (e.g., through reflector gaps and fluidic diode or check valve to decay heat removal system).

The single principal thermal-fluids figure of merit during normal operation of the PHTS, listed in Section 3.1, is peak bulk coolant outlet temperature.

3.2.2 Top-Down Scaling for Normal Steady-State Operation

Using the set of assumptions listed at the beginning of Section 3.2, and focusing on the idealized PHTS, a simplified set of conservation equations is used to derive characteristic time ratios for normal operation. The top-down scaling analysis covers two levels: the integral system level, which provides similarity criteria for the loop as a whole, and the module/component level, which in this example provides similarity criteria for the pebble-bed core and the twisted tube IHX.

The loop integrated momentum conservation equation in the entire idealized KP-FHR primary loop (core, pump, IHX and hot and cold leg piping) and constituent-level energy balance equation for the reactor core (which is one of the five modules/components in the idealized PHTS) during steady-state normal operation are written as:

$$\Delta p + \rho g \beta \Delta T_{loop} - \frac{\dot{m}^2}{\rho A_{ref}^2} \sum_{j=1}^{N} \left[\frac{1}{2} \left(K_j + f_j \frac{l_j}{d_j} \right) \left(\frac{A_{ref}}{A_j} \right)^2 \right] = 0 \tag{11}$$

$$\dot{m} c_{pf} (T_H - T_C) = Q_{Rx} = Q_{HX} \tag{12}$$

where Δp is the pressure differential developed by the primary salt pump, ρ the average fluid density in the idealized PHTS, g gravitational acceleration, β the average coefficient of thermal expansion of the salt in the PHTS, ΔT_{loop} the effective temperature difference between the hot and cold legs of the loop (defined in Eq. (36) in Section 3.3), which is approximately equal to $T_H - T_C$, l_{HT} the elevation difference between the centerline of the core and the centerline of the IHX (see Figure 6) $\dot{m}$ the fluid mass flow rate in the PHTS, A_{ref} a reference cross-sectional area (typically core area, as seen in Figure 6), K_j the form loss coefficient of module/component j, f_j the friction loss coefficient of module/component j, l_j the effective length of any module/component j in the loop, d_j the effective hydraulic diameter of module/component j, A_j the effective cross-sectional area of module/component j, c_{pf} the average fluid specific heat capacity in the PHTS, T_H the bulk coolant temperature at the outlet of the core, T_C the reactor coolant minimum temperature, Q_{Rx} the thermal power generated in the reactor core, and Q_{Hx} the heat removed in the heat exchanger.

Note that T_H and T_C are key figures of merit listed in Section 3.2.1 for the normal operation scenario.

Equation (11) may be non-dimensionalized using the following normalized parameters (marked with $*$ or θ), based on the normal operation temperature difference in the loop $(T_{H0} - T_{C0})$, normal operation mass flow rate $\dot{m}_{ref}$, and normal operation pressure drop of the pump Δp_0:

$$\theta = \frac{(T_H - T_C)}{(T_{H0} - T_{C0})}, \dot{m}^* = \frac{\dot{m}}{\dot{m}_{ref}}, \Delta p^* = \frac{\Delta p}{\Delta p_0} \tag{13}$$

By substituting normalized parameters (Eq. (13)) into Eq. (11), the momentum conservation equation may be presented as follows:

$$\Delta p^* \Delta p_0 + \theta \rho g \beta \Delta T_{loop} l_{HT} - (\dot{m}^*)^2 \frac{\dot{m}_{ref}^2}{\rho A_{ref}^2} \sum_{j=1}^{N} \left[\frac{1}{2} \left(K_j + f_j \frac{l_j}{d_j} \right) \left(\frac{A_{ref}}{A_j} \right)^2 \right] = 0 \tag{14}$$

Using u_{ref}, the reference fluid velocity in the PHTS during normal operation, the momentum conservation equation may be stated as:

$$\Delta p^* \Delta p_0 + \theta \rho g \beta \Delta T_{loop} l_{HT} - (\dot{m}^*)^2 \rho u_{ref}^2 \sum_{j=1}^{N} \left[\frac{1}{2} \left(K_j + f_j \frac{l_j}{d_j} \right) \left(\frac{A_{ref}}{A_j} \right)^2 \right] = 0 \tag{15}$$

By dividing out the ρu_{ref}^2 term from both sides of Eq. (15), the final form of the momentum conservation equation before identifying characteristic time ratios may be stated as:

$$\Delta p^* \frac{\Delta p_0}{\rho u_{ref}^2} + \theta \frac{g \beta \Delta T_{loop} l_{HT}}{u_{ref}^2} - (\dot{m}^*)^2 \sum_{j=1}^{N} \left[\frac{1}{2} \left(K_j + f_j \frac{l_j}{d_j} \right) \left(\frac{A_{ref}}{A_j} \right)^2 \right] = 0 \tag{16}$$

The non-dimensional equation for the loop may now be presented using characteristic time ratios:

$$\Pi_{Eu} \Delta p^* + \Pi_{Ri} \theta - \Pi_F (\dot{m}^*)^2 = 0 \tag{17}$$

The characteristic time ratios consist of Π_{Eu} (Euler number of the loop), Π_{Ri} (Richardson number of the loop), and Π_F (loop flow resistance number):

$$\begin{aligned} \Pi_{Eu} &= \frac{\Delta p_0}{\rho u_{ref}^2} = \frac{g H_0}{u_{ref}^2}, \\ \Pi_{Ri} &= \frac{g \beta \Delta T_{loop} l_{HT}}{u_{ref}^2}, \\ \Pi_F &= \sum_{j=1}^{N} \left[\frac{1}{2} \left(K_j + f_j \frac{l_j}{d_j} \right) \left(\frac{A_{ref}}{A_j} \right)^2 \right] \end{aligned} \tag{18}$$

where $H_0 = \Delta p_0 / \rho g$ is the pump head, commonly used in sizing pumps. Note that the friction factors in Π_F are functions of the local Reynolds number, and therefore Π_F is not a constant. The bottom-up scaling approach presented in Section 0 addresses the question of local friction factors f_i in Π_F.

Using Newton's law of cooling for the reactor core, Eq. (12) may be written as:

$$\dot{m} c_{pf} (T_H - T_C) = \varepsilon_{Rx} h_{Rx} A_{s,Rx} \left(T_{si,Rx} - T_{f,Rx} \right) \tag{19}$$

where ε_{Rx} is a heat transfer effectiveness correction factor that accounts for flow non-uniformity in the core and bypass flow in the reflector structure, h_{Rx} the average heat transfer coefficient between the solid and fluid phases in the core, $A_{s,Rx}$ the heat transfer surface area in the core, $T_{si,Rx}$ the average solid (i.e., fuel) interface (surface) temperature in the core, and $T_{f,Rx}$ the average fluid temperature in the core.

The energy balance equation is non-dimensionalized using the following normalized parameter in addition to those used to non-dimensionalize the momentum equation (Eq. (13)):

$$\theta_{feg,Rx} = \frac{T_{si,Rx} - T_{f,Rx}}{\left(T_{si,Rx} - T_{f,Rx}\right)_0} \tag{20}$$

Substituting the normalized parameters in Eq. (13) and Eq. (20) into Eq. (19) yields the following equation:

$$\dot{m}^* \dot{m}_{ref} c_{pf} \theta (T_{H0} - T_{C0}) = \varepsilon_{Rx} h_{Rx} A_{s,Rx} \theta_{feg,Rx} \left(T_{si,Rx} - T_{f,Rx}\right)_0 \tag{21}$$

By dividing both sides of the equation by $\dot{m}_{ref} c_{pf} (T_{H0} - T_{C0})$:

$$\dot{m}^* \theta = \varepsilon_{Rx} h_{Rx} A_{s,Rx} \theta_{feg,Rx} \frac{\left(T_{si,Rx} - T_{f,Rx}\right)_0}{\dot{m}_{ref} c_{pf} (T_{H0} - T_{C0})} \tag{22}$$

The non-dimensional form of the energy balance equation may be stated as:

$$\dot{m}^* \theta = \Pi_{St,m-Rx} \theta_{feg,Rx} \tag{23}$$

The characteristic time ratio shown in Eq. (23), relating mass flow rate to the fluid's reference velocity, consists of the modified Stanton number for the reactor core.

$$\Pi_{St,m-Rx} = \frac{\varepsilon_{Rx} h_{Rx} A_{s,Rx} \left(T_{si,Rx} - T_{f,Rx}\right)_0}{\rho u_{ref} A_{ref} c_{pf} (T_{H0} - T_{C0})} \tag{24}$$

The steady-state energy balance equation as stated in Eq. (12) may also be written at the constituent level for the IHX as:

$$\dot{m} c_{pf} (T_H - T_C) = Q_{HX} \tag{25}$$

where Q_{HX} is the thermal power removed by the IHX. In this case, the non-dimensional form of the energy balance equation may be stated as:

$$\dot{m}^* \theta = \Pi_{St,m-HX} \theta_{feg,HX} \tag{26}$$

The characteristic time ratio shown in Eq. (26) consists of the modified Stanton number for the IHX.

$$\Pi_{St,m-HX} = \frac{\varepsilon_{HX} U_{HX} A_{s,HX} \Delta T_{LMTD,0}}{\rho u_{ref} A_{ref} c_{pf} (T_{H0} - T_{C0})} \tag{27}$$

where U_{HX} is the total thermal resistance of the IHX and $\Delta T_{LMTD,0}$ the reference logarithmic mean temperature difference in the IHX.

3.2.3 Bottom-Up Scaling for Normal Operation

Bottom-up scaling for normal operation of the KP-FHR PHTS requires local behavior to be captured in individual constituents, namely the heat source (reactor core), heat sink (IHX), primary salt pump, and PHTS hot and cold leg piping. To determine required items for bottom-up scaling, the characteristic time ratios derived from top-down scaling (Section 3.2.2) may be examined for each constituent, and further scaling constraints may be identified.

The component frictional and form losses to be matched between the scaled experiment and the prototype are expressed as follows (from Eq. (18)):

$$\Pi_{F,m} = \Pi_{F,p} \Leftrightarrow \sum_{j=1}^{N}\left[\frac{1}{2}\left(K_j + f_j\frac{l_j}{d_j}\right)\left(\frac{A_{ref}}{A_j}\right)^2\right]_m = \sum_{j=1}^{N}\left[\frac{1}{2}\left(K_j + f_j\frac{l_j}{d_j}\right)\left(\frac{A_{ref}}{A_j}\right)^2\right]_p \tag{28}$$

If scaling of module/component j allows the scaled hydraulic diameter of flow channels to be preserved, then since the friction factors f_j in Π_F are functions of the local Reynolds number, Π_F may be preserved by preserving the Reynolds number between the prototypical system and scaled experiment. The Reynolds number in each module/component j is expressed as:

$$\Pi_{Re,j} = \frac{\rho_j u_j d_j}{\mu_j} \tag{29}$$

Alternatively, in cases where it is not practical to preserve the scaled hydraulic diameter in some modules/components, the relationship in Eq. (28) allows for varying friction factors and minor or form losses for individual modules/components as long as the overall loop's Π_F is preserved from a prototypical system to a scaled experiment.

For heat transfer, the relationship between the scaled experiment and the idealized PHTS prototype is expressed by matching the modified Stanton numbers in the core ($j = Rx$) and IHX ($j = HX$) (from Eqs. (24) and (27)):

$$\begin{aligned}&\left(\Pi_{St,m-Rx}\right)_m = \left(\Pi_{St,m-Rx}\right)_p \\ &\Leftrightarrow \left(\frac{\varepsilon_{Rx} h_{Rx} A_{s,Rx}\left(T_{si,Rx} - T_{f,Rx}\right)_0}{\rho u_{ref} A_{ref} c_{pf}(T_{H0} - T_{C0})}\right)_m = \left(\frac{\varepsilon_{Rx} h_{Rx} A_{s,Rx}\left(T_{si,Rx} - T_{f,Rx}\right)_0}{\rho u_{ref} A_{ref} c_{pf}(T_{H0} - T_{C0})}\right)_p\end{aligned} \tag{30}$$

$$\begin{aligned}&\left(\Pi_{St,m-HX}\right)_m = \left(\Pi_{St,m-HX}\right)_p \\ &\Leftrightarrow \left(\frac{\varepsilon_{HX} U_{HX} A_{s,HX} \Delta T_{LMTD,0}}{\rho u_{ref} A_{ref} c_{pf}(T_{H0} - T_{C0})}\right)_m = \left(\frac{\varepsilon_{HX} U_{HX} A_{s,HX} \Delta T_{LMTD,0}}{\rho u_{ref} A_{ref} c_{pf}(T_{H0} - T_{C0})}\right)_p\end{aligned} \tag{31}$$

Individual behaviors in the reactor core and IHX influence the modified Stanton numbers through the heat transfer coefficients for each component (heat transfer in other parts of the loop is neglected, since it was assumed that the idealized PHTS piping is adiabatic).

[[

]] Since the heat transfer coefficient is related to the Nusselt number through the length scale and thermal conductivity of the fluid, the Nusselt number dependence may be matched between the model and prototypical IHX. A common functional form of the Nusselt number for forced circulation results in a relation that is a function of both Reynolds and Prandtl numbers, and is defined as follows:

$$Nu = aRe^m Pr^n \tag{32}$$

where a, m and n are condition-dependent coefficients, the Reynolds number is defined in Eq. (29), and the Prandtl number is defined as follows

$$\Pi_{Pr} = \frac{\nu}{\alpha} \tag{33}$$

where ν is fluid kinematic viscosity and α thermal diffusivity of the fluid. Alternatively, the relationships in Eqs. (30) and (31) allow matching of hA_s instead of h and A_s individually, in which case matching of the Nusselt number would not be as important.

To conclude the bottom-up IHX scaling analysis presented here, Π_{Re} and Π_{Pr} are the two relevant characteristic time ratios for the IHX during steady-state, normal operation. In general, one would apply the bottom-up scaling approach laid out above (resulting in matching of Π_{Re} and Π_{Pr}) when geometric scaling is feasible (e.g., for the IHX), and therefore the specific heat structure behavior may be matched. Conversely, alternative solutions may be used when it is not practical to match the specific heat structure geometry of a component (e.g., pebble bed core).

3.2.4 Summary of Normal Operation Similitude Criteria

Following the H2TS methodology for the KP-FHR PHTS under steady-state, normal operation, characteristic time ratios have been identified from both top-down and bottom-up scaling analyses. They are summarized in Table 1.

Sections 3.4.1 and 3.4.2 show that all the normal operation characteristic time ratios derived above may be matched in scaled experiments using heat transfer oil. This similitude is important, because steady-state forced circulation is the normal initial condition for initiating events where the subsequent transition to natural circulation and passive residual heat removal is of interest.

3.3 NATURAL CIRCULATION SCALING ANALYSIS

The natural circulation class of scenarios assumes that, from normal operation conditions (as described in Section 3.2), the primary pumps trip because of some initiating event (e.g., pump motor failure, loss of heat sink). The reactor protection system is actuated as off-normal conditions are detected and the reactor scrams.

Because the primary salt pump shuts down and no active auxiliary cooling is initiated, the simplified scenario involves a transition to natural circulation in the PHTS where only the density difference in the loop between the reactor core and heat removal system causes the primary salt to circulate. The systems and components credited for decay heat removal in the context of this document are used for illustration of the scaling methodology only and do not reflect the actual KP-FHR system used for passive residual heat removal. This example is similar to the approaches taken in References 12, 20, 21, and 22.

A flow diagram for natural circulation scaling analysis, building on the steps laid out through the generic scaling methodology in Figure 5, is shown in Figure 8.

The following assumptions are made to simplify the scaling analysis for the natural circulation class of scenarios, as an illustration of the methodology developed in this report:

1. The temperature rise across the core once the system reaches quasi-steady natural circulation is assumed to be similar to the normal operation temperature rise;
2. [[ ]]
3. The flow is assumed to be incompressible and the Boussinesq approximation is applied;
4. The flow is treated as 1-D around the entire loop (i.e., the fluid properties are considered constant across every cross-section in the loop);
5. Parasitic heat losses from the system are neglected (i.e., adiabatic boundary conditions are assumed outside of the core and heat removal system).

For KP-FHRs it is considered good design practice to design natural circulation flow systems for decay heat removal to operate with similar temperature differences as during forced circulation, full power operation. Assumption 1 is based upon this good design practice, however it is important to note that the scaling will still result in correct temperature differences occurring in natural circulation, even if the assumption is not correct.

3.3.1 Natural Circulation Phenomena and Figures of Merit

In addition to the phenomena identified for the normal operation case and listed in Section 3.2.1, thermal-fluids phenomena of interest during natural circulation in the PHTS, addressed in this section, include:

- Single-phase natural circulation in the reactor core;
- Potential for freezing of the primary salt, Flibe, around 460°C, for long-term natural circulation.

Thermal radiation heat transfer can be important at the operating temperatures of the KP-FHR, however under natural circulation conditions thermal radiation can generally be neglected compared to convective heat transfer. For convective heat transfer in flow channels under natural circulation, surfaces

that view each other (opposite sides of channels) have similar temperature and small thermal radiation heat transfer. While Flibe absorbs in the far infrared, path lengths in flow channels are short, therefore reducing net radiative heat transfer. Bardet and Peterson provide additional discussion on scaling distortion from thermal radiation (Reference 25). However, it is emphasized that thermal radiation must always be considered as a potential source of distortion in scaling of IET experiments.

Principal thermal-fluids figures of merit during natural circulation in the PHTS, listed in Section 3.1, include:

- Time at elevated temperature and magnitude of temperature for structural components;
- Peak temperature gradients in structural components;
- Peak bulk coolant outlet temperature;
- Reactor coolant minimum temperature.

The following sections cover the top-down and bottom-up scaling analyses for two phases of the natural circulation class of scenarios, namely onset of natural circulation, then quasi-steady natural circulation in the PHTS.

3.3.2 Natural Circulation Transient Evolution

3.3.2.1 Top-Down Scaling for Onset of Natural Circulation

Using the set of assumptions listed at the beginning of Section 3.3, and focusing on the PHTS, a simplified set of conservation equations is used to derive characteristic time ratios for onset of natural circulation. Similar to the analysis for normal operation, the top-down scaling analysis covers two levels: the integral system level, which provides similarity criteria for the loop as a whole, and the constituent level, which in this example provides similarity criteria for the core and the heat removal system.

The integrated momentum conservation equation in the entire KP-FHR PHTS (core, heat removal system and PHTS piping system) and integrated energy balance equation during the onset of natural circulation transient, which relates to the single-phase natural circulation phenomenon highlighted in Section 3.3.1, are written as:

$$\frac{d\dot{m}}{dt}\sum_{j=1}^{N}\frac{l_j}{A_j} = \rho_f g\beta\Delta T_{loop} l_{HT} - \frac{\dot{m}^2}{\rho_f A_{ref}^2}\sum_{j=1}^{N}\left[\frac{1}{2}\left(K_j + f_j\frac{l_j}{d_j}\right)\left(\frac{A_{ref}}{A_j}\right)^2\right] \tag{34}$$

$$m_{loop}c_{ploop}\frac{\partial T_{loop}}{\partial t} = Q_{Rx} - Q_{HX} \tag{35}$$

where l_{HT} is the elevation difference between the centerlines of the heat source (i.e., reactor core) and the decay heat removal system.

Equation (34) uses much of the same nomenclature as in Section 3.2, Eq. (11). However, in transient natural circulation, buoyancy forces, which are small under forced circulation, provide the dominant forces to drive flow, where the effective temperature difference ΔT_{loop} emerges from integration of temperature variation around the loop:

$$\Delta T_{loop} = \frac{1}{l_{HT}} \oint (T(z) - T_{C0}) dz = \frac{1}{l_{HT}} \sum_{j=1}^{N} (T_{fj} - T_{C0}) \Delta z_j \approx T_H - T_C \quad (36)$$

where T_{fj} is the average fluid temperature in module/component j and Δz_j the height of module/component j (negative if there is downflow in the module/component). In the case where the temperature distributions in the core and in the heat exchanger are linear with elevation, ΔT_{loop} equals the difference between the core outlet and inlet temperatures ($T_H - T_C$).

Equation (35) also adds transient terms to account for the thermal inertia of fluid and structures in the loop. Here, the total heat capacity of the loop fluid and solid structures is given by:

$$m_{loop} c_{ploop} = \sum_{j=1}^{N} \left[\rho_{fj} c_{pfj} V_{CVj} + m_{sj} c_{psj} \right] \quad (37)$$

where c_{ploop} is the loop-average specific heat. The average temperature of fluid and structures in the loop, T_{loop}, found in Eq. (35), is then given by:

$$T_{loop} - T_{C0} = \frac{\sum_{j=1}^{N} \left[\rho_{fj} c_{pfj} V_{CVj} (T_{fj} - T_{C0}) + m_{sj} c_{psj} (T_{sj} - T_{C0}) \right]}{m_{loop} c_{ploop}} \quad (38)$$

where T_{fj} and V_{CVj} are the bulk temperature and volume of the fluid in module/component j, T_{sj} and m_{sj} the bulk temperature and mass of solid material in module/component j, and c_{pfj} and c_{psj} the specific heat of the fluid and solid material in module/component j.

The energy conservation equation, Eq. (35), plays a major role in governing the transient evolution under natural circulation. Immediately after reactor shutdown, decay heat generation Q_{Rx} exceeds the passive heat removal rate Q_{HX} and heat is absorbed into the coolant and the solid heat structures around the loop. As the loop temperature increases, the heat removal rate Q_{HX} also increases due to the increasing driving temperature. As decay heat drops over time the decay heat and heat removal rate become equal and then the heat removal rate exceeds decay heat, and the fluid and structure temperatures begin to drop. An important goal for IET scaling is to correctly match the heat capacity and thermal coupling of solid heat structures for modules/component in the system so that the transient evolution of the fluid temperature distribution, and resulting natural circulation flow, are accurately reproduced in the model. At the system level, this requires matching the solid structures heat capacity number:

$$\Pi_{HS} = \frac{1}{m_f c_{pf}} \sum_{j=1}^{N} \left[\rho_{fj} c_{pfj} V_{CVj} + m_{sj} c_{psj} \right] = \frac{m_{loop} c_{ploop}}{m_f c_{pf}} \quad (39)$$

where m_f is the total mass of coolant in the system.

In KP-FHRs, the heat capacity of the coolant and of solid heat structures are comparable. The energy conservation equation, Eq. (35), using the average loop temperature defined in Eq. (38), shows how the transient change of temperature of solid heat structures affects the overall system transient response.

Transient heat transfer from the fluid in a module/component j to the solid heat structure depends on the history of the temperature difference between the fluid and the component.

Equation (34) may be non-dimensionalized using the following normalized parameters based on the time constant of the loop for natural circulation, initial temperature difference in the loop, reference mass flow rate in the loop for natural circulation, and the elevation difference between the centerlines of the heat source and the decay heat removal system:

$$\theta_{fj} = \frac{T_{fj} - T_{C0}}{T_{H0} - T_{C0}}, \theta_{sj} = \frac{T_{sj} - T_{C0}}{T_{H0} - T_{C0}}, \Delta\theta_{loop} = \frac{\Delta T_{loop}}{T_{H0} - T_{C0}}, \Delta z_j^* = \frac{\Delta z_j}{l_{HT}}$$
$$t^* = \frac{t}{\tau_{loop,NC}}, \ \dot{m}^* = \frac{\dot{m}}{\dot{m}_{ref,NC}} \tag{40}$$

The time constant of the loop in Eq. (40) is based on the residence time of the fluid in the entire loop (i.e., total amount of time it takes for the fluid to circulate through the loop once) as the loop reaches quasi-steady natural circulation:

$$\tau_{loop,NC} = \frac{m_f}{\dot{m}_{ref,NC}} = \frac{m_f}{\rho u_{ref,NC} A_{ref}} \tag{41}$$

Using the design-goal assumption listed at the beginning of Section 3.3 that the natural-circulation temperature rise across the core with decay heat power is similar to the normal forced-circulation operation temperature rise at full power, the reference mass flow rate for natural circulation, which is taken to be the mass flow rate in the loop as the system reaches quasi-steady-state, can be expressed as a function of the normal operation mass flow rate, normal operation power level in the core Q_{FC}, and decay heat level of power generation in the core Q_{NC}, and similarly, the time constant of the loop for natural circulation can be expressed as a function of the normal operation time constant, normal operation power level in the core, and decay heat level of power generation in the core:

$$\dot{m}_{ref,NC} = \dot{m}_{ref} \frac{Q_{NC}}{Q_{FC}} \tag{42}$$

$$\tau_{loop,NC} = \tau_{loop} \frac{Q_{FC}}{Q_{NC}} \tag{43}$$

By substituting normalized parameters (Eq. (40)) into Eq. (34), the momentum conservation equation may be presented as follows:

$$\frac{d\dot{m}^*}{dt^*} \frac{\dot{m}_{ref,NC}}{\tau_{loop,NC}} \sum_{j=1}^{N} \frac{l_j}{A_j} = \Delta\theta_{loop} \rho g \beta (T_{H0} - T_{C0}) l_{HT}$$
$$- (\dot{m}^*)^2 \frac{\dot{m}_{ref,NC}^2}{\rho A_{ref}^2} \sum_{j=1}^{N} \left[\frac{1}{2} \left(K_j + f_j \frac{l_j}{d_j} \right) \left(\frac{A_{ref}}{A_j} \right)^2 \right] \tag{44}$$

where the nondimensional loop temperature difference $\Delta\theta_{loop}$ is derived from Eq. (36):

$$\Delta\theta_{loop} = \frac{1}{l_{HT}(T_{H0} - T_{C0})}\sum_{j=1}^{N}(T_{fj} - T_{C0})\Delta z_j = \sum_{j=1}^{N}\theta_{fj}\Delta z_j^* \tag{45}$$

Using $u_{ref,NC}$, the reference fluid velocity during quasi-steady natural circulation as shown in Eq. (41), and the reference length of the loop based on the total mass of fluid in the loop:

$$l_{ref} = \frac{m_f}{\rho A_{ref}} \tag{46}$$

the momentum conservation equation may be expressed as:

$$\begin{aligned}&\frac{d\dot{m}^*}{dt^*}\rho u_{ref,NC}^2\frac{A_{ref}}{l_{ref}}\sum_{j=1}^{N}\frac{l_j}{A_j} = \Delta\theta_{loop}\rho g\beta(T_{H0} - T_{C0})l_{HT}\\&-(\dot{m}^*)^2\rho u_{ref,NC}^2\sum_{j=1}^{N}\left[\frac{1}{2}\left(K_j + f_j\frac{l_j}{d_j}\right)\left(\frac{A_{ref}}{A_j}\right)^2\right]\end{aligned} \tag{47}$$

By dividing out the $\rho u_{ref,NC}^2$ term from both sides of Eq. (47), the final form of the momentum conservation equation before identifying characteristic time ratios may be stated as:

$$\frac{d\dot{m}^*}{dt^*}\sum_{j=1}^{N}\frac{l_j}{A_j}\frac{A_{ref}}{l_{ref}} = \Delta\theta_{loop}\frac{g\beta(T_{H0} - T_{C0})l_{HT}}{u_{ref,NC}^2} - (\dot{m}^*)^2\sum_{j=1}^{N}\left[\frac{1}{2}\left(K_j + f_j\frac{l_j}{d_j}\right)\left(\frac{A_{ref}}{A_j}\right)^2\right] \tag{48}$$

The non-dimensional form of the momentum equation for the loop may now be presented using characteristic time ratios:

$$\Pi_G\frac{d\dot{m}^*}{dt^*} = \Pi_{Ri,NC}\Delta\theta_{loop} - \Pi_F(\dot{m}^*)^2 \tag{49}$$

The characteristic time ratios consist of Π_G (geometry number for the loop, also important for matching fluid heat capacity distribution around the loop), $\Pi_{Ri,NC}$ (Richardson number of the loop for natural circulation), and Π_F (loop flow resistance number):

$$\begin{aligned}\Pi_G &= \sum_{j=1}^{N}\frac{l_j}{A_j}\frac{A_{ref}}{l_{ref}},\\\Pi_{Ri,NC} &= \frac{g\beta(T_{H0} - T_{C0})l_{HT}}{u_{ref,NC}^2},\\\Pi_F &= \sum_{j=1}^{N}\left[\frac{1}{2}\left(K_j + f_j\frac{l_j}{d_j}\right)\left(\frac{A_{ref}}{A_j}\right)^2\right]\end{aligned} \tag{50}$$

It is worthwhile to note that:

$$u_{ref,NC} = u_{ref}\frac{Q_{NC}}{Q_{FC}} \tag{51}$$

Therefore:

$$\Pi_{Ri,NC} = \Pi_{Ri}\left(\frac{Q_{FC}}{Q_{NC}}\right)^2 \tag{52}$$

This report presents approximate closure models to complete the scaling analysis for the idealized PHTS. This presents the methodology needed for the scaling and modeling of transient heat transport between fluids and solid structures (both the convective heat transfer from the fluid to the surface of the heat structures and conduction in the heat structures).

Applying Newton's law of cooling for the reactor core, *j* = *Rx*, and heat exchanger, *j* = *HX*, Eq. (35) may be expressed as:

$$\begin{aligned}\rho_f c_{pf}\left(V_{CV,Rx}\frac{\partial T_{fRx}}{\partial t} + V_{CV,HX}\frac{\partial T_{fHX}}{\partial t}\right) + m_{s,Rx}c_{ps,Rx}\frac{\partial T_{s,Rx}}{\partial t} + m_{s,HX}c_{ps,HX}\frac{\partial T_{s,HX}}{\partial t}\\ = m_{loop}c_{ploop}\frac{\partial T_{loop}}{\partial t}\\ = \varepsilon_{Rx}h_{Rx}A_{s,Rx}\left(T_{si,Rx} - T_{f,Rx}\right) + \varepsilon_{HX}U_{HX}A_{s,HX}\Delta T_{LMTD,HX}\end{aligned} \tag{53}$$

The integrated energy balance equation is non-dimensionalized using the following normalized parameter, in addition to the same normalized parameters used previously:

$$\theta_{loop} = \frac{T_{loop} - T_{C0}}{T_{H0} - T_{C0}} \tag{54}$$

This yields:

$$\begin{aligned}m_{loop}c_{ploop}\frac{1}{\tau_{loop,NC}}\frac{\partial}{\partial t^*}\left[T_{C0} + \theta_{loop}(T_{H0} - T_{C0})\right]\\ = \varepsilon_{Rx}h_{Rx}A_{s,Rx}\theta_{feg,Rx}\left(T_{si,Rx} - T_{f,Rx}\right)_0 + \varepsilon_{HX}U_{HX}A_{s,HX}\theta_{feg,HX}\Delta T_{LMTD,HX,0}\end{aligned} \tag{55}$$

It is further recognized that:

$$\frac{m_f}{\tau_{loop,NC}} = \frac{m_{loop}c_{ploop}}{\Pi_{HS}c_{pf}\tau_{loop,NC}} = \dot{m}_{ref,NC} \tag{56}$$

$$\frac{\partial T_{C0}}{\partial t^*} = 0 \tag{57}$$

Therefore:

$$\dot{m}_{ref,NC}\Pi_{HS}c_{pf}(T_{H0}-T_{C0})\frac{\partial\theta_{loop}}{\partial t^*} = \varepsilon_{Rx}h_{Rx}A_{s,Rx}\theta_{feg,Rx}\left(T_{si,Rx}-T_{f,Rx}\right)_0 + \varepsilon_{HX}U_{HX}A_{s,HX}\theta_{feg,HX}\Delta T_{LMTD,HX,0} \quad (58)$$

By dividing both sides of Eq. (58) by $\dot{m}_{ref,NC}c_{pf}(T_{H0}-T_{C0})$:

$$\Pi_{HS}\frac{\partial\theta_{loop}}{\partial t^*} = \varepsilon_{Rx}h_{Rx}A_{s,Rx}\theta_{feg,Rx}\frac{\left(T_{si,Rx}-T_{f,Rx}\right)_0}{\dot{m}_{ref,NC}c_{pf}(T_{H0}-T_{C0})} + \varepsilon_{HX}U_{HX}A_{s,HX}\theta_{feg,HX}\frac{\Delta T_{LMTD,HX,0}}{\dot{m}_{ref,NC}c_{pf}(T_{H0}-T_{C0})} \quad (59)$$

The non-dimensional form of the energy balance equation may be presented as:

$$\Pi_{HS}\frac{\partial\theta_{loop}}{\partial t^*} = \Pi_{St,m-Rx,NC}\theta_{feg,Rx} + \Pi_{St,m-HX,NC}\theta_{feg,HX} \quad (60)$$

In addition to the solid structures heat capacity number Π_{HS}, the characteristic time ratios shown in Eq. (60) consist of the modified Stanton numbers for the reactor core and the heat exchanger, respectively, during natural circulation:

$$\Pi_{St,m-Rx,NC} = \frac{\varepsilon_{Rx}h_{Rx}A_{s,Rx}\left(T_{si,Rx}-T_{f,Rx}\right)_0}{\rho u_{ref,NC}A_{ref}c_{pf}(T_{H0}-T_{C0})},$$
$$\Pi_{St,m-HX,NC} = \frac{\varepsilon_{HX}U_{HX}A_{s,HX}\Delta T_{LMTD,HX,0}}{\rho u_{ref,NC}A_{ref}c_{pf}(T_{H0}-T_{C0})} \quad (61)$$

Heat transfer to solid structures is important in KP-FHR transients, because of important figures of merit related to temperatures and temperature gradients in structural components as listed in Section 3.3.1, and because solid structures comprise a significant share of the total heat capacity in the PHTS as given by the solid structures heat capacity number Π_{HS}. The energy balance at the solid/fluid boundary of each constituent in the system may be stated as:

$$q''_{cond} = q''_{conv} \quad (62)$$

where q''_{cond} is the heat flux through conduction in the solid and q''_{conv} the heat flux through convection between the solid and fluid. Fourier's law may be applied for the heat conduction term, and Newton's law of cooling may be applied for the heat convection term in Eq. (62):

$$-k_s\frac{dT_s}{dy}\bigg|_{y=0} = h\left(T_{si}-T_f\right) \quad (63)$$

where the subscript s specifies quantities associated with the solid and y the length in the solid normal to the heat transfer surface (this specific example uses Cartesian coordinates, however it may readily be translated to cylindrical or spherical coordinates).

The normalized parameters for Eq. (63) may be defined as follows:

$$y^* = \frac{y}{l_s}, \theta = \frac{T - T_{C0}}{T_{H0} - T_{C0}} \tag{64}$$

where l_s is the characteristic length of the solid, defined as:

$$l_s = \frac{A_{s,cross-section}}{P} \tag{65}$$

where $A_{s,cross-section}$ is the solid structure cross-sectional area and P the wetted perimeter. The normalized parameters in Eq. (64) may be substituted into Eq. (63) to yield the following after dividing both left and right sides by $-k_s$:

$$\frac{1}{l_s}\frac{d}{dy^*}[\theta_s(T_{H0} - T_{C0}) + T_{C0}]\Big|_{y^*=0} = -\frac{h}{k_s}(\theta_{si} - \theta_f)(T_{H0} - T_{C0}) \tag{66}$$

The reference temperature difference $(T_{H0} - T_{C0})$ may be divided out on both sides of the equation to yield the non-dimensional form of the solid/fluid boundary energy balance equation:

$$\frac{d\theta_s}{dy^*}\Big|_{y^*=0} = -\Pi_{Bi}(\theta_{si} - \theta_f) \tag{67}$$

The characteristic time ratio in Eq. (67) is the Biot number for any of the loop components:

$$\Pi_{Bi} = \frac{hl_s}{k_s} \tag{68}$$

For low values of the Biot number, temperature gradients in the solid heat structure are small compared to other temperature differences in the system and the heat structure may be assumed to be isothermal and to respond as a lumped mass. In this case, the solution of the transient conduction equation is not required. Conversely, for high Biot number values, transient conduction is important, and the conduction equation must be scaled.

The conduction equation at the constituent level for solid heat structures may be considered to determine the energy-related characteristic time ratios associated with the solids. To simplify this analysis, only a rectangular geometry is considered here, although the derivation of characteristic time ratios in cylindrical and spherical coordinates is similar:

$$\rho_s c_{ps}\frac{\partial T_s}{\partial t} = k_s\frac{\partial^2 T_s}{\partial y^2} + q'''_{source,s} \tag{69}$$

The energy equation for the solids in the loop is non-dimensionalized using the following normalized parameters:

$$y^* = \frac{y}{l_s}, t^* = \frac{t}{\tau_s}, \theta_{seg} = \frac{T_s - T_{C0}}{(T_{H0} - T_{C0})} \tag{70}$$

where τ_s is the characteristic time constant of the solid and θ_{seg} the temperature scaling factor specific to the solid energy conservation equation. The time constant τ_s found in Eq. (70) is based on the time needed for heat to conduct through the solid:

$$\tau_s = \frac{l_s^2}{\alpha_s} \tag{71}$$

This time constant is specific to each solid constituent in the loop with its own characteristic length and thermal diffusivity. By substituting Eqs. (70) and (71) into Eq. (69) and dividing both sides by $\rho_s c_{ps}$, the following is found:

$$\frac{1}{\tau_s}\frac{\partial}{\partial t^*}\left[\theta_{seg}(T_{H0} - T_{C0}) + T_{C0}\right] = \frac{k_s}{\rho_s c_{ps}}\frac{1}{l_s^2}\frac{\partial^2}{\partial (y^*)^2}\left[\theta_{seg}(T_{H0} - T_{C0}) + T_{C0}\right] + \frac{q'''_{source,s}}{\rho_s c_{ps}} \tag{72}$$

Using Eq. (57), and multiplying both sides of the equation by the solid time constant τ_s, the following equation results:

$$\frac{\partial}{\partial t^*}\left[\theta_{seg}(T_{H0} - T_{C0})\right] = \frac{\partial^2}{\partial (y^*)^2}\left[\theta_{seg}(T_{H0} - T_{C0})\right] + \tau_s \frac{q'''_{source,s}}{\rho_s c_{ps}} \tag{73}$$

The term $T_{H0} - T_{C0}$ is divided out on by both sides of Eq. (73) to get the following:

$$\frac{\partial \theta_{seg}}{\partial t^*} = \frac{\partial^2 \theta_{seg}}{\partial (y^*)^2} + \frac{l_s^2 q'''_{source,s}}{\rho_s c_{ps} \alpha_s (T_{H0} - T_{C0})} \tag{74}$$

The last term on the right is simplified in Eq. (74) by canceling out the common quantities found in the thermal diffusivity ($\alpha_s = \frac{k_s}{\rho_s c_{ps}}$).

$$\frac{\partial \theta_{seg}}{\partial t^*} = \frac{\partial^2 \theta_{seg}}{\partial (y^*)^2} + \frac{l_s^2 q'''_{source,s}}{k_s (T_{H0} - T_{C0})} \tag{75}$$

The non-dimensionalized form of the conduction equation may be stated as:

$$\frac{\partial \theta_{seg}}{\partial t^*} = \frac{\partial^2 \theta_{seg}}{\partial (y^*)^2} + \Pi_{q'''_{source,s}} \tag{76}$$

The characteristic time ratio for conduction in individual solid constituents (e.g., reactor core) in the loop is the heat source number:

$$\Pi_{q'''_{source,s}} = \frac{l_s^2 q'''_{source,s}}{k_s (T_{H0} - T_{C0})} \tag{77}$$

3.3.2.2 Bottom-Up Scaling for Natural Circulation Transient Evolution

Bottom-up scaling for transition to natural circulation in the KP-FHR PHTS requires local behavior to be captured in individual constituents, namely the heat source (reactor core), heat removal system heat exchanger, and PHTS piping. To determine required items for bottom-up scaling, the characteristic time ratios derived from top-down scaling (Section 3.3.2.1) may be examined for each constituent, and further scaling constraints may be identified.

Similar to the normal operation case, because the friction factors in Π_F are functions of the local Reynolds number, Π_F may be preserved by preserving the Reynolds number between the prototypical system and scaled experiment. Alternatively, friction factors and minor or form losses may be varied in individual components as long as the overall loop's Π_F is preserved from a prototypical system to a scaled experiment.

For heat transfer, the relationship between the scaled experiment and the prototype is expressed by matching the modified Stanton numbers in the core and heat removal system heat exchanger during natural circulation, given in Eq. (61). Individual behaviors in the reactor core and heat exchanger influence the modified Stanton numbers through the heat transfer coefficients for each component (heat transfer in other parts of the loop is neglected, since it was assumed that the PHTS piping is adiabatic, however the same methodology may be applied to the PHTS hot and cold legs).

[[

]] Since the heat transfer coefficient is related to the Nusselt number through the length scale and thermal conductivity of the fluid, the Nusselt number dependence may be matched between the model and prototypical heat exchanger. A common functional form of the Nusselt number for onset of natural circulation, where the Reynolds number is still relatively high, was given in Eq. (32). Alternatively, the relationships in Eq. (61) allow matching of hA_s instead of h and A_s individually, in which case matching of the Nusselt number would not be as important.

Based on the bottom-up scaling analysis presented here, similar to the steady-state, normal operation case, Π_{Re} and Π_{Pr} are the two relevant characteristic time ratios for the heat removal system heat exchanger during onset of natural circulation. In general, one would apply the bottom-up scaling approach laid out above (resulting in matching of Π_{Re} and Π_{Pr}) when geometric scaling is feasible (e.g., for the heat exchanger), and therefore the specific heat structure behavior may be matched. Conversely, alternative solutions may be used when it is not practical to match the specific heat structure behavior of a component (e.g., pebble bed core).

3.3.3 Quasi-Steady Natural Circulation

The quasi-steady natural circulation phase of the natural circulation scenario is, from a scaling analysis standpoint, a simplified version of the onset of natural circulation phase detailed in Section 3.3.2.

This results in a subset of the characteristic time ratios derived in Section 3.3.2, and no new characteristic time ratios are derived from top-down scaling.

From bottom-up scaling, the only difference is that a usual functional form of the Nusselt number for quasi-steady natural circulation, as Reynolds number becomes very low, is a function of Grashof and Prandtl numbers, and is defined as follows (Reference 23):

$$Nu = aGr^m Pr^n \tag{78}$$

The Prandtl number was defined in Eq. (33), and the Grashof number is defined as follows:

$$\Pi_{Gr} = \frac{g\beta(T_{H0} - T_{C0})d^3}{\nu^2} \tag{79}$$

Note that when Π_{Re} and Π_{Ri} are matched, then Π_{Gr} is also matched. Based on the bottom-up scaling analysis presented here, Π_{Pr} and Π_{Gr} are the two relevant characteristic time ratios for the heat exchanger. In general, one would apply the bottom-up scaling approach laid out above (resulting in matching of Π_{Pr} and Π_{Gr}) when geometric scaling is feasible (e.g., for the heat exchanger), and therefore the specific heat structure behavior may be matched. [[

]]

3.3.4 Summary of Natural Circulation Similitude Criteria

Following the H2TS methodology for the KP-FHR PHTS during a natural circulation scenario, characteristic time ratios have been identified from both top-down and bottom-up scaling analyses. They are summarized in Table 2.

Sections 3.4.3 and 3.4.4 show that all the transient and quasi-steady natural circulation similitude ratios derived above can be matched in scaled experiments using heat transfer oil. This shows that it is feasible to design scaled surrogate fluid IETs that can replicate both forced circulation and transient natural circulation phenomena.

3.4 DESIGN SPECIFICATIONS AND QUANTIFICATION OF SCALING DISTORTIONS

As mentioned in Section 3.1, the experimental objectives for a scaled test resulting from this scaling effort would be to cover normal operation as well as both phases of the natural circulation scenario in a single facility. In this Section, design specifications for such a test facility, based on the characteristics of the idealized KP-FHR PHTS and the sets of characteristic time ratios listed in Table 1 and Table 2, are developed. Such design specifications include dimensional parameters such as lengths, velocities, temperature differences, power levels, etc.

3.4.1 System-Level Scaling Implementation for Normal Operation

Three characteristic time ratios for forced circulation in the KP-FHR PHTS during normal operation, listed in Table 1, apply to the system-level design of the PHTS: Π_{Pr}, Π_{Ri} and Π_{Eu}. For a forced circulation surrogate fluid IET, there are six adjustable parameters in the scaled model IET system that can be varied to achieve similitude: average temperature ($(T_{H0} + T_{C0})/2$), temperature difference ($T_{H0} - T_{C0}$), height

(l_{HT}), flow area (A_{ref}), velocity (u_{ref}), and pump head ($H_0 = \Delta p_0/\rho g$). The availability of three extra adjustable parameters provides important flexibility in IET scaling.

Π_{Pr} only depends on the thermophysical properties of the fluid used in the scaled test. Therefore, it is chosen as the first characteristic time ratio to match between the prototype and scaled model. Kairos Power is requesting NRC concurrence with the use of a specific class of surrogate fluids, as detailed in Section 5. This class of heat transfer fluids matches the average Π_{Pr} of Flibe in the PHTS (Π_{Pr} = 18.6 at $(T_{H0} + T_{C0})_p/2 = 600$°C) at a much reduced temperature ($(T_{H0} + T_{C0})_m/2 = 73$°C). The selection of the temperature determines average thermophysical properties of the model and prototypical fluids, which can then be used in quantifying other characteristic time ratios. Thus, the scaled surrogate model average temperature $(T_{H0} + T_{C0})_m/2$ is selected so that:

$$(Pr)_R = \frac{Pr_m}{Pr_p} = 1 \tag{80}$$

where the subscript R is used, here and in the rest of the report, to refer to the ratio between model and prototype parameters.

The second adjustable parameter is the scaled surrogate model temperature difference $(T_{H0} - T_{C0})_m$. This is scaled so that density changes due to heating and cooling are matched:

$$\left(\beta(T_{H0} - T_{C0})\right)_R = \frac{\left(\beta(T_{H0} - T_{C0})\right)_m}{\left(\beta(T_{H0} - T_{C0})\right)_p} = 1 \tag{81}$$

For the specific surrogate fluid, detailed in Section 5, density changes can be matched by selecting $(T_{H0} - T_{C0})_R = 1/3.43$, that is, for a typical prototype value of $(T_{H0} - T_{C0})_p = 100$°C, the scaled model uses $(T_{H0} - T_{C0})_m = 29.2$°C.

The two next most important scaling parameters for IETs are the scaled height $(l_{HT})_R$ and scaled area $\left(A_{ref}\right)_R$, because with power-to-volume scaling these parameters determine physical size and power required for the IET. The optimal selection of these parameters, to minimize scaling distortion for a prototypical KP-FHR, falls outside the scope of this report. Instead, for illustration of the scaling methodology for the idealized PHTS example, the height scale is selected as:

$$(l_{HT})_R = 1/2 \tag{82}$$

Full area scaling is selected for the idealized PHTS scaled model, which maintains geometric similitude, so:

$$\left(A_{ref}\right)_R = (l_{HT})_R^2 = 1/4 \tag{83}$$

A key question for scaling of IETs, at the component level, involves the scaling of hydraulic diameters d and lengths l of flow channels, particularly in cases for modules/components j where there are $(n)_{R,j} = \left(A_{ref}\right)_R/d_{R,j}^2$ multiple, parallel flow channels with similar flow conditions, for example in heat exchangers. Given full-area geometric scaling, for the idealized PHTS the number of parallel flow channels is preserved in each module/component j:

$$(n)_{R,j} = 1 \tag{84}$$

so, for the idealized PHTS:

$$(l)_{R,j} = (d)_{R,j} = (l_{HT})_R = 1/2 \tag{85}$$

The final steps involve selecting the velocity (u_{ref}), and pump head ($H_0 = \Delta p_0/\rho g$) scales for the IET, to match Π_{Ri} and Π_{Eu} between the scaled model and the prototype.

Π_{Ri} depends on fluid temperature (through temperature-dependent coefficient of thermal expansion), fluid reference velocity, temperature difference in the system, and length scale:

$$\Pi_{Ri} = \frac{g\beta(T_{H0} - T_{C0})l_{HT}}{u_{ref}^2} \tag{86}$$

Given the scaling of the temperature differences, Eq. (81), Π_{Ri} is then matched by selecting the velocity scale:

$$\left(u_{ref}\right)_R = \left(\sqrt{l_{HT}}\right)_R = 0.707 \tag{87}$$

This scaling is equivalent to matching the Froude number:

$$\Pi_{Fr} = \frac{u_{ref}^2}{g l_{HT}} \tag{88}$$

which also preserves free surface phenomena in the IET, in particular the relative elevations of different free surfaces in the system. Matching Π_{Fr} with reduced height scaling results in accelerated time scaling

$$\left(\tau_{loop}\right)_R = \left(\frac{l_{HT}}{u_{ref}}\right)_R = 0.707 \tag{89}$$

The pump Euler number Π_{Eu} depends on fluid temperature (through temperature-dependent density), fluid reference velocity, and the pump pressure drop and head,

$$\Pi_{Eu} = \frac{\Delta p_0}{\rho u_{ref}^2} = \frac{g H_0}{u_{ref}^2} \tag{90}$$

The pump Euler number is preserved by matching the pump head to the height scale, so

$$(H_0)_R = (l_{HT})_R = 1/2 \tag{91}$$

and

$$(\Delta p_0)_R = (\rho)_R (l_{HT})_R \tag{92}$$

Pump head and pressure can generally be matched in the scaled model by using variable frequency drive.

In addition to identifying important system dimensional parameter ratios through matching the characteristic time ratios identified in Section 3.2.4, it is helpful to quantify two other system parameter ratios relevant to experiment design: the heating power ratio and the pumping power ratio. The heating power Q_h is defined as follows:

$$Q_h = \rho c_{pf}(T_H - T_C)Q_{ref} = \rho c_{pf}(T_H - T_C)u_{ref}A_{ref} \quad (93)$$

where Q_{ref} is the average volumetric flow rate through the heated section of the system.

$$(Q_h)_R = (\rho)_R\left(c_{pf}\right)_R(\Delta T)_R\left(u_{ref}\right)_R\left(A_{ref}\right)_R \quad (94)$$

Another benefit of using a surrogate fluid, besides the large improvement in experimental measurement accuracy, is a very large reduction in heater power, $(Q_h)_R$ = 1/53.1.

The pumping power Q_p is defined as follows:

$$Q_p = \Delta p_o Q_{ref} = \Delta p_o u_{ref} A_{ref} \quad (95)$$

$$\left(Q_p\right)_R = (\Delta p_o)_R\left(u_{ref}\right)_R\left(A_{ref}\right)_R \quad (96)$$

The use of a surrogate fluid also enables a very large reduction in the pumping power, $\left(Q_p\right)_R$ = 1/22.9.

Model-to-prototype ratios of heating and pumping powers are entirely defined through other ratios of dimensional parameters derived previously and correspond to changes in requirements for input heat and input mechanical pumping action to the system. The fact that a significant reduction can be achieved for both ratios emphasizes the benefits of using surrogate fluid in IET experiments.

The steps for system-level scaling implementation for normal operation are summarized below:

1. [[

]]

Model-to-prototype ratios for all dimensional parameters identified in this Section, as well as resulting characteristic time ratios, are summarized in Table 3.

At this point, an appropriate surrogate fluid, as well as reasonable dimensional parameter scales for sizing a scaled IET for normal operation of the idealized KP-FHR PHTS, have been identified. Relevant characteristic time ratios between the prototype and model at a system level have also been identified and matched. The next step is to examine the design of components within the model system.

3.4.2 Component-Level Scaling Implementation for Normal Operation

The scaling parameter from Table 1 used to scale all components as an integrated system is the loop flow resistance number, Π_F.

To match Π_F between the model and prototypical systems, major frictional and form losses between the model and prototypical systems must be matched as follows:

$$\Pi_F = \sum_{j=1}^{N} \left[\frac{1}{2} \left(K_j + f_j \frac{l_j}{d_j} \right) \left(\frac{A_{ref}}{A_j} \right)^2 \right] \tag{97}$$

$$(\Pi_F)_R = 1 \Leftrightarrow \left(\sum_{j=1}^{N} \left[\left(K_j + f_j \frac{l_j}{d_j} \right) \left(\frac{A_{ref}}{A_j} \right)^2 \right] \right)_R = 1 \tag{98}$$

In KP-FHRs, the very high volumetric heat capacity of the reactor coolant results in low volumetric flow rates, so that Reynolds numbers are commonly in the transition or laminar regimes in heat exchangers. For this reason, KP-FHR designs optimize to use enhanced heat transfer surfaces, such as the pebble bed core and twisted tube IHX of the idealized PHTS. In heat exchange systems with surface enhancement, form losses generally dominate over friction losses in causing pressure drop. To simplify matching Π_F in the model and prototypical systems, we assume that form losses are much more significant than frictional losses in the idealized PHTS:

$$\sum_{j=1}^{N} K_j \gg \sum_{j=1}^{N} f_j \frac{l_j}{d_j} \tag{99}$$

This is justified by assuming that pressure drops from form losses through the pebble bed core and the twisted tube IHX in the PHTS will dominate overall loop pressure drop, compared to friction losses through the hot and cold leg piping in the PHTS during normal operation. This assumption may be verified once designs of the KP-FHR PHTS and scaled test facility have been finalized, and simplifies the relationship to match Π_F as follows:

$$(\Pi_F)_R = 1 \Leftrightarrow \left(\sum_{j=1}^{N} \left[\frac{K_j}{A_j^2} \right] \right)_R = \frac{1}{\left(A_{ref} \right)_R^2} \tag{100}$$

In KP-FHR designs where the component form loss coefficients dominate pressure losses, the model system flow resistances may be adjusted by the system designer through the use of orifice plates, needle valves, or other methods of adjusting pressure drop in the flow branches.

Looking more specifically at the reactor core and IHX components of the idealized PHTS, three characteristic time ratios from Table 1 should be matched between the model and prototype: $\Pi_{St,m-Rx}$, $\Pi_{St,m-HX}$ and $\Pi_{Re,HX}$.

The modified Stanton numbers for the reactor core and IHX ($\Pi_{St,m-Rx}$ and $\Pi_{St,m-HX}$) are important to match in order to preserve the steady state heat transfer behavior between solid structures and fluid in these components. In designing the reactor core and IHX in the model system, $\Pi_{St,m}$ may be matched by adjusting the heat transfer coefficient and heat transfer surface area within each component as follows:

$$\Pi_{St,m-x} = \frac{\varepsilon_x h_x A_{s,x} \left(T_{si,x} - T_{f,x} \right)_0}{\rho u_{ref} A_{ref} c_{pf} (T_{H0} - T_{C0})} \tag{101}$$

In particular, for the reactor core:

$$\left(\Pi_{St,m-Rx}\right)_R = 1 \Leftrightarrow \left(\varepsilon_{Rx} h_{Rx} A_{s,Rx}\right)_R = (\rho)_R \left(c_{pf}\right)_R \left(u_{ref}\right)_R \left(A_{ref}\right)_R \quad (102)$$

and for the twisted tube IHX:

$$\left(\Pi_{St,m-HX}\right)_R = 1 \Leftrightarrow \left(\varepsilon_{HX} h_{HX} A_{s,HX}\right)_R = (\rho)_R \left(c_{pf}\right)_R \left(u_{ref}\right)_R (n)_R (d)_R^2 \quad (103)$$

Given that for the pebble reactor core, $\Pi_{St,m-Rx}$ may be matched in an electrically heated model through adjusting several experimental parameters (heat transfer effectiveness correction factor, heat transfer coefficient and heat transfer surface area), the IET designer must be strategic in considering which parameter is most worth the effort in adjusting. In general, the heat transfer coefficient is highly dependent on the process fluid, process operational regime, and pebble bed core design, which makes adjusting this parameter challenging, although it is possible by using enhanced surfaces or other heat transfer enhancement/reduction means. Once heat transfer coefficient is well known for the model, partly based on separate effects testing for heated elements geometry of interest, heat transfer surface area may be adjusted to meet the relationship in Eq. (102).

Similar to $\Pi_{St,m}$, the IHX's Reynolds number (Π_{Re}) may be matched between the model and prototypical systems to ensure similar flow regime behavior in the IHX. However, all dimensional parameters that define Π_{Re}, as seen in Eq. (29), are fully defined at this stage:

$$(\Pi_{Re})_R = \frac{(\rho)_R (u)_R (d)_R}{(\mu)_R} \quad (104)$$

When listing final design parameter specification for the scaled IET facility, distortion factors, including for Π_{Re}, will be quantified. It is important to note that, while for SETs matching of Π_{Re} will be important, scaled IETs may accept some distortion as long as it is properly quantified and propagated through system models.

The steps for component-level scaling implementation for normal operation are summarized below:

1. [[

]]

Model-to-prototype ratios for all dimensional parameters identified in this Section, as well as resulting characteristic time ratios, are summarized in Table 4.

3.4.3 System-Level Scaling Implementation for Natural Circulation

Three characteristic time ratios for natural circulation in the KP-FHR PHTS, listed in Table 2, apply to the system-level design of the PHTS: $\Pi_{Ri,NC}$, Π_{HS} and Π_{Pr}.

Working fluid and average operating temperature ($(T_{H0} + T_{C0})/2$) for the scaled test facility were already chosen in Section 3.4.1 so that $(\Pi_{Pr})_R = 1$. Using the assumption listed at the beginning of

Section 3.3 that the average temperature and temperature rise across the core during the natural circulation scenario is similar to the normal operation average temperature and temperature rise, $(\Pi_{Pr})_R = 1$ remains true for the natural circulation scenario using the same scaled test facility as for normal operation.

As seen in Eq. (52), the Richardson number for the natural circulation case, $\Pi_{Ri,NC}$, is directly related to the Richardson number during normal operation, Π_{Ri}, and the ratio of decay heat power to normal operation power. The scaled temperature difference $(T_{H0} - T_{C0})$ has been selected so buoyancy forces match in the prototype and model systems, $\left(\beta(T_{H0} - T_{C0})\right)_R = 1$. Therefore, matching of the Richardson number is achieved by matching the ratio of natural circulation, decay-heat power Q_{NC} to forced circulation, full power Q_{FC}:

$$\left(\frac{Q_{NC}}{Q_{FC}}\right)_R = 1 \Leftrightarrow \left(\Pi_{Ri,NC}\right)_R = (\Pi_{Ri})_R = 1 \tag{105}$$

Similarly, because of the relationships listed in Eqs. (43) and (51):

$$\left(\frac{Q_{NC}}{Q_{FC}}\right)_R = 1 \Leftrightarrow \left(\tau_{loop,NC}\right)_R = \left(\tau_{loop}\right)_R \text{ and } \left(u_{ref,NC}\right)_R = \left(u_{ref}\right)_R \tag{106}$$

Once system-level scaling has been implemented for normal operation, system-level scaling for the natural circulation transient evolution scenario may be summarized in two steps:

1. [[

]]

Model-to-prototype ratios for all dimensional parameters identified in this Section for the idealized PHTS, as well as resulting characteristic time ratios, are summarized in Table 5. Dimensional parameter ratios are not repeated from Table 3 when they are identical (e.g., geometric scales).

3.4.4 Component-Level Scaling Implementation for Natural Circulation

The two scaling parameters from Table 2 used to scale all components as an integrated system are the loop geometry number, Π_G, and the loop resistance number, Π_F.

To match Π_G between the model and prototypical systems, the sum of the length-to-area ratios of all components in the model system must scale to the same sum of ratios in the prototypical system as follows:

$$\Pi_G = \sum_{j=1}^{N} \frac{l_j}{l_{ref}} \frac{A_{ref}}{A_j} \tag{107}$$

$$(\Pi_G)_R = 1 \Leftrightarrow \left(\sum_{j=1}^{N} \frac{l_j}{A_j}\right)_R = \frac{(l_{ref})_R}{(A_{ref})_R} \tag{108}$$

Preserving Π_G between the model and prototypical systems ensures that system-level geometric phenomena are preserved (volume ratios in the system are preserved, and therefore relative residence times are preserved). Note that this similarity criterion is automatically met if geometric similitude is adopted between the model and prototype, however, this methodology may extend to cases where geometric similitude is not preserved for added degrees of freedom in the scaled experiment.

Component-level form loss coefficients were already adjusted in Section 3.4.2 so that $(\Pi_F)_R = 1$. This remains true for the natural circulation scenario using the same scaled test facility as for normal operation.

Looking more specifically at the reactor core and heat exchanger components, six characteristic time ratios from Table 2 in Section 3.3.4 must be matched between the model and prototype: $\Pi_{St,m-Rx,NC}$, $\Pi_{St,m-HX,NC}$, $\Pi_{Re,HX}$, $\Pi_{Gr,HX}$, $\Pi_{Bi,HX}$ and $\Pi_{q'''_{source,s}}$.

For convective heat transport, $\left(h_{Rx}A_{s,Rx}\right)_R$ and $\left(h_{HX}A_{s,HX}\right)_R$ were already adjusted in Section 3.4.2 so that $\left(\Pi_{St,m-Rx}\right)_R = 1$ and $\left(\Pi_{St,m-HX}\right)_R = 1$. Since $\left(u_{ref,NC}\right)_R = \left(u_{ref}\right)_R$ (Eq. (106)), this automatically results in $\left(\Pi_{St,m-Rx,NC}\right)_R = 1$ and $\left(\Pi_{St,m-HX,NC}\right)_R = 1$ for the natural circulation scenario, using the same scaled test facility as for normal operation.

Similar to $\Pi_{St,m}$, the heat exchanger's Reynolds and Grashof numbers (Π_{Re} and Π_{Gr}) may be matched between the model and prototypical systems to ensure similar natural circulation behavior in the heat exchanger during onset of natural circulation and steady-state natural circulation, respectively. However, all dimensional parameters that define Π_{Re} and Π_{Gr}, as seen in Eqs. (29) and (79), are fully defined at this stage:

$$(\Pi_{Re})_R = \frac{(\rho)_R(u)_R(d)_R}{(\mu)_R} \tag{109}$$

$$(\Pi_{Gr})_R = \frac{(\beta)_R(\Delta T)_R(d)_R^3}{(\nu)_R^2} \tag{110}$$

When listing final design parameter specification for the scaled facility, distortion factors, including for Π_{Re} and Π_{Gr}, will be quantified. It is important to note that, while for SETs matching of Π_{Re} and Π_{Gr} will be important, scaled IETs may accept some distortion as long as it is properly quantified and propagated through system models.

The Biot number (Π_{Bi}) is important to scale correctly to capture the relative importance of conduction and convection at the heat transfer surfaces in the heat exchanger. Π_{Bi} for the model may be adjusted to match Π_{Bi} in the prototypical system as follows:

$$\Pi_{Bi} = \frac{hl_s}{k_s} \tag{111}$$

$$(\Pi_{Bi})_R = 1 \Leftrightarrow (l_s)_R = \frac{(k_s)_R}{(h)_R} \quad (112)$$

To match Π_{Bi} between the model and prototypical systems, the design parameters that may be adjusted are the solid characteristic length (generally its thickness) and the solid material selection, which dictates its thermophysical properties (thermal conductivity k_s in particular). [[

]] Alternatively, distortions in Π_{Bi} may be acceptable to better match solid time constants in the heat exchanger during natural circulation transients. In particular, overall flow and energy distribution will not be strongly affected in slow transients typical of a natural circulation system.

The time constants for solid structures in the reactor core and heat exchanger, $\tau_{s,Rx}$ and $\tau_{s,HX}$, are defined as follows:

$$\tau_{s,Rx} = \frac{{l_{s,Rx}}^2}{\alpha_{s,Rx}}, \tau_{s,HX} = \frac{{l_{s,HX}}^2}{\alpha_{s,HX}} \quad (113)$$

To appropriately match time response of conjugate heat transfer between fluid and solid structures in the system, an effort is made to match the loop time constant ratio and solid time constant ratios:

$$\left(\tau_{s,Rx}\right)_R = \left(\tau_{s,HX}\right)_R = \left(\tau_{loop,NC}\right)_R \quad (114)$$

Using the definition of the solid time constants (Eq. (113)) and the definition of the loop time constant:

$$\left(\tau_{s,Rx}\right)_R = \left(\tau_{loop,NC}\right)_R \Leftrightarrow \frac{\left(l_{s,Rx}\right)_R^2}{\left(\alpha_{s,Rx}\right)_R} = \frac{\left(l_{ref}\right)_R}{\left(u_{ref,NC}\right)_R} \quad (115)$$

$$\left(\tau_{s,HX}\right)_R = \left(\tau_{loop,NC}\right)_R \Leftrightarrow \frac{\left(l_{s,HX}\right)_R^2}{\left(\alpha_{s,HX}\right)_R} = \frac{\left(l_{ref}\right)_R}{\left(u_{ref,NC}\right)_R} \quad (116)$$

The solid length scale ratio between the model and prototype $\left(l_{s,j}\right)_R$ may be chosen to be constant (e.g., at 1/2 to reduce the thickness of solid structures in the scaled test facility), and solid materials are then chosen so that:

$$\left(\alpha_{s,j}\right)_R = \frac{\left(l_{s,j}\right)_R^2 \left(u_{ref,NC}\right)_R}{\left(l_{ref}\right)_R} \quad (117)$$

This may require the [[

]]

[[

]]

Finally, to match the heat source number in the reactor core between the model and prototype, using Eq. (77):

$$\left(\Pi_{q'''_{source,s}}\right)_R = 1 \Leftrightarrow \left(q'''_{source,s}\right)_R = \frac{\left(k_{s,Rx}\right)_R (\Delta T)_R}{\left(l_{s,Rx}\right)_R^2} \tag{118}$$

The steps for component-level scaling implementation for the natural circulation transient, using the same scaled test facility for both normal operation and natural circulation, are summarized below:

1. [[

]]

Model-to-prototype ratios for all dimensional parameters identified in this Section, as well as resulting characteristic time ratios, are summarized in Table 6.

3.4.5 Summary of Design Specifications and Quantification of Scaling Distortions

Sections 3.4.1 through 3.4.4 detailed system- and component-level scaling implementation to replicate normal operation, initial onset of natural circulation and long-term quasi-steady-state natural circulation scenarios in the KP-FHR PHTS using a single scaled test facility. Table 7 provides a summary of design specifications for such a facility as a list of dimensional parameters relative to a prototypical KP-FHR PHTS. Table 8 lists characteristic time ratios relevant for each of the two scenarios and associated as-designed distortion factors.

This generic scaling implementation demonstrates that, due to beneficial scaling attributes between a specific surrogate heat transfer oil at 73°C and KP-FHR PHTS prototypical fluid Flibe at 600°C average operating temperature, a single test facility may be designed that replicates both normal operation and natural circulation transients (onset of natural circulation and steady-state natural circulation). As seen in Table 8, this may be done with no distortions to most relevant characteristic time ratios for both scenarios, except for Π_{Re} and Π_{Gr} in the heat exchanger, due to simplicity of the single-phase, near-atmospheric pressure salt coolant in the KP-FHR PHTS, compared to other classes of reactors (e.g., PWRs, BWRs, gas-cooled reactors).

A number of conclusions may be drawn from this analysis. Surrogate heat transfer fluid temperatures needed to simulate the expected temperature range in the KP-FHR PHTS are low and well within operational constraints of the identified class of heat transfer oils, which have a freezing point of 12°C, flash and fire points near 115°C, and boiling point of 257°C. This, along with advantageous scaling ratios for length, fluid velocity, temperature change, area, system pressure drop, fluid mass, fluid volume, and solid heat structure thermal capacities (combination of length and area scales), emphasizes the advantage of using a surrogate fluid to model the steady state and transient thermal-fluids performance of Flibe systems in general. Further, the accuracy of experimental measurements for pressure, flow and temperature are much higher for the low temperature surrogate fluid system, the heating and pumping power ratios are also very small.

Note that, following this generic scaling implementation, the practical scaling of such a surrogate fluid IET facility would be based on final dimensional parameters for the KP-FHR PHTS. Then, as-built dimensional parameters would be adopted to be as close as possible to as-designed parameters, in order to minimize additional distortions relative to as-designed distortion factors listed in Table 8. Potential causes of distortions between as-designed and as-built scaled test facilities are listed in Section 2.4.

4 APPLICATION OF SCALING METHODOLOGY TO SEPARATE EFFECTS TESTS

SETs are used to understand the physical phenomena or processes of interest in specific modules or components, develop closure models and correlations, and address technical questions such as how to scale up components (Reference 7). This section discusses the implementation of scaling in SETs for both fluid dynamics and heat transfer phenomena experienced in the KP-FHR design. As described in Section 2, IETs may not fully characterize component-specific and phenomena-specific effects. Focusing solely on isothermal fluid dynamics, the relevant non-dimensional groups or scaling parameters are traditionally Reynolds number (turbulence structure, viscous and form drag forces on surfaces and structures), Froude number (liquid free surface dynamics, buoyancy forces on pebbles), and Weber number (surface tension effects on droplet and bubble generation) (Reference 24). For convective heat transfer, the relevant non-dimensional parameters or scaling parameters are the Prandtl number, Reynolds number, Grashof number, and Rayleigh number (Reference 24). These non-dimensional parameters are not prescriptive of all situations expected to be encountered but serve as a valuable starting point. This section provides methods for scaling SETs appropriately for fluid dynamics and heat transfer phenomena, as well as expected KP-FHR design specific phenomena.

4.1 FORCED CIRCULATION FLUID DYNAMICS

The investigation of fluid dynamics behavior of various geometries that are relevant to the KP-FHR require matching of specific non-dimensional numbers and resulting scaling parameters. At a fundamental level, the fluid dynamics in geometrically scaled flow channels involve the regime of flow (laminar, transitional, or turbulent). For single-phase flows, the flow regime is determined by the Reynolds number, resulting from non-dimensionalization of the Navier-Stokes equation and defined below:

$$Re \equiv \frac{\rho u d}{\mu} \tag{119}$$

The Reynolds number is an important factor in correlations for quantities such as friction factor for various geometries (e.g., flow inside tubes or across pebbles, applicable to key components of the KP-FHR PHTS such as pebble bed core). The Reynolds number is scaled between a prototypical system and a scaled experiment using the following relationship:

$$Re_m = Re_p \Leftrightarrow \frac{\rho_m u_m d_m}{\mu_m} = \frac{\rho_p u_p d_p}{\mu_p} \Leftrightarrow \frac{u_m}{u_p} = \frac{\rho_p}{\rho_m}\frac{\mu_m}{\mu_p}\frac{d_p}{d_m} \tag{120}$$

Matching Reynolds number enables use of surrogate fluids (e.g., heat transfer oil or water) to be scaled to prototypic fluids (e.g., Flibe or nitrate salt) to reproduce fluid dynamics phenomena which are controlled by the balance of inertial and viscous forces.

For liquid flow involving free surfaces or coupling with buoyant objects like fuel pebbles and other solid structures, the Froude number is used to quantify the significance of buoyant vs. inertial forces of the flow. This is especially important for experiments characterizing the motion of fuel pebbles in the KP-FHR core, as well as investigation of the dynamics of various fluid free surfaces in the KP-FHR PHTS. The Froude number is defined as follows:

$$Fr \equiv \frac{u}{\sqrt{gd}} \tag{121}$$

The Froude number is scaled between a prototypical system and a scaled experiment using the following relationship:

$$Fr_m = Fr_p \Leftrightarrow \left(\frac{u}{\sqrt{gd}}\right)_m = \left(\frac{u}{\sqrt{gd}}\right)_p \Leftrightarrow \frac{u_m}{u_p} = \left(\frac{d_m}{d_p}\right)^{1/2} \tag{122}$$

In scenarios involving both convective and buoyant effects (e.g., pebble bed flow dynamics), where it is important to match both Reynolds and Froude numbers, scaling of the relevant length scale (d) may be dependent on scaling of fluid properties only, using both Eqs. (120) and (122):

$$\frac{d_m}{d_p} = \left(\frac{\rho_p}{\rho_m}\frac{\mu_m}{\mu_p}\right)^{2/3} \tag{123}$$

The velocity ratio between the scaled experiment and prototypic system may be determined as well, using Eqs. (120) and (123) to yield:

$$\frac{u_m}{u_p} = \left(\frac{d_m}{d_p}\right)^{1/2} = \left(\frac{\rho_p}{\rho_m}\frac{\mu_m}{\mu_p}\right)^{1/3} \tag{124}$$

The time scale ratio is also determined, where the reduced length scale model has accelerated time:

$$\frac{t_m}{t_p} = \frac{d_m/u_m}{d_p/u_p} = \left(\frac{d_m}{d_p}\right)^{1/2} = \left(\frac{\rho_p}{\rho_m}\frac{\mu_m}{\mu_p}\right)^{1/3} \tag{125}$$

While scaling of the Froude number reproduces large-scale liquid free surface effects, in cases where generation of small liquid droplets and gas bubbles occurs, surface tension effects may be important. The Weber number, which determines the relative role of surface tension and inertia, is defined as:

$$We \equiv \frac{\rho u^2 d}{\sigma} \tag{126}$$

where σ is the surface tension.

The Weber number is normally not matched in SET experiments but may be used to evaluate distortion in generation of liquid droplets or gas bubbles, for example as a consequence of operation of a cantilevered pump shaft extending through a liquid free surface.

4.2 CONVECTIVE HEAT TRANSFER

The investigation of convective heat transfer behavior of various flow-channel geometries that are relevant to the KP-FHR (e.g., pebble bed core, IHX, downcomer) requires matching of both fluid dynamics- and heat transfer-related non-dimensional numbers, as well as related scaling parameters, as discussed

in this Section, for scaled experiments. Forced, mixed, and natural convection heat transfer of any geometry is characterized by the Nusselt number, which in turn is a function of Reynolds, Prandtl and/or Grashof numbers depending on the scenario of interest:

$$\begin{aligned} &Nu = f(Re, Pr, F) \text{ (forced circulation and natural circulation at high Reynolds)} \\ &Nu = f(Gr, Re, Pr, F) \text{ (mixed convection and natural circulation at low Reynolds)} \\ &Nu = f(Gr, Pr, F) \text{ (natural convection)} \end{aligned} \quad (127)$$

where F is a generic correction factor that changes with various heat transfer scenarios. Specific forms of Nusselt number correlations vary depending on the scenario of interest, with one example provided in APPENDIX A, Section A.2. All Nusselt number correlations depend on the Prandtl number, which characterizes the ratio of momentum diffusivity to thermal diffusivity in a fluid:

$$Pr \equiv \frac{\nu}{\alpha} = \frac{{}^{\mu}/_{\rho}}{{}^{k}/_{\rho c_p}} = \frac{c_p \mu}{k} \quad (128)$$

The fact that Prandtl number is only dependent on fluid properties enables a simple means of evaluating the suitability of surrogate fluids for use in scaled experiments, prior to defining other parameters of a test (e.g., geometries, flow rates). Evaluation of distortions may be done by comparing the range of Prandtl numbers between prototypical and surrogate fluids, as discussed in Section 5.2.

For scenarios where forced circulation is dominant, or for natural circulation scenarios with relatively large Reynolds number, the first form of the Nusselt number in Eq. (127) is used for scaling (Reference 24). In this case, both Reynolds number and Prandtl number need to be matched:

$$Re_m = Re_p \Leftrightarrow \frac{\rho_m u_m d_m}{\mu_m} = \frac{\rho_p u_p d_p}{\mu_p} \Leftrightarrow \frac{u_m}{u_p} = \frac{\rho_p}{\rho_m}\frac{\mu_m}{\mu_p}\frac{d_p}{d_m} \quad (129)$$

$$Pr_m = Pr_p \Leftrightarrow \left(\frac{c_p \mu}{k}\right)_m = \left(\frac{c_p \mu}{k}\right)_p \quad (130)$$

For natural convection scenarios, or for natural circulation scenarios with very low Reynolds number, the second or third form of the Nusselt number in Eq. (127) is used for scaling (Reference 24). Instead of the Reynolds number alone, the Grashof number based on the characteristic length scale (i.e., pipe diameter or hydraulic diameter) and average fluid properties is used for length and temperature scaling:

$$Gr \equiv \frac{g\beta\Delta T d^3}{\nu^2} \quad (131)$$

$$Gr_m = Gr_p \Leftrightarrow \left(\frac{g\beta\Delta T d^3}{\nu^2}\right)_m = \left(\frac{g\beta\Delta T d^3}{\nu^2}\right)_p \Leftrightarrow \left(\frac{d_m}{d_p}\right)^3 = \left(\frac{\beta_p \Delta T_p}{\beta_m \Delta T_m}\right)\left(\frac{\nu_m}{\nu_p}\right)^2 \quad (132)$$

Correlations for mixed convection are commonly in the form of Gr/Re or Gr/Re^2, while for natural convection they are in the form of Gr. From Eq. (132), matching of the Grashof number may be split into separate matching of scaling parameters for temperature difference ratio and length scale ratio:

$$\frac{\Delta T_m}{\Delta T_p} = \frac{\beta_p}{\beta_m} \tag{133}$$

$$\frac{d_m}{d_p} = \left(\frac{\nu_m}{\nu_p}\right)^{2/3} = \left(\frac{\rho_p}{\rho_m}\frac{\mu_m}{\mu_p}\right)^{2/3} \tag{134}$$

Note that the scaling in Eq. (134) to match Grashof number is identical to the scaling in Eq. (135) that matches Reynolds and Froude number simultaneously. Thus as noted by Bardet and Peterson (Reference 25), when temperature differences are scaled according to Eq. (133) scaled experiments can simultaneously match the Prandtl, Reynolds, Grashof, and Froude numbers to reproduce natural convection, mixed convection, and forced convection heat transfer phenomena. Additionally, the Rayleigh number ($Ra = GrPr$) associated with buoyancy-driven flow is also matched, and for mixed momentum/buoyancy-driven flows, the Richardson number ($Ri = Gr/Re^2$), which quantifies the relative intensity of either driving force, is also matched.

4.3 CONJUGATE HEAT TRANSFER WITH SOLID STRUCTURES

[[

]]

[[

]]

[[

]]

4.4 CHANNEL FLOW EXPERIMENTS

Channel flow phenomena with molten salts is defined by laminar, transitional, or turbulent regimes of flow. Flows in channels can be driven by a pump under forced circulation, or by buoyancy forces under natural circulation. Characterization of such regimes in scaled experiments may be particularly important to replicate and investigate flow dynamics phenomena in modules/components of the KP-FHR PHTS such as hot and cold leg piping. The Reynolds number is the key parameter prescriptive of these regimes:

$$Re \equiv \frac{\rho u D}{\mu} \tag{143}$$

for a channel of hydraulic diameter D.

If an analyst or designer is attempting to observe behavior in PHTS piping in a scaled experiment with a different working fluid, the following relationship is used for guidance of the design of an experiment as a ratio of the scaled over the prototypical conditions:

$$Re_m = Re_p \Leftrightarrow \frac{\rho_m u_m D_m}{\mu_m} = \frac{\rho_p u_p D_p}{\mu_p} \Leftrightarrow \frac{u_m}{u_p} = \frac{\rho_p}{\rho_m}\frac{\mu_m}{\mu_p}\frac{D_p}{D_m} \tag{144}$$

Equation (144) provides the following: if the prototypical fluid and process conditions, diameter and reference velocity are known, the analyst or designer has freedom of selecting two out of three parameters between surrogate fluid, piping diameter and reference velocity for the scaled experiment.

Using scaled velocities, the analyst or designer may determine pumping power requirements for pipe flow experiments with the following equation:

$$P = \Delta pQ = \frac{1}{2} f \frac{l_{pipe}}{D} \rho u^3 \frac{\pi}{4} D^2 = \frac{\pi}{8} f l_{pipe} \rho u^3 D \tag{145}$$

This requires the analyst or designer to determine the friction factor f using appropriate empirical correlations (see Eqs. (172) and (173) for laminar and turbulent flow, respectively), and appropriate piping length.

4.5 TWISTED ELLIPTICAL TUBE EXPERIMENTS

Flow dynamics and heat transfer phenomena on the tube and shell sides of twisted elliptical tube bundles may be relevant to KP-FHR IHX design configuration. Early investigations into twisted elliptical tube heat exchangers were performed almost four decades ago, showing good promise to reduce heat exchanger volume and helping to alleviate some of the challenges associated with fouling. Since that time, the technology has been commercialized in a number of variations, with a handful of companies across the globe manufacturing several similar products. For KP-FHR, the application of twisted elliptical tube [[

]] However, the specifics of the tube geometry vary from company to company, and correlations in the literature show a large range of predicted performance. In addition, there are multiple parameters in the tube geometry that can be optimized for a specific application. By performing its own experiments, Kairos Power can confirm performance for its specific thermal-fluids conditions where literature-reported correlations are widely varying and narrow down the optimal tube parameter range for its application. The use of simulant fluids enables Kairos Power to perform these experiments at reduced cost and with higher fidelity instrumentation.

The flow in twisted elliptical tubes is described by the Reynolds number based on the hydraulic diameter of the tube or shell side:

$$Re_D \equiv \frac{\rho u D}{\mu} \tag{146}$$

The geometric features that characterize a twisted elliptical tube are shown in Figure 9 and Figure 10. Twisting of the tube is characterized by a twist pitch shown in Figure 9, usually denoted as s. The cross-section of the twisted tube is characterized by the maximum and minimum diameters of the elliptic tube, on both inner and outer surfaces of the tube, as shown in Figure 10.

Geometric scaling of the twisted elliptical tube is based on the aspect ratio of the cross-section, the twist or torsional pitch ratio, and the modified Froude number. The aspect ratio of the cross-section is defined as:

$$XS - AR \equiv \frac{D_{min,in\ or\ out}}{D_{max,in\ or\ out}} \tag{147}$$

The twist or torsional pitch ratio is defined as:

$$Twist\ Pitch\ Ratio \equiv \frac{s}{D_{max,in\ or\ out}} \tag{148}$$

The modified Froude number is an indication of the flow swirling based on the geometry of the shell side of the tube. It is defined as:

$$Fr_m \equiv \frac{s^2}{D_{max,out} D_{h,shell}} \tag{149}$$

The shell side hydraulic diameter $D_{h,shell}$ is determined based on either the unit cell or realistic bundle geometries.

Velocity scaling results from matching of the Reynolds number (Eq. (146)) between the prototype and scaled model:

$$Re_m = Re_p \Leftrightarrow \frac{\rho_m u_m D_m}{\mu_m} = \frac{\rho_p u_p D_p}{\mu_p} \Leftrightarrow \frac{u_m}{u_p} = \frac{\rho_p}{\rho_m}\frac{\mu_m}{\mu_p}\frac{D_p}{D_m} \tag{150}$$

[[

]]

[[ ]] (155)

For characterization of forced convective heat transfer, following appropriate convective heat transfer guidance from Section 4.2, Prandtl number must be matched between the prototype and scaled experiment on both shell and tube side (see Eq. (130)).

Similitude criteria to preserve flow and heat transfer characteristics between the prototype and scaled experiment are summarized in Table 9. In summary, the following steps may be followed to design a scaled system for twisted elliptical tube flow and heat transfer experiments:

1. [[

]]

4.6 PEBBLE BED FLOW AND FUEL ELEMENT DYNAMICS EXPERIMENTS

The fluid dynamics for pebble buoyancy in a stagnant fluid are important for behavior involving pebble movement in the KP-FHR, including introduction and extraction of fuel pebbles to/from a control volume without coolant flow. In order to determine the required density of the pebble and appropriate material used in a scaled experiment, a force balance on the pebble in stagnant liquid using a free body diagram is done (Figure 11).

The force balance at equilibrium may be expressed using the following relationship:

$$W_{pebble} = F_{buoyancy} \Leftrightarrow \rho_{pebble} V_{pebble} g = \rho_f V_{sub} g \quad (156)$$

where W_{pebble} is the weight of the pebble, $F_{buoyancy}$ buoyancy force, ρ_{pebble} density of the pebble, V_{pebble} volume of the pebble, and V_{sub} submerged volume of the pebble.

Equation (156)(156) may be rearranged into the ratio of the density of the pebble over the density of the fluid, referred to as relative density or specific gravity SG. For a specific gravity larger than one, the pebble will sink into the fluid whereas for a specific gravity smaller than one, the pebble will float upwards until it is partially submerged.

$$SG = \frac{\rho_{pebble}}{\rho_{fluid}} = \frac{V_{sub}}{V_{pebble}} \quad (157)$$

By matching the specific gravity of pebble material in a scaled experiment, based on the surrogate fluid used in the experiment (e.g., water), the static behavior of pebbles in the coolant is preserved:

$$SG_m = SG_p \Leftrightarrow \frac{\rho_{pebble,m}}{\rho_{pebble,p}} = \frac{\rho_{fluid,m}}{\rho_{fluid,p}} \tag{158}$$

In the case of a pebble or pebbles immersed in a moving fluid, such as the KP-FHR reactor core with a moving packed bed of pebbles and coolant flowing around the pebbles, as indicated in Section 4.1, the Reynolds and Froude numbers must be matched in addition to specific gravity. The Reynolds and Froude numbers use the diameter of a pebble D_{pebble} as the characteristic length. Matching of both non-dimensional numbers allows the analyst/designer to determine the appropriate pebble diameter, flow velocity, and fluid properties in the scaled experiment. The same derivation as 4.1 yields:

$$\frac{D_{pebble,m}}{D_{pebble,p}} = \left(\frac{\rho_{f,p}}{\rho_{f,m}}\frac{\mu_{f,m}}{\mu_{f,p}}\right)^{2/3} \tag{159}$$

$$\frac{u_{f,m}}{u_{f,p}} = \left(\frac{\rho_{f,p}}{\rho_{f,m}}\frac{\mu_{f,m}}{\mu_{f,p}}\right)^{1/3} \tag{160}$$

Equations (157), (159), and (160) provide the appropriate scaling parameters to design an experiment to appropriately scale the inertial, viscous, and buoyancy forces from prototypical conditions, and therefore replicate flow and pebble bed dynamics applicable to the KP-FHR core.

In summary, the following steps may be followed to design a scaled system for pebble bed flow and fuel element dynamics:

1. [[

]]

Assuming the model pebble density is constant with temperature, it may be necessary to take the average SG-matched model pebble density across the temperature range of interest as the true model pebble density and quantify distortions in the SG ratio at the extreme ends of the temperature range.

This scaling approach is illustrated with physical parameters in Table 10. In particular, at [[ ]] geometric scale and [[ ]] velocity scale, pebble bed flow and fuel element dynamics may be investigated using polypropylene spheres (average density of 880 kg/m^3) in 20°C water to simulate KP-

FHR fuel elements in 600°C Flibe. Note that Table 10 is listed for illustrative purposes only and values do not represent the final design of the KP-FHR.

4.7 POROUS MEDIA OR PACKED BED EXPERIMENTS

Flow dynamics and heat transfer in a packed bed or other porous media are important to investigate temperature distribution in key KP-FHR modules/components such as the reactor pebble bed core to close heat transfer coefficient relationships developed in Section 3. Packed bed reactors have been investigated for chemical engineering and nuclear engineering applications. Despite the significant scale difference between the two fields, thermal-fluids characteristics such as pressure drop, heat transfer and species transport are key factors in both fields. Most correlations found in the literature for packed bed phenomena are based on experimental data using air- or water-cooled systems over a limited range of Reynolds numbers, flow regimes (forced convection/mixed or free convection), and pebble bed packing fractions. For applications in the nuclear industry, most experience with packed bed reactors has been focused on gas-cooled reactor designs, and applicable heat transfer and pressure drop correlations have been developed (e.g., KTA correlation for pressure drop). While the Reynolds number range applicable to gas-cooled reactors covers the range applicable to KP-FHR, which allows Kairos Power to use available pressure drop correlations, heat transfer correlations developed for gas-cooled reactor applications are out of the applicable range for KP-FHR, due to the high Prandtl number of KP-FHR coolant, Flibe. Therefore, new heat transfer correlations must be developed for different flow regimes and Reynolds number ranges applicable to KP-FHR, which will feed into Preliminary and Final Safety Analysis Reports ("Standard Review Plan for the Review of Safety Analysis Reports for Nuclear Power Plants, Chapter 4 and 15"). These correlations will be obtained using scaled SET experiments and will serve as inputs for future porous media analyses, to model convective heat transfer from solid phase (fuel pebbles) to liquid phase (Flibe coolant) in the KP-FHR core.

Note that such experiments would not cover conductive heat transfer inside fuel elements, which may be easily modeled knowing fuel geometry and thermal conductivity of fuel constituents. Instead, for scaled SETs investigating packed bed flow and heat transfer, high thermal conductivity materials (e.g., copper) may be used and pebbles may be treated as lumped capacitances (see Section 4.3).

In order to appropriately model the porous media behavior in a scaled experiment, the porosity of the media needs to be matched between the prototype and scaled experiment. Porosity is defined as the ratio between void space volume (i.e., liquid volume in KP-FHR reactor core) and total bulk volume of the region, which includes both solid and void. For beds of randomly packed spheres of uniform diameter, porosity may vary between 0.2595 (associated with rhombohedral packing) and 0.4764 (associated with cubic packing) (Reference 26).

$$\varphi \equiv \frac{V_{void}}{V_{tot}} \tag{161}$$

where φ is porosity, V_{void} void volume and V_{tot} total volume.

A cylindrical packed bed is a usual geometry found in pebble bed reactor types – including the reference KP-FHR reactor core design – with a defined diameter (D_{vol}), height (H_{vol}) and pebble diameter (D_{pebble}). The volume of the cylinder is calculated using ($V_{cylinder} = \frac{\pi D_{vol}^2 H_{vol}}{4}$) and the volume of each

sphere is calculated using $V_{pebble} = \frac{\pi D_{pebble}^3}{6}$. Porosity may be calculated for a cylindrical packed bed using both volumes:

$$\varphi = \frac{V_{void}}{V_{tot}} = \frac{V_{cylinder} - N_{pebble} V_{pebble}}{V_{cylinder}} = 1 - \frac{2}{3} N_{pebble} \frac{D_{pebble}^3}{H_{vol} D_{vol}^2} \tag{162}$$

where N_{pebble} is the number of pebbles in the packed bed.

Permeability of the porous media is usually dependent on porosity and diameter of the "pores," or pebbles in the case of a pebble bed. Permeability is expressed as:

$$K \equiv \frac{\varphi^3 D_{pebble}^2}{A(1-\varphi)^2} \tag{163}$$

where K is permeability and A is a constant. The value of A commonly found in the literature in the case of randomly packed beds, such as the KP-FHR core, is 180 (Reference 26).

For characterization of forced convective heat transfer in a packed bed, following appropriate heat transfer guidance from Section 4.2, Reynolds and Prandtl numbers must be matched between the prototype and scaled experiment. Prandtl number, as seen in Eq. (130) (repeated below as Eq. (164)), only depends on fluid properties that are solely temperature-dependent. Therefore, Prandtl number may be matched between prototype and scaled experiment by selecting an appropriate surrogate fluid and adjusting the fluid average temperature and temperature bounds for the process fluid. Once temperature range is known based on desired Prandtl number range, thermophysical properties of the fluid – density and viscosity in particular – are known:

$$Pr_m = Pr_p \Leftrightarrow \left(\frac{c_p \mu}{k}\right)_m = \left(\frac{c_p \mu}{k}\right)_p \tag{164}$$

Reynolds number for porous media flow is defined using either the pebble diameter D_{pebble} or square root of permeability K as characteristic length:

$$\begin{aligned} Re_{D_{pebble}} &\equiv \frac{\rho_f u D_{pebble}}{\mu_f} \\ Re_K &\equiv \frac{\rho_f u K^{1/2}}{\mu_f} \end{aligned} \tag{165}$$

The fluid velocity u in Eq. (165) is the superficial velocity, or equivalent velocity in the total volume without pebbles:

$$u = \frac{\dot{m}}{\rho_f A_{vol}} \tag{166}$$

where $\dot{m}$ is the fluid mass flow rate in the volume and A_{vol} the cross-sectional area of the volume, which in the case of a cylinder mentioned above is expressed as:

$$A_{vol} = \frac{\pi D_{vol}^2}{4} \tag{167}$$

In the case of a packed bed with a significant number of pebbles, the ratio of pebble diameter to diameter of the channel, duct, or generic volume should be maintained between the prototype and scaled experiment if possible:

$$\left(\frac{D_{pebble}}{D_{vol}}\right)_m = \left(\frac{D_{pebble}}{D_{vol}}\right)_p \tag{168}$$

At a minimum, when scaling to a large bed where wall effects are minimal, $\frac{D_{vol}}{D_{pebble}}$ in the scaled experiment should be larger than 15 to reduce impact of the walls on void fraction or porosity (Reference 27).

From Eq. (162), matching of porosity between the scaled experiment and prototype yields:

$$\varphi_m = \varphi_p \Leftrightarrow \frac{D_{pebble,m}}{D_{pebble,p}} = \left(\frac{D_{vol,m}}{D_{vol,p}}\right)^{2/3} \left(\frac{N_{pebble,p}}{N_{pebble,m}} \frac{H_{vol,m}}{H_{vol,p}}\right)^{1/3} \tag{169}$$

Substituting Eq. (168) into Eq. (169) yields a relationship between ratios of pebble diameter, number of pebbles and height of the volume:

$$\frac{N_{pebble,m}}{N_{pebble,p}} \frac{D_{pebble,m}}{D_{pebble,p}} = \frac{H_{vol,m}}{H_{vol,p}} \tag{170}$$

The superficial velocity ratio between the prototype and scaled experiment is determined by matching Reynolds number between the two systems, using Eq. (165). The ratio is a function of both fluid properties and pebble diameter as follows:

$$\frac{u_m}{u_p} = \left(\frac{\rho_p}{\rho_m} \frac{\mu_m}{\mu_p}\right) \left(\frac{D_{pebble,p}}{D_{pebble,m}}\right) \tag{171}$$

In summary, the following steps may be followed to design a scaled system for packed bed flow and heat transfer experiments:

1. [[

]]

This scaling approach is illustrated with physical parameters in Table 11. In particular, at [[ ]] geometric scale and [[ ]] velocity scale, packed bed flow and heat transfer may be investigated using copper spheres (high thermal conductivity) in 73°C heat transfer oil to simulate KP-FHR fuel elements in 600°C Flibe. Note that most numbers are listed for illustrative purposes only and may evolve with the final design of the KP-FHR.

5 USE OF SURROGATE FLUIDS IN SCALED EXPERIMENTS

The use of surrogate fluids in scaled experimental activities is critical to the research and development of novel thermal-fluids systems such as the KP-FHR. One of the main motivations is that surrogate fluids allow the investigation of relevant fluid and heat transfer phenomena at significantly smaller scale and required resources, which enables the realization of Kairos Power's rapid analysis, prototyping and iterative design cycle while providing high-quality data for safety analysis code validation. The use of surrogate fluids enables direct and comprehensive measurements of the phenomena under investigation due to the higher compatibility of instrumentation (temperature, velocity, and other measurements) in surrogate fluids vs. prototypical molten salts at high temperatures (molten salts in the context of this section refers to clean salt coolant, where the thermophysical properties are not expected to change throughout the lifetime of the reactor). This ensures Kairos Power is able to appropriately inform the scaling, safety analysis, and code validation efforts required for design and licensing activities.

For molten salts, the working requirements involve higher temperature operation (> 460°C for Flibe), high power demand, and the difficulty and hazards of working with molten salts, which are strong motivations for using surrogate fluids. Fortunately, for both SETs and IETs, surrogate fluids have been shown to match relevant scaling parameters with reduced power, temperature and size requirements without these associated difficulties (Reference 25). This enables scaled experiments in fluids such as air, water, and heat transfer oil before testing with the molten salt of choice, depending on the physics of interest being investigated. Ultimately, this should enable the motivations suggested earlier and reduce the resources needed to develop the KP-FHR in an expedited fashion while maintaining a safe and consistent approach.

5.1 HISTORICAL USE OF SURROGATE FLUIDS IN SCALED EXPERIMENTS

Surrogate fluids have been used extensively in past and current experimental efforts for nuclear reactor development in both single- and multi-phase flow systems. For light water reactors and two-phase systems in general, refrigerants have been used extensively for scaled experiments instead of water due to lower power, temperature and pressure requirements, as discussed by Yadigaroglu and Zeller (Reference 28) and recently by Estrada-Perez et al. (Reference 29). For liquid metal reactors, fluid dynamics and heat transfer involving measurements of heat transfer, pressure drop, and liquid-gas interfaces has been investigated using air, water, or p-Cymene for regimes of flow where the Reynolds, Peclet, Richardson, or Froude numbers are matching (References 30 and 31).

Scaling of an integral natural convection residual heat removal facility for a liquid metal-cooled reactor has also been done using water, although significant distortions were observed, which need to be considered in the design and subsequent use for safety analysis (Reference 32). In this case, distortions appear when attempting to simultaneously match the Reynolds or Peclet numbers and the Richardson number when buoyancy is considered for sodium. Conversely, as supported by analysis in this report, scaling of Flibe to water for hydrodynamic tests, and to heat transfer oil for heat transfer tests only introduces very minor distortions.

For reactor systems involving the molten salt Flibe, water has been shown to match Reynolds and Froude numbers, with moderate distortion of the Weber number, for investigating behavior of oscillating Flibe sheet jets for use in a fusion reactor (Reference 33). For FHRs, the pebble and fluid dynamic behavior of graphite pebbles in Flibe salt at different temperatures have been shown to scale to polypropylene spheres in water at 20°C (Reference 34). The Reynolds number (using superficial velocity and pebble

diameter as characteristic velocity and length, respectively), Froude number, and pebble-fluid density ratio may match with minor distortions, resulting in minor distortions for pebble drag to buoyancy force ratio over a relevant range of flow conditions, as discussed in further detail in Section 4.6.

Similarly, the behavior and proof of concept of thermal-buoyancy-driven shutdown rod insertion in FHRs were investigated by matching the Froude and Reynolds numbers of water to Flibe and using the addition of sugar to modify the water density to match the density change associated with temperature change in Flibe. The desired specific gravity ratio of the simulated shutdown rod to sugar water was matched as well to ensure applicability to a potential prototype (Reference 35). In the case of mass transfer for use in tritium management, a mixture of water and glycerol has been shown to match Flibe for the Schmidt number (Reference 36). This was done to analyze the impact of ultrasonic horns on gas sparging to maximize tritium removal.

The overall system behavior of a generic FHR has been investigated using DOWTHERM™ A in a compact IET (CIET) at UC Berkeley for forced and natural circulation during simulated transients (Reference 22). Lastly, the flow behavior of fluidic diodes in a passive safety system for FHRs has been investigated in isothermal experiments with and without buoyancy effects. For the experiment without buoyancy effects, water and DOWTHERM™ A were used to match the Reynolds number, Euler number, and diodicity to Flibe in a fluidic diode (Reference 37). For an experimental concept involving bulk buoyancy effects, the DirEX^2 fluidic diode concept was investigated using water and sugar water. The water and sugar water were able to match the Reynolds number and specific gravity ratio of hot and cold Flibe (Reference 38). The referenced literature provides a supporting basis for using surrogate fluids in place of Flibe for scaled experimental efforts involving design, development, and licensing efforts.

5.2 APPLICATION OF SURROGATE FLUIDS FOR MOLTEN SALTS TOP-DOWN SCALING ANALYSIS

In order to show the direct scaling of different fluids to liquid fluoride salts, Bardet and Peterson discussed the matching of the Reynolds, Froude, Prandtl, and Grashof numbers of Flibe at 600°C or FLiNaK at 700°C to specific heat transfer oils such as DOWTHERM™ A (from Dow Chemical) or Therminol® VP-1 (from Eastman) heated to 80°C (Reference 25). Supporting the motivation in the opening paragraphs of Section 5, heat transfer oil allows for significantly smaller length, velocity, and temperature scaling ratios compared to Flibe for use in experimental efforts involving both forced and natural circulation heat transfer phenomena. This also enables testing activities for both IETs and SETs to occur at significantly reduced pumping and heating powers using heat transfer oil based on Bardet's and Peterson's calculations (Reference 25).

For illustration, the prototypical fluid specific to the KP-FHR PHTS, Flibe, is compared to the surrogate heat transfer oil in Table 12, at average operating temperatures, in order to simultaneously match Reynolds, Prandtl, Grashof and Froude numbers.

5.3 DISTORTIONS BETWEEN MOLTEN SALTS AND SURROGATE FLUIDS

Distortions must be quantified between molten salt and surrogate fluid systems, due to constraints of designing and constructing scaled experiments, and complexity of the physics and systems being investigated. Such distortions are balanced by the much higher precision of experimental measurements possible with lower-temperature surrogate fluids. Scaling distortions resulting from use of surrogate fluids may be captured in terms of the characteristic time ratios, as described in Section 2.3 and illustrated in Section 3.4.5 for a scaled IET.

Radiative heat transfer in the KP-FHR will also introduce distortions when scaling down to a surrogate fluid system using heat transfer oil or water, due to lower temperature operating conditions as compared to prototypical operating temperatures. The impact of these distortions is expected to be more significant for laminar, forced and natural convective flows, due to the lower convective heat transfer for these flow regimes. For turbulent flow regimes, heat transfer due to convection is significantly higher and radiative heat transfer may be neglected. In both cases, distortions between the prototype and scaled system will be quantified when designing scaled IETs.

5.4 MATCHING OF PRANDTL NUMBER USING SURROGATE FLUIDS

The general process of matching non-dimensional groups of a prototypical system using surrogate fluids is based on the desired operating temperature range of the KP-FHR. The KP-FHR PHTS uses Flibe coolant between 550°C and 650°C during normal operations. For an appropriate surrogate fluid to be used, the difference between the average Prandtl number of Flibe in the KP-FHR PHTS and the average Prandtl number of a surrogate fluid such as heat transfer oil should be minimized. The temperature range of the surrogate fluid is selected to cover the same range of Prandtl numbers as Flibe in the prototype. Distortion factors between the Prandtl numbers at each temperature may be calculated using Eq. (10). Based on the Prandtl number ranges and distortions, the heat transfer oil temperature range may be varied until distortions are minimized. This process is summarized in the following steps:

1. [[

]]

The matching of Prandtl number for Flibe against heat transfer oil is shown in Figure 12 for prototypical temperature ranges of Flibe in the KP-FHR PHTS during both normal and off-normal operations, and lab-suitable temperature ranges for heat transfer oil. Operating temperatures for heat transfer oil are selected so that Prandtl number exactly matches that of prototypical salt at the average operating temperature of 600°C during normal operations. From the figure, the Prandtl numbers match over the majority of the temperature ranges with reasonably low distortions. Distortion factors range from +5.6% at the lower end of the temperature range to -21.1% at the upper end of the temperature range. This supports the use of heat transfer oil for SETs or IETs operating over this range of Prandtl numbers as a surrogate for Flibe.

5.5 MATCHING OF FLOW DYNAMICS BEHAVIOR USING SURROGATE FLUIDS

Matching of flow behavior between surrogate fluids and molten salts in SETs is illustrated through the friction factor used to calculate pressure drop in prototypical piping. The friction factor usually depends on the non-dimensional Reynolds number, and pipe surface roughness. This places two degrees of freedom to ensure friction factor is matched, but only friction factors based on the Reynolds number are considered for this derivation. The pipe roughness is considered to be similar, since experiments of this type will be using similar variants of stainless steel for both the prototype and scaled experiments.

Darcy friction factor as a function of Reynolds number is shown for water, heat transfer oil, Flibe and solar salt in Figure 13, based on correlations listed in Section A.1. The different working fluids are at different temperatures within the expected range of operating conditions for the KP-FHR and lab experiments. The KP-FHR is expected to experience laminar, transitional, and turbulent regimes of flow. However, because friction factor correlations only depend on Reynolds number, friction factors are matched with no distortions if Reynolds number is matched (all curves superimposed in Figure 13).

This capability to match friction factor with no distortions through matching of Reynolds number implies that for hydrodynamic phenomena investigated through SETs, a variety of fluids, including room-temperature water, may be used as surrogates for salts with very minimal distortions for expected KP-FHR conditions. It is important to note that this approach, while valid for SETs, may be more challenging to implement for many components in reduced area IETs, as further discussed in Section 3.

5.6 MATCHING OF HEAT TRANSFER BEHAVIOR USING SURROGATE FLUIDS

Heat transfer behavior is characterized by the Nusselt number, which may be calculated for water, heat transfer oil, Flibe and solar salt systems at different temperature points. The Nusselt number is used in calculating heat transfer coefficients in components such as the reactor core and IHX and depends on the Reynolds and Prandtl numbers in forced convection situations. Figure 14 shows Nusselt number for a range of Reynolds numbers between 2,300 and $5x10^6$ using the Gnielinski correlation (Eq. (175)) found in Todreas & Kazimi as an illustration (Reference 39).

Because of the dependence of Nusselt number on Reynolds and Prandtl numbers only in this case (Eq. (175)), and because both Reynolds and Prandtl numbers may be matched with minimal distortions as explained in Sections 5.4 and 5.5, the distortions in Nusselt numbers for each of the fluid pairs (heat transfer oil to Flibe and water to solar salt) are shown to be minimal, except for water at 72.5°C matching solar salt above ~610°C, due to larger distortions in Prandtl number for these conditions (illustrated in Figure 14). The other three fluid pairs exhibit less than 1% distortion over the entire range of Reynolds numbers experienced in the KP-FHR. The fluid pair of water at 72.5°C and solar salt above ~610°C has significant distortions that need to be avoided if possible. This may be partly due to the extrapolation of fluid thermophysical properties for solar salt above 600°C, however it is not expected that the salt will reach higher temperatures in the KP-FHR IHTS.

This capability to match Nusselt number with minimal distortions through matching of Prandtl and Reynolds numbers implies that for heat transfer phenomena investigated through SETs, a select set of fluids may be used as surrogates for salts with minimal distortions for expected KP-FHR conditions. Similar to flow dynamics behavior scaling illustrated in Section 5.5, it is important to note that this approach, while valid for SETs, may be more challenging to implement for many components in reduced area IETs, as further discussed in Section 3.

6 CONCLUSIONS

This report presents the H2TS methodology selected for Kairos Power scaling efforts that will be applied to IETs for system level testing and SETs for component and phenomenon level testing. The scaling methodology for thermal-fluids IETs that will model the KP-FHR PHTS under normal operations and transient condition was detailed in Section 3. The methodology was also presented for a comprehensive set of SETs for phenomena and component level tests in Section 4. Section 5 described the scalable surrogate fluids that can be used for Flibe in IETs and SETs.

Kairos Power is requesting NRC review and approval to use the scaling methodology as described in Section 3 and Section 4 along with the use of heat transfer oil and water as surrogate fluids for Flibe as described in Section 5 of this report for testing included in the assessment base of evaluation models supporting KP-FHR safety analysis required by 10 CFR 50.34 (a)(4), 10 CFR 50.34(b)(4), 10 CFR 52.47(a)(4), 10 CFR 52.79(a)(5), 10 CFR 52.137(a)(4), or 10 CFR 52.157(f)(1).

7 REFERENCES

1. Andreades, C., Cisneros, A. T., Choi, J. K., Chong, A. Y. K., Fratoni, M., Hong, S., … Zweibaum, N. (2016). Design Summary of the Mark-I Pebble-Bed, Fluoride Salt–Cooled, High-Temperature Reactor Commercial Power Plant. Nuclear Technology, 195(3), 223-238.
2. Kairos Power LLC, "Design Overview of the Kairos Power Fluoride Salt Cooled, High Temperature Reactor (KP-FHR)", KP-TR-001, November 2018.
3. Kairos Power LLC, "Testing and Development Program Overview for the Kairos Power Fluoride Salt Cooled, High Temperature Reactor", KP-TR-002, November 2018.
4. Kairos Power LLC, "Regulatory Analysis for the Kairos Power Fluoride Salt-Cooled, High Temperature Reactor", KP-TR-004, January 2019.
5. US Nuclear Regulatory Commission, "Severe Accident Research Program Plan Update", NUREG-1365, Revision 1, December 1992.
6. US Nuclear Regulatory Commission, "An Integrated Structure and Scaling Methodology for Severe Accident Technical Issue Resolution", NUREG/CR-5809, Draft Report, November 1991.
7. Zuber, N., Wilson, G. E., Ishii, M., Wulff, W., Boyack, B. E., Dukler, A. E., … Valente, J. (1998). An Integrated Structure and Scaling Methodology for Severe Accident Technical Issue Resolution: Development of Methodology. Nuclear Engineering and Design, 186(1), 1-21.
8. Reyes, J. N., & Hochreiter, L. (1998). Scaling Analysis for the OSU AP600 Test Facility (APEX). Nuclear Engineering and Design, 186(1), 53-109.
9. Reyes, J. N. (2001). Scaling Analysis for the OSU APEX-CE Integral System Test Facility. Washington DC: U.S. Nuclear Regulatory Commission.
10. Reyes, J. N., Groome, J. T., Woods, B. G., Jackson, B., & Marshall, T. D. (2010). Scaling Analysis for the High Temperature Gas Reactor Test Section (GRTS). Nuclear Engineering and Design, 240(2), 397-404.
11. Arcilesi, D. J., Ham, T. K., Kim, I. H., Sun, X., Christensen, R. N., & Oh, C. H. (2015). Scaling and Design Analyses of a Scaled-Down, High-Temperature Test Facility for Experimental Investigation of the Initial Stages of a VHTR Air-Ingress Accident. Nuclear Engineering and Design, 288, 141-162.
12. Graves, J. D. (2012). Top-Down Scaling Analysis of the Integral Reactor Vessel Test Facility. Corvallis, OR: Oregon State University.
13. Peterson, P. F., Schrock, V. E., & Greif, R. (1998). Scaling for Integral Simulation of Mixing in Large, Stratified Volumes. Nuclear Engineering and Design, 186(1), 213-224.
14. Zuber, N., Rohatgi, U. S., Wulff, W., & Catton, I. (2007). Application of fractional scaling analysis (FSA) to loss of coolant accidents (LOCA) - Methodology development. Nuclear Engineering and Design, 237, 1593-1607.
15. Huddar, L., Kendrick, J. C., Poresky, C., Wang, X., & Peterson, P. F. (2018). Application of Frequency Response Methods in Separate and Integral Effects Tests for Molten Salt Cooled and Fueled Reactors. Nuclear Engineering and Design, 329, 3-11.

16. Zuber, N., Wulff, W., Rohatgi, U. S., & Catton, I. (2005). Application of fractional scaling analysis (FSA) to loss of coolant accidents (LOCA). Proceedings of the 11th International Topical Meeting on Nuclear Reactor Thermal-Hydraulics (NURETH-11). Avignon, France.
17. Levy, S. (1999). Two-Phase Flow in Complex Systems. John Wiley & Sons.
18. Scarlat, R. O., Laufer, M. R., Blandford, E. D., Zweibaum, N., Krumwiede, D. L., Cisneros, A. T., … Peterson, P. F. (2014). Design and Licensing Strategies for the Fluoride-Salt-Cooled, High-Temperature Reactor (FHR) Technology. Progress in Nuclear Energy, 77, 406-420.
19. Crawford, J. D., & Knobloch, E. (1991). Symmetry and Symmetry-Breaking Bifurcations in Fluid Dynamics. Annual Review of Fluid Mechanics, 23, 341-387.
20. Vijayan, P. K. (2002). Experimental Observations on the General Trends of the Steady State and Stability Behaviour of Single-Phase Natural Circulation Loops. Nuclear Engineering and Design, 215(1), 139-152.
21. Lv, Q., Wang, X., Kim, I. H., Sun, X., Christensen, R. N., Blue, T. E., … Sabharwall, P. (2015). Scaling Analysis for the Direct Reactor Auxiliary Cooling System for FHRs. Nuclear Engineering and Design, 285, 197-206.
22. Zweibaum, N., Guo, Z., Kendrick, J. C., & Peterson, P. F. (2016). Design of the Compact Integral Effects Test Facility and Validation of Best-Estimate Models for Fluoride Salt–Cooled High-Temperature Reactors. Nuclear Technology, 196(3), 641-660.
23. Gebhart, B., Jaluria, Y., Mahajan, R., & Sammakia, B. (1988). Buoyancy-Induced Flows and Transport. CRC Press.
24. Bejan, A. (2013). Convection Heat Transfer, Fourth Edition. Wiley & Sons.
25. Bardet, P. M., & Peterson, P. F. (2008). Options for Scaled Experiments for High Temperature Liquid Salt and Helium Fluid Mechanics and Convective Heat Transfer. Nuclear Technology, 163(3), 344-357.
26. Nield, D. A., & Bejan, A. (2006). Convection in Porous Media. New York: Springer-Verlag.
27. Yoder, G. L., Aaron, A., Cunningham, B., Fugate, D., Holcomb, D., Kisner, R., … Wilson, D. (2014). An Experimental Test Facility to Support Development of the Fluoride-Salt-Cooled High-Temperature Reactor. Annals of Nuclear Energy, 64, 511-517.
28. Yadigaroglu, G., & Zeller, M. (1994). Fluid-to-Fluid Scaling for a Gravity- and Flashing-Driven Natural Circulation Loop. Nuclear Engineering and Design, 151(1), 49-64.
29. Estrada-Pérez, C. E., Hassan, Y. A., Alkhudhiri, B., & Yoo, J. (2018). Time-Resolved Measurements of Liquid–Vapor Thermal Interactions throughout the Full Life-Cycle of Sliding Bubbles at Subcooled Flow Boiling Conditions. International Journal of Multiphase Flow, 99, 94-110.
30. Moriya, S., & Ohshima, I. (1990). Hydraulic Similarity in the Temperature Fluctuation Phenomena of Non-Isothermal Coaxial Jets. Nuclear Engineering and Design, 120(2), 385-393.
31. Goth, N., Jones, P., Nguyen, T. D., Vaghetto, R., Hassan, Y., Salpeter, N., & Merzari, E. (2018). PTV/PIV Measurements of Turbulent Flows in Interior Subchannels of a 61-Pin Wire-Wrapped Hexagonal Fuel Bundle. International Journal of Heat and Fluid Flow, 71, 295-304.

32. Heisler, M. P. (1982). Development of Scaling Requirements for Natural Convection Liquid-Metal Fast Breeder Reactor Shutdown Heat Removal Test Facilities. Nuclear Science and Engineering, 80(3), 347-359.

33. Cavanaugh, C. J., & Peterson, P. F. (1994). Scaled Modeling of Oscillating Sheet Jets for the HYLIFE-II Inertial Confinement Fusion Reactor. Fusion Technology, 26, 917-921.

34. Zweibaum, N., Huddar, L., Hughes, J., Laufer, M., Blandford, E., Scarlat, R., & Peterson, P. (2015). Role and Status of Scaled Experiments in the Development of Fluoride-Salt-Cooled, High-Temperature Reactors. International Congress on Advances in Nuclear Power Plants (ICAPP '15). Nice, France.

35. Blandford, E., & Peterson, P. F. (2013). A Buoyantly-Driven Shutdown Rod Concept for Passive Reactivity Control of a Fluoride Salt-Cooled High-Temperature Reactor. Nuclear Engineering and Design, 262, 600-610.

36. Rubio, F., Bond, L., & Blandford, E. (2017). Scaled Experiment Investigating Sonomechanically Enhanced Inert Gas Sparging Mass Transfer. Nuclear Engineering and Design, 324, 171-180.

37. Qu, S.-X., Wu, Y.-H., He, Z.-Z., & Chen, K. (2018). Surrogate Fluid Experimental Study and CFD Simulation on the Hydraulic Characteristics of Vortex Diode. Nuclear Science and Engineering, 189(3), 282-289.

38. Hughes, J. T., & Blandford, E. (2016). Experimental Investigation of a Directionally Enhanced DHX Concept for High Temperature Direct Reactor Auxiliary Cooling Systems. Nuclear Engineering and Design, 303, 132-152.

39. Todreas, N. E., & Kazimi, M. S. (1990). Nuclear Systems: Thermal Hydraulic Fundamentals. Hemisphere Pub. Corp.

40. Kairos Power LLC, “Reactor Coolant for the Kairos Power Fluoride Salt-Cooled High Temperature Reactor”, KP-TR-005, March 2019.

Table 1. Scaling Groups from Top-down and Bottom-up Scaling Analysis for Normal Operation of the KP-FHR PHTS.

Scaling Group	Expression	Material	Comments
Top-down scaling groups			
Π_{Eu}	$\frac{\Delta p_0}{\rho u_{ref}^2}$	Fluid	Loop Euler number (ratio of pump head to dynamic pressure in the fluid).
Π_{Ri}	$\frac{g\beta\Delta T_{loop} l_{HT}}{u_{ref}^2}$	Fluid	Loop Richardson number (ratio of buoyancy to momentum in the loop).
Π_F	$\sum_{j=1}^{N}\left[\frac{1}{2}\left(K_j + f_j\frac{l_j}{d_j}\right)\left(\frac{A_{ref}}{A_j}\right)^2\right]$	Fluid	Loop frictional and form losses.
$\Pi_{St,m-Rx}$	$\frac{\varepsilon_{Rx} h_{Rx} A_{s,Rx}\left(T_{si,Rx} - T_{f,Rx}\right)_0}{\rho u_{ref} A_{ref} c_{pf}(T_{H0} - T_{C0})}$	Fluid	Stanton number for the reactor core (ratio of heat transfer into the coolant to thermal capacity of the coolant).
$\Pi_{St,m-HX}$	$\frac{\varepsilon_{HX} U_{HX} A_{s,HX} \Delta T_{LMTD,0}}{\rho u_{ref} A_{ref} c_{pf}(T_{H0} - T_{C0})}$	Fluid	Stanton number for the IHX (ratio of heat transfer into the coolant to thermal capacity of the coolant).
Bottom-up scaling groups (for IHX)			
Π_{Re}	$\frac{\rho u d}{\mu}$	Fluid	Reynolds number for the IHX.
Π_{Pr}	$\frac{\nu}{\alpha}$	Fluid	Prandtl number of the fluid in the IHX.

Table 2. Scaling Groups from Top-down and Bottom-up Scaling Analysis for Natural Circulation in the KP-FHR PHTS.

Scaling Group	Expression	Material	Comments
Top-down scaling groups			
Π_G	$\sum_{j=1}^{N} \frac{l_j}{A_j} \frac{A_{ref}}{l_{ref}},$	Fluid	Parameter for power/volume and fluid residence time similarity.
$\Pi_{Ri,NC}$	$\frac{g\beta\Delta T_{loop} l_{HT}}{u_{ref,NC}^2}$	Fluid	Loop Richardson number (ratio of buoyancy to momentum in the loop).
Π_F	$\sum_{j=1}^{N} \left[\frac{1}{2}\left(K_j + f_j \frac{l_j}{d_j}\right)\left(\frac{A_{ref}}{A_j}\right)^2\right]$	Fluid	Loop frictional and form losses.
$\Pi_{St,m-Rx,NC}$	$\frac{\varepsilon_{Rx} h_{Rx} A_{s,Rx} \left(T_{si,Rx} - T_{f,Rx}\right)_0}{\rho u_{ref,NC} A_{ref} c_{pf} (T_{H0} - T_{C0})}$	Fluid	Stanton number for the reactor core (ratio of heat transfer into the coolant to thermal capacity of the coolant).
$\Pi_{St,m-HX,NC}$	$\frac{\varepsilon_{HX} U_{HX} A_{s,HX} \Delta T_{LMTD,0}}{\rho u_{ref,NC} A_{ref} c_{pf} (T_{H0} - T_{C0})}$	Fluid	Stanton number for the heat exchanger (ratio of heat transfer into the coolant to thermal capacity of the coolant).
Π_{HS}	$\frac{1}{m_f c_{pf}} \sum_{j=1}^{N} \left[\rho_{fj} c_{pfj} V_{CVj} + m_{sj} c_{psj}\right]$	Solid	Solid structures heat capacity number.
$\Pi_{Bi,HX}$	$\frac{h_{HX} l_{s,HX}}{k_{s,HX}}$	Solid	Biot number for the heat exchanger (ratio of convective heat transfer to conduction at solid/fluid boundary).
Bottom-up scaling groups (for heat exchanger)			
Π_{Re}	$\frac{\rho u d}{\mu}$	Fluid	Reynolds number for the heat exchanger.
Π_{Gr}	$\frac{g\beta(T_{H0} - T_{C0}) d^3}{\nu^2}$	Fluid	Grashof number for the heat exchanger.
Π_{Pr}	$\frac{\nu}{\alpha}$	Fluid	Prandtl number of the fluid in the heat exchanger.

Table 3. Summary of Dimensional Parameter Ratios and Resulting Scaling Groups for Normal Operation at the System Level.

Prototypical Fluid (Temperature)	Flibe (600°C)
Surrogate Fluid (Temperature)	Heat transfer oil (73°C)
Dimensional Parameter Ratios	
Length Ratio, $(l)_R$	1:2 [a]
Hydraulic Diameter Ratio, $(d)_R$	1:2 [a]
Area Ratio, $(A)_R$	1:4 [a]
Fluid Volume Ratio, $(V)_R$	1:8 [a]
Velocity Ratio, $(u)_R$	1:1.43
Temperature Difference Ratio, $(\Delta T)_R$	1:3.43
Pressure Drop Ratio, $(\Delta p_o)_R$	1:4
Heating Power Ratio, $(Q_h)_R$	1:53.1
Pumping Power Ratio, $\left(Q_p\right)_R$	1:22.9
Loop Time Constant Ratio, $\left(\tau_{loop}\right)_R$	1:1.40
Scaling Group Ratios	
Prandtl Number Ratio, $(\Pi_{Pr})_R$	1:1
Euler Number Ratio, $(\Pi_{Eu})_R$	1:1
Richardson Number Ratio, $(\Pi_{Ri})_R$	1:1

[a] Here, an attempt is made to maintain geometric similitude between the model and prototype, and the length scale ratio between the model and prototype is chosen to be constant at 1/2. Future implementations of this scaling methodology may choose to select different scaling ratios for height, length and area scaling for added degrees of freedom without compromising the validity of this method.

Table 4. Summary of Dimensional Parameter Ratios and Resulting Scaling Groups for Normal Operation at the Component Level.

Prototypical Fluid (Temperature)	Flibe (600°C)
Surrogate Fluid (Temperature)	Heat transfer oil (73°C)
Dimensional Parameter Ratios	
Form Losses Ratio, $\left(\sum_{j=1}^{N}\left[\frac{K_j}{A_j^2}\right]\right)_R$	1:0.06
Solid-Fluid Temperature Difference Ratio in Reactor Core, $(\Delta T_{Rx})_R$	1:3.43
Solid-Fluid Temperature Difference Ratio in IHX, $(\Delta T_{HX})_R$	1:3.43
Heat Transfer Ratio in Reactor Core, $\left(h_{Rx}A_{s,Rx}\right)_R$	1:15.5
Heat Transfer Ratio in IHX, $\left(h_{HX}A_{s,HX}\right)_R$	1:15.5
Scaling Group Ratios	
Flow Resistance Number Ratio, $(\Pi_F)_R$	1:1
Reactor Core Modified Stanton Number Ratio, $\left(\Pi_{St,m-Rx}\right)_R$	1:1
IHX Modified Stanton Number Ratio, $\left(\Pi_{St,m-HX}\right)_R$	1:1
IHX Reynolds Number Ratio, $\left(\Pi_{Re,HX}\right)_R$	1:0.92

Table 5. Summary of Dimensional Parameter Ratios and Resulting Scaling Groups for Natural Circulation Scenario at the System Level.

Prototypical Fluid (Temperature)	Flibe (600°C)
Surrogate Fluid (Temperature)	Heat transfer oil (73°C)
Dimensional Parameter Ratios	
Velocity Ratio, $(u_{NC})_R$	1:1.43
Temperature Difference Ratio, $(\Delta T)_R$	1:3.43
Heating Power Ratio, $(Q_{NC})_R$	1:53.1
Loop Time Constant Ratio, $\left(\tau_{loop,NC}\right)_R$	1:1.40
Scaling Group Ratios	
Prandtl Number Ratio, $(\Pi_{Pr})_R$	1:1
Richardson Number Ratio, $\left(\Pi_{Ri,NC}\right)_R$	1:1
Solid Structures Heat Capacity Number Ratio, $(\Pi_{HS})_R$	1:1

Table 6. Summary of Dimensional Parameter Ratios and Resulting Scaling Groups for Natural Circulation Scenario at the Component Level.

Prototypical Fluid (Temperature)	Flibe (600°C)
Surrogate Fluid (Temperature)	Heat transfer oil (73°C)
Dimensional Parameter Ratios	
Sum of Length-to-Area Ratio, $\left(\sum_{j=1}^{N}\frac{l_j}{A_j}\right)_R$	1:0.5
Solid-Fluid Temperature Difference Ratio in Reactor Core, $(\Delta T_{Rx})_R$	1:3.43
Solid-Fluid Temperature Difference Ratio in Heat Exchanger, $(\Delta T_{HX})_R$	1:3.43
Heat Transfer Ratio in Reactor Core, $\left(h_{Rx}A_{s,Rx}\right)_R$	1:15.5
Heat Transfer Ratio in Heat Exchanger, $\left(h_{HX}A_{s,HX}\right)_R$	1:15.5
Solid Characteristic Length Ratio in Reactor Core, $\left(l_{s,Rx}\right)_R$	1:2
Solid Characteristic Length Ratio in Heat Exchanger, $\left(l_{s,HX}\right)_R$	1:2
Solid Thermal Diffusivity Ratio in Reactor Core, $\left(\alpha_{s,Rx}\right)_R$	1:2.86
Solid Thermal Diffusivity Ratio in Heat Exchanger, $\left(\alpha_{s,HX}\right)_R$	1:2.86
Solid Time Constant Ratio in Reactor Core, $\left(\tau_{s,Rx}\right)_R$	1:1.40
Solid Time Constant Ratio in Heat Exchanger, $\left(\tau_{s,HX}\right)_R$	1:1.40
Scaling Group Ratios	
Loop Geometry Number Ratio, $(\Pi_G)_R$	1:1
Flow Resistance Number Ratio, $(\Pi_F)_R$	1:1
Reactor Core Modified Stanton Number Ratio, $\left(\Pi_{St,m-Rx,NC}\right)_R$	1:1
Heat Exchanger Modified Stanton Number Ratio, $\left(\Pi_{St,m-HX,NC}\right)_R$	1:1
Heat Exchanger Reynolds Number Ratio, $\left(\Pi_{Re,HX}\right)_R$	1:0.92
Heat Exchanger Grashof Number Ratio, $\left(\Pi_{Gr,HX}\right)_R$	1:0.84
Heat Exchanger Biot Number Ratio, $\left(\Pi_{Bi,HX}\right)_R$	See Discussion
Reactor Core Heat Source Number Ratio, $\left(\Pi_{q'''_{source,s}}\right)_R$	1:1

Table 7. Summary of Dimensional Parameter Ratios for Scaled Test Facility.

Prototypical Fluid (Temperature)	Flibe (600°C)
Surrogate Fluid (Temperature)	Heat transfer oil (73°C)
Geometry Parameter Ratios	
Length Ratio, $(l)_R$	1:2
Hydraulic Diameter Ratio, $(d)_R$	1:2
Area Ratio, $(A)_R$	1:4
Fluid Volume Ratio, $(V)_R$	1:8
Fluid Parameter Ratios	
Velocity Ratio, $(u)_R$	1:1.43
Temperature Difference Ratio, $(\Delta T)_R$	1:3.43
Solid-Fluid Temperature Difference Ratio in Reactor Core, $(\Delta T_{Rx})_R$	1:3.43
Solid-Fluid Temperature Difference Ratio in Heat Exchanger, $(\Delta T_{HX})_R$	1:3.43
Pressure Drop Ratio, $(\Delta p_o)_R$	1:4
Heating Power Ratio, $(Q_h)_R$	1:53.1
Pumping Power Ratio, $\left(Q_p\right)_R$	1:22.9
Loop Time Constant Ratio, $\left(\tau_{loop}\right)_R$	1:1.40
Form Losses Ratio, $\left(\sum_{j=1}^{N}\left[\frac{K_j}{A_j^2}\right]\right)_R$	1:0.06
Fluid-Solid Interface Parameter Ratios	
Heat Transfer Ratio in Reactor Core, $\left(h_{Rx}A_{s,Rx}\right)_R$	1:15.5
Heat Transfer Ratio in Heat Exchanger, $\left(h_{HX}A_{s,HX}\right)_R$	1:15.5
Solid Parameter Ratios	
Solid Characteristic Length Ratio in Reactor Core, $\left(l_{s,Rx}\right)_R$	1:2
Solid Characteristic Length Ratio in Heat Exchanger, $\left(l_{s,HX}\right)_R$	1:2
Solid Thermal Diffusivity Ratio in Reactor Core, $\left(\alpha_{s,Rx}\right)_R$	1:2.86
Solid Thermal Diffusivity Ratio in Heat Exchanger, $\left(\alpha_{s,HX}\right)_R$	1:2.86
Solid Time Constant Ratio in Reactor Core, $\left(\tau_{s,Rx}\right)_R$	1:1.40
Solid Time Constant Ratio in Heat Exchanger, $\left(\tau_{s,HX}\right)_R$	1:1.40

Table 8. Summary of Scaling Groups and Associated As-designed Distortion Factors for Scaled Test Facility.

Scaling Group	Value	Distortion Factor
Normal Operation		
Prandtl Number Ratio, $(\Pi_{Pr})_R$	1:1	0.00
Euler Number Ratio, $(\Pi_{Eu})_R$	1:1	0.00
Richardson Number Ratio, $(\Pi_{Ri})_R$	1:1	0.00
Flow Resistance Number Ratio, $(\Pi_F)_R$	1:1	0.00
Reactor Core Modified Stanton Number Ratio, $\left(\Pi_{St,m-Rx}\right)_R$	1:1	0.00
IHX Modified Stanton Number Ratio, $\left(\Pi_{St,m-HX}\right)_R$	1:1	0.00
IHX Reynolds Number Ratio, $\left(\Pi_{Re,HX}\right)_R$	1:0.92	-0.09
Natural Circulation		
Prandtl Number Ratio, $(\Pi_{Pr})_R$	1:1	0.00
Richardson Number Ratio, $\left(\Pi_{Ri,NC}\right)_R$	1:1	0.00
Loop Geometry Number Ratio, $(\Pi_G)_R$	1:1	0.00
Flow Resistance Number Ratio, $(\Pi_F)_R$	1:1	0.00
Reactor Core Modified Stanton Number Ratio, $\left(\Pi_{St,m-Rx,NC}\right)_R$	1:1	0.00
Heat Exchanger Modified Stanton Number Ratio, $\left(\Pi_{St,m-HX,NC}\right)_R$	1:1	0.00
Heat Exchanger Grashof Number Ratio, $\left(\Pi_{Gr,HX}\right)_R$	1:0.84	-0.19
Heat Exchanger Biot Number Ratio, $\left(\Pi_{Bi,HX}\right)_R$	See Section 3.4.4	
Reactor Core Heat Source Number Ratio, $\left(\Pi_{q'''_{source,s}}\right)_R$	1:1	0.00

Table 9. Similitude Criteria to Preserve Flow Characteristics Between Prototype and Scaled Experiment in Twisted Elliptical Tube Tests.

Category	Similitude Criteria
Geometry	$\frac{D_{max,in,m}}{D_{max,in,p}} = \frac{D_{min,in,m}}{D_{min,in,p}}$
	$\frac{D_{max,out,m}}{D_{max,out,p}} = \frac{D_{min,out,m}}{D_{min,out,p}}$
	$\frac{s_m}{s_p} = \frac{D_{max,in,m}}{D_{max,in,p}}$
Flow	$\frac{D_{h,shell,m}}{D_{h,shell,p}} = \frac{D_{max,out,m}}{D_{max,out,p}}$
	$\frac{u_m}{u_p} = \frac{\rho_p}{\rho_m}\frac{\mu_m}{\mu_p}\frac{D_{max,out,p}}{D_{max,out,m}}$
Heat transfer	$\left(\frac{c_p\mu}{k}\right)_{m,tube} = \left(\frac{c_p\mu}{k}\right)_{p,tube}$
	$\left(\frac{c_p\mu}{k}\right)_{m,shell} = \left(\frac{c_p\mu}{k}\right)_{p,shell}$

Table 10. Physical Parameters for Prototype and Scaled Experiment to Investigate Pebble Bed Flow and Fuel Element Dynamics.

Parameter	Prototype	Model
Fluid (temperature)	Flibe (600°C)	Water (20°C)
Fluid density (kg/m^3)	1,987	998
Fluid dynamic viscosity (Pa-s)	8.55 x 10^{-3}	1.00 x 10^{-3}
Pebble diameter (cm)	[[ ]]	1.52
Reference velocity (m/s)	0.16	0.10
Average pebble density (kg/m^3)	1,745	877

Table 11. Physical Parameters for Prototype and Scaled Experiment to Investigate Packed Bed Flow and Heat Transfer.

Parameter	Prototype	Model
Fluid (temperature)	Flibe (600°C)	Heat transfer oil (73°C)
Dimensional parameters		
Fluid density (kg/m^3)	1,987	1,018
Fluid dynamic viscosity (Pa-s)	8.55 x 10^{-3}	1.40 x 10^{-3}
Pebble diameter (cm)	[[ ]]	0.50
Core/test section diameter (cm)	[[ ]]	32
Core/test section height (cm)	[[ ]]	40
Number of pebbles in core/test section	[[ ]]	300,000
Reference velocity (m/s)	0.16	0.41
Scaling group ratios		
Porosity ratio, $\frac{\varphi_m}{\varphi_p}$	1.0	
Reynolds number ratio, $\frac{Re_m}{Re_p}$	1.0	
Prandtl number ratio, $\frac{Pr_m}{Pr_p}$	1.0	

Table 12. Scaling of Surrogate Fluid to KP-FHR PHTS Fluid to Simultaneously Match Reynolds, Prandtl, Grashof and Froude Numbers.

	Flibe at 600°C
Surrogate Fluid	Heat transfer oil
Surrogate Fluid Temperature	73°C
Scaling ratios of dimensional quantities	
Length Ratio, $(l)_R$	0.47
Velocity Ratio, $(u)_R$	0.68
Temperature Difference Ratio, $(\Delta T)_R$	0.30
Pumping Power Ratio, $(Q_p)_R$	0.036
Heating Power Ratio, $(Q_h)_R$	0.017
Matching of non-dimensional groups	
Reynolds Number Ratio, $(\Pi_{Re})_R$	1.0
Prandtl Number Ratio, $(\Pi_{Pr})_R$	1.0
Grashof Number Ratio, $(\Pi_{Gr})_R$	1.0
Froude Number Ratio, $(\Pi_{Fr})_R$	1.0

Figure 1. Evaluation Model Development and Assessment Process (EMDAP) from RG 1.203.

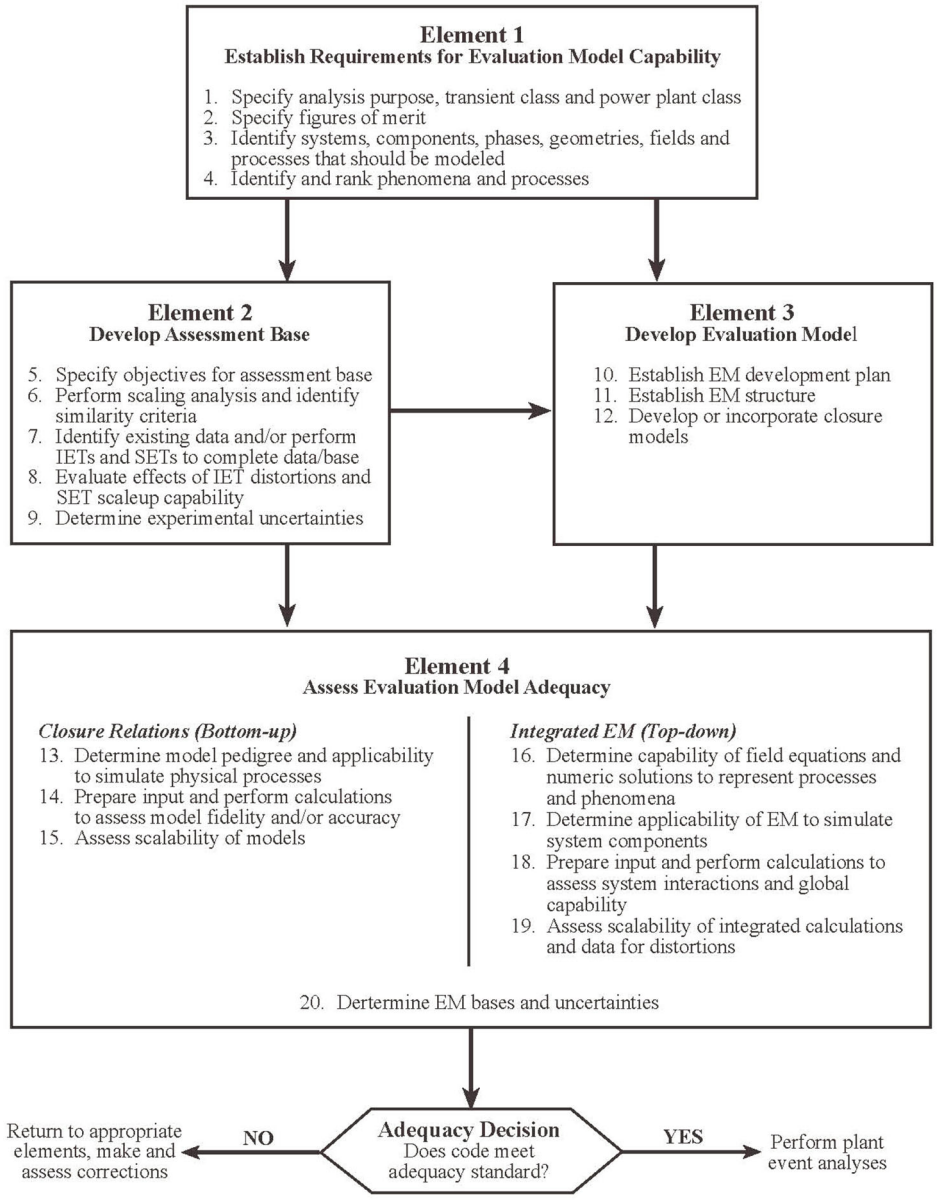

Figure 2. H2TS Methodology Flow Diagram (Reference 7).

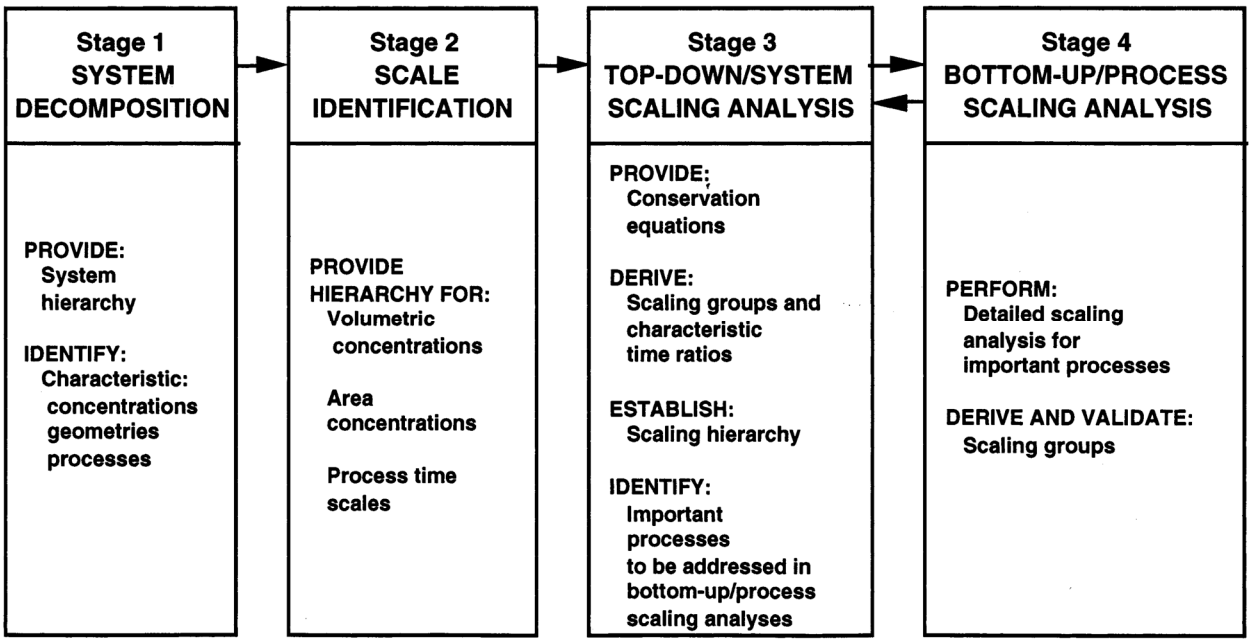

Figure 3. Decomposition of a Hierarchical System (Reference 7).

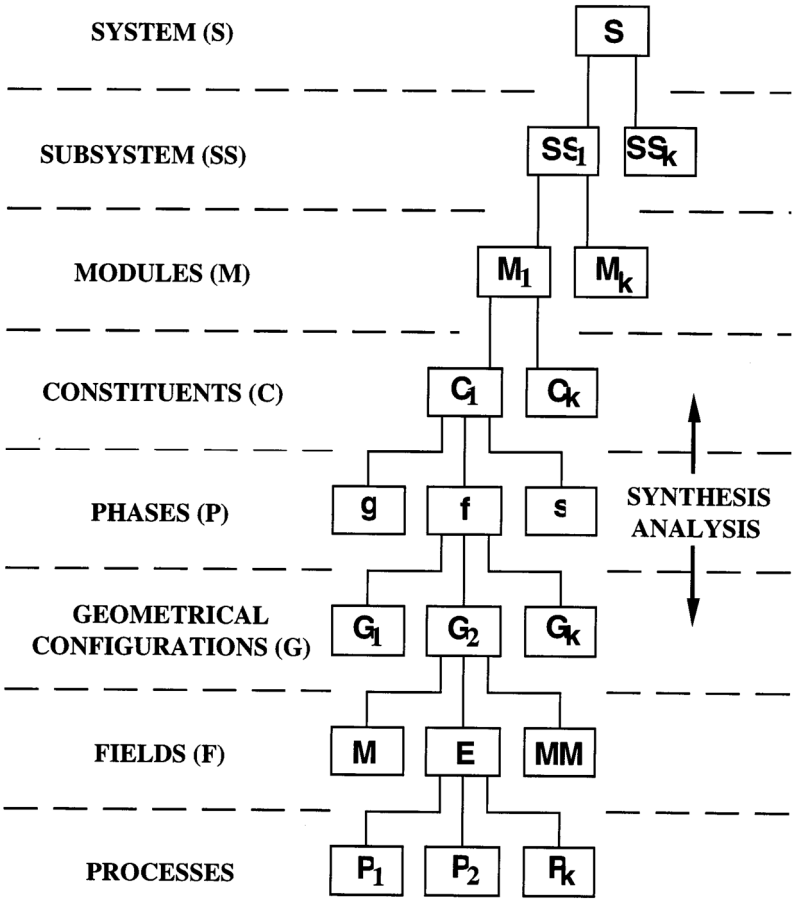

Figure 4. Characteristic Scales at Different Levels in a Hierarchical System (Reference 7).

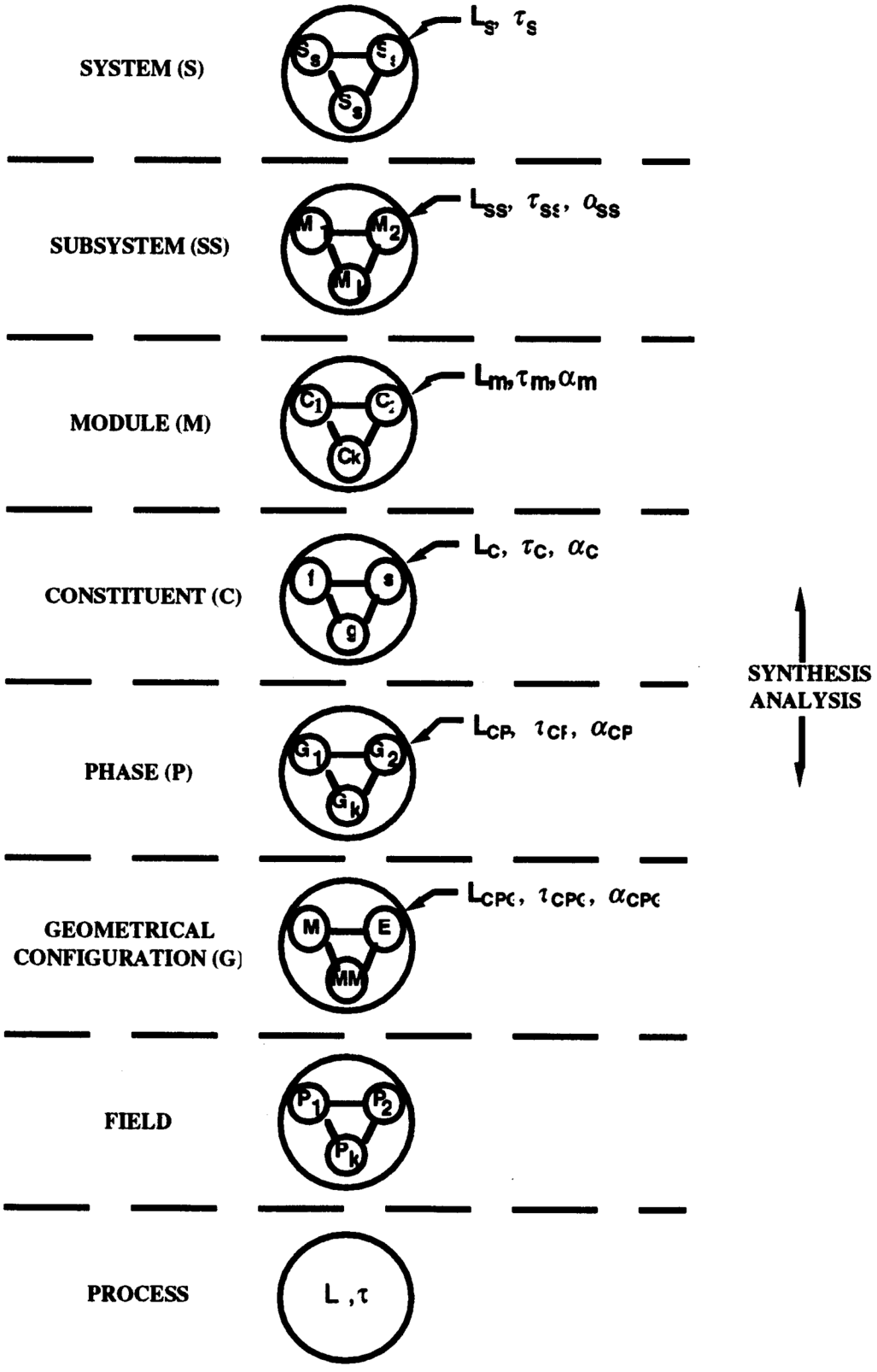

Figure 5. Generic KP-FHR Scaling Methodology Flow Chart.

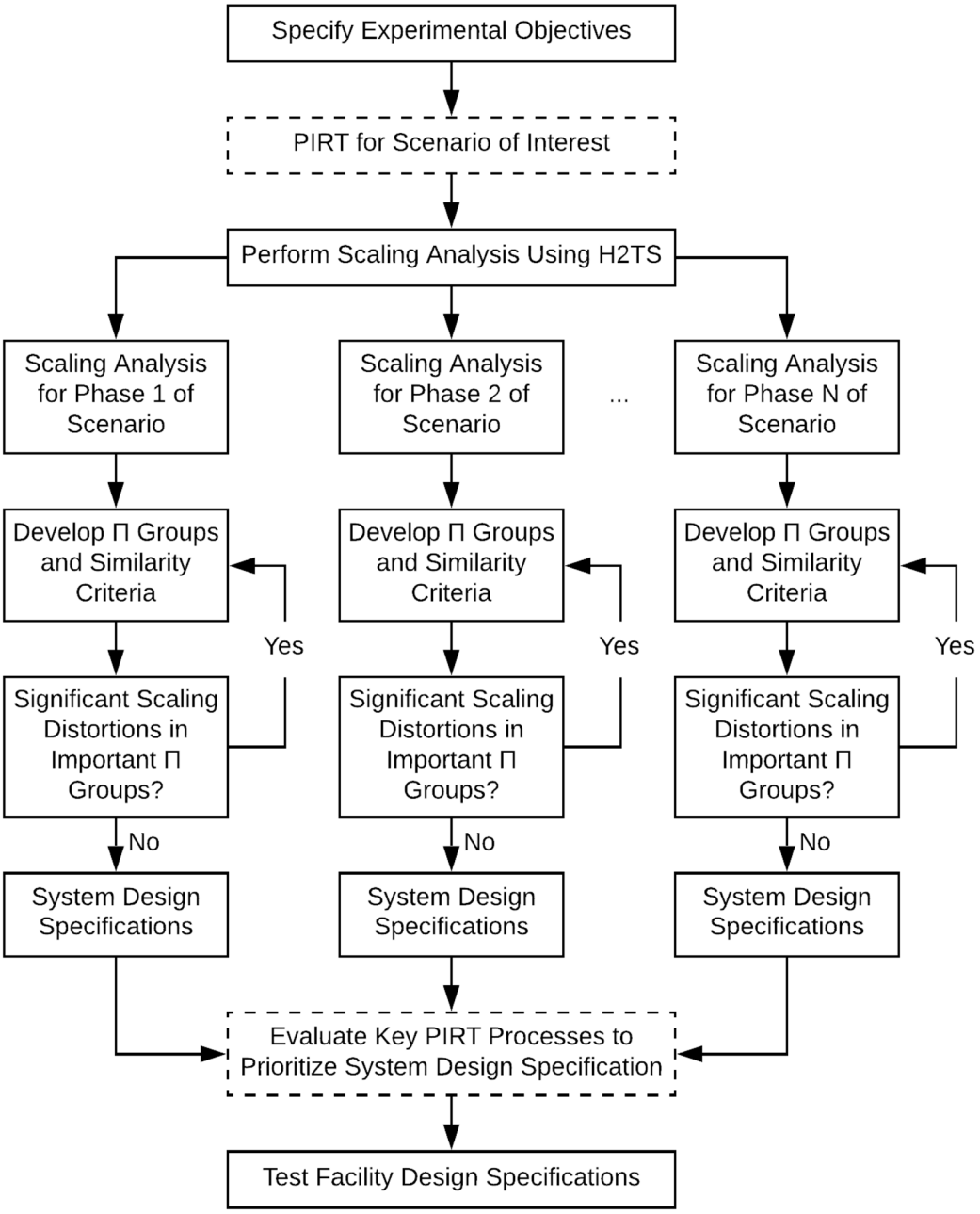

Figure 6. Idealized KP-FHR Primary Heat Transport System (PHTS).

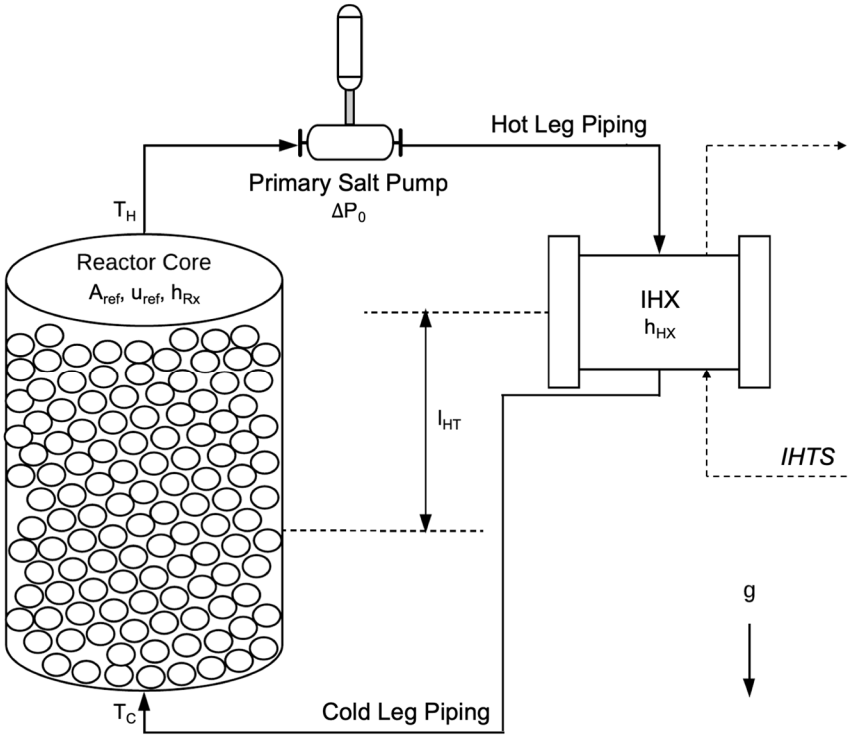

Figure 7. Normal Operation Scaling Flow Chart.

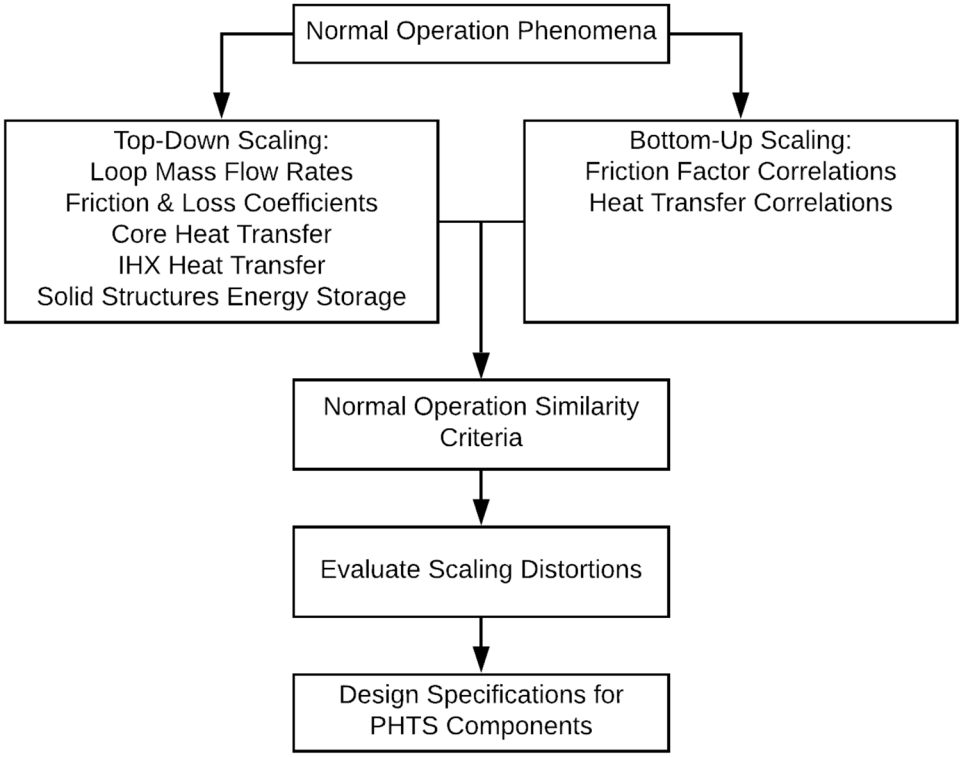

Figure 8. Natural Circulation Flow Chart.

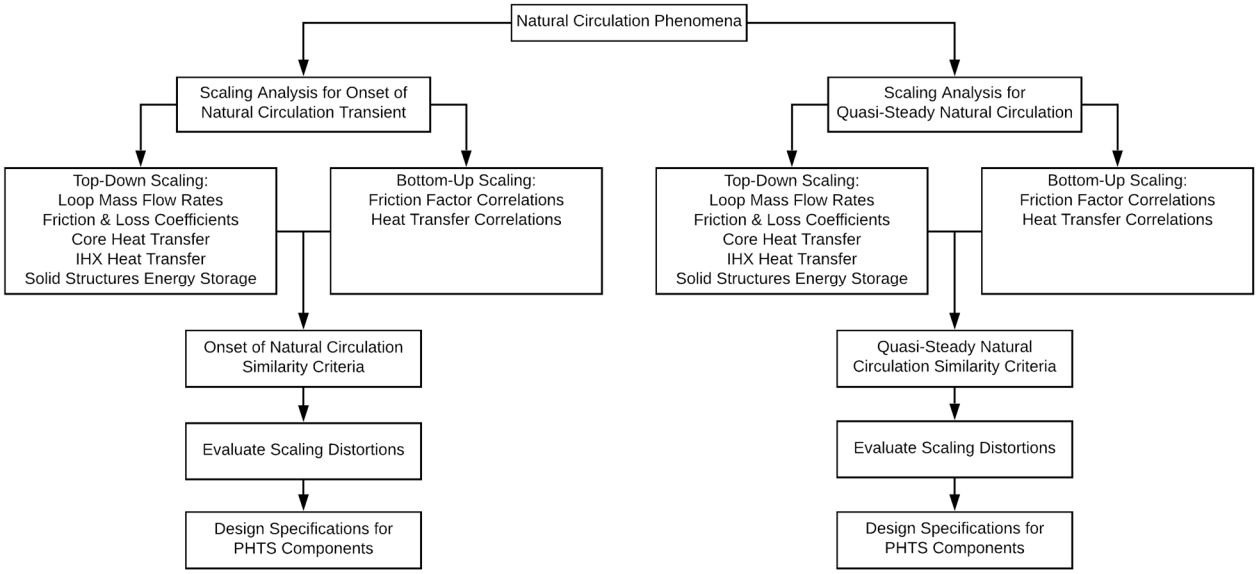

Figure 9. Diagram of a Twisted Elliptical Tube.

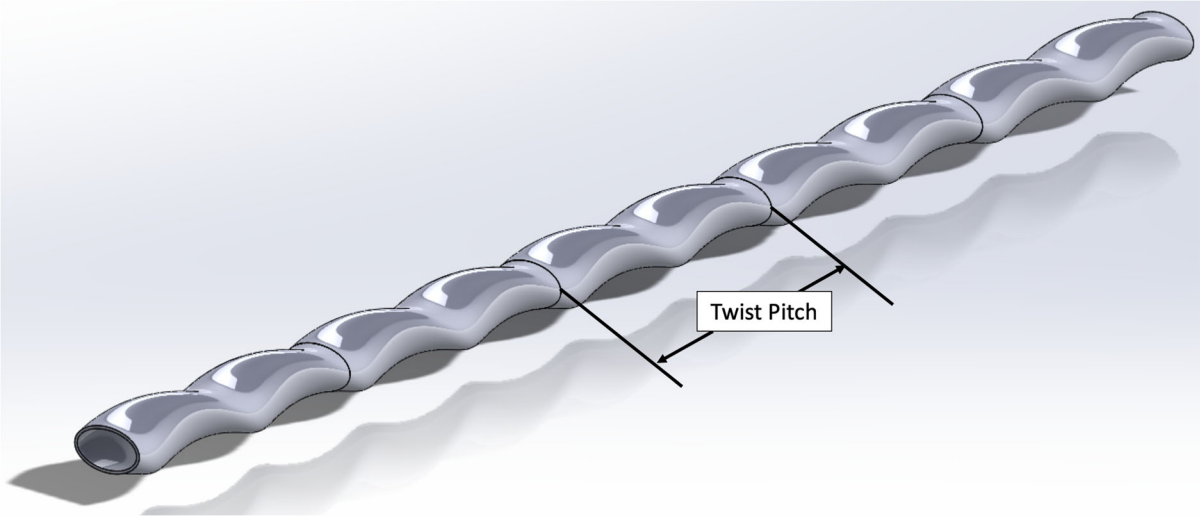

Figure 10. Twisted Elliptical Tube Cross-section.

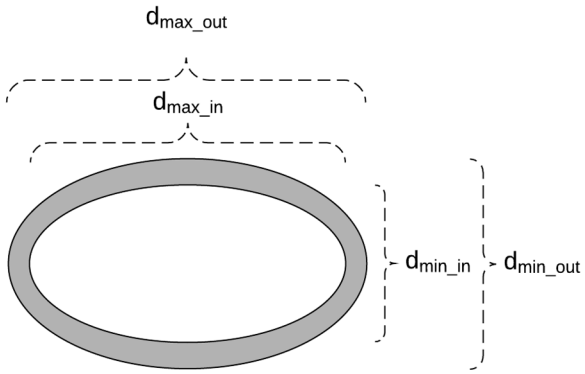

Figure 11. Free Body Diagram of Pebble Immersed in Stagnant Liquid.

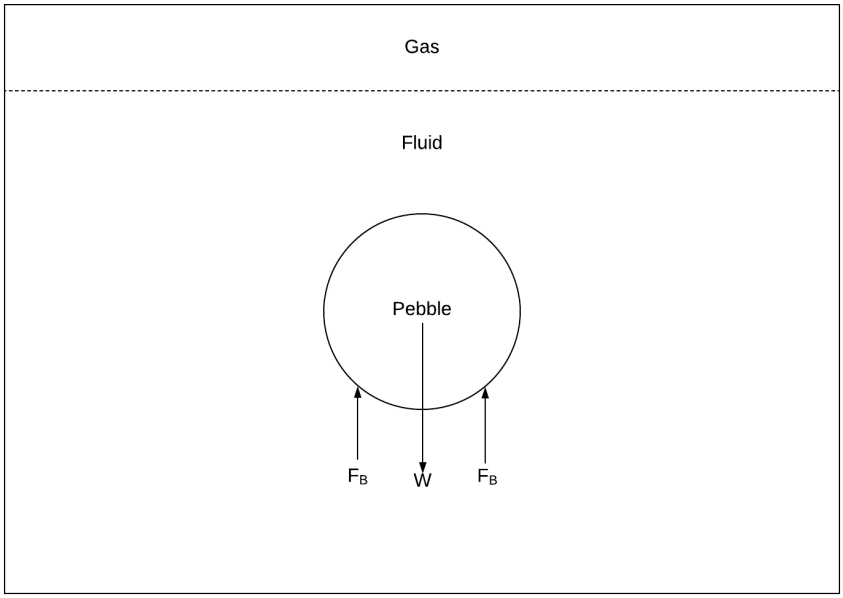

Figure 12. Prandtl Number Matching and Distortions for Flibe at Temperatures Between 550°C and 750°C [1], and Heat Transfer Oil at Temperatures Between 58°C and 118°C [2].

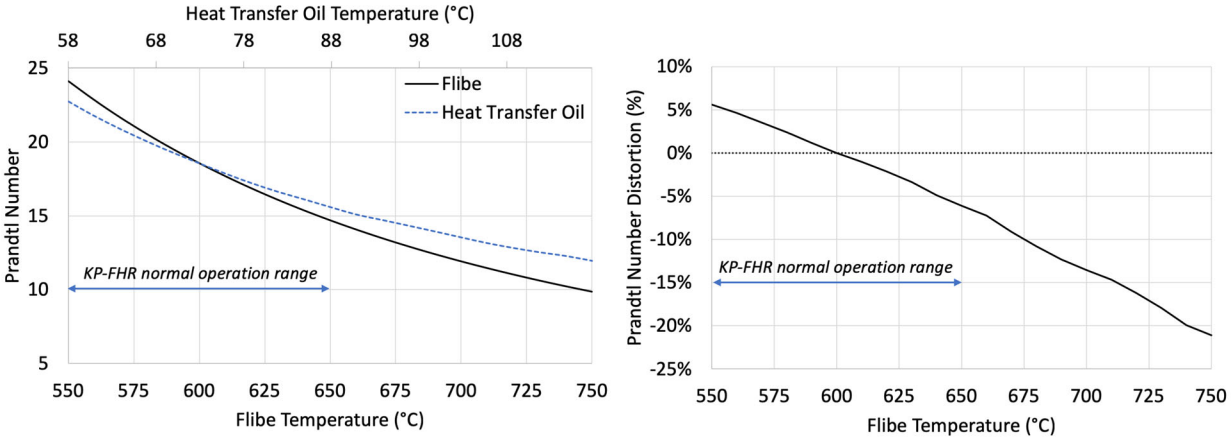

[1] For Flibe, this plot uses average thermophysical properties listed in Reference 40.

[2] For heat transfer oil, this plot uses average thermophysical properties of DOWTHERM™ A listed in APPENDIX B.

Figure 13. Darcy Friction Factor Matching for Flibe at 550°C and 650°C [3], Solar Salt at 350°C and 650°C, Heat Transfer Oil at 52°C and 93°C [4], and Water at 22.5°C and 72.5°C.

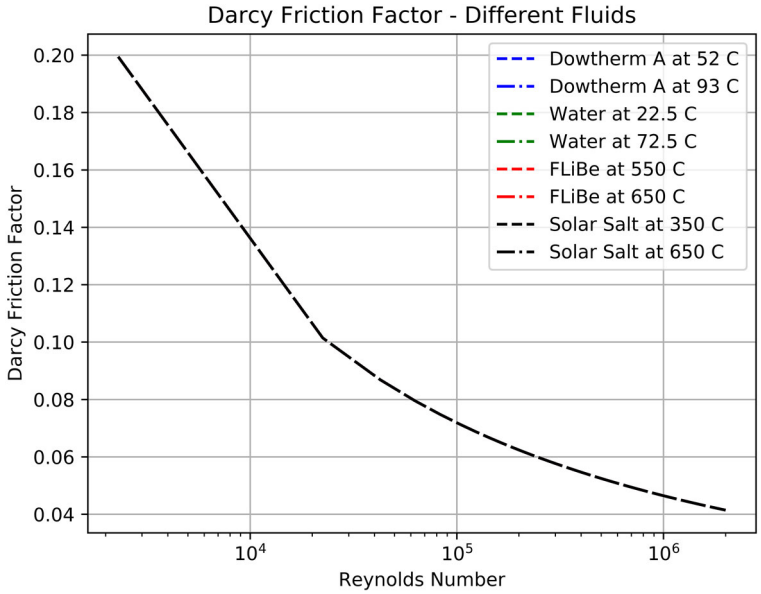

[3] For Flibe, this plot uses average thermophysical properties listed in Reference 40.

[4] For heat transfer oil, this plot uses average thermophysical properties of DOWTHERM™ A listed in APPENDIX B.

Figure 14. Nusselt Number Matching and Distortions for Flibe at 550°C and 650°C [5], Solar Salt at 350°C and 650°C, Heat Transfer Oil at 52°C and 93°C [6], and Water at 22.5°C and 72.5°C.

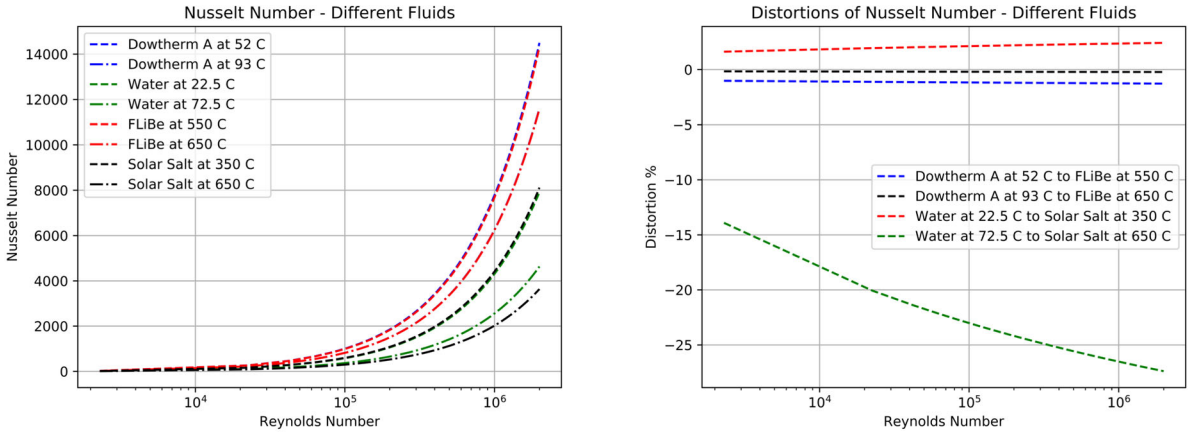

[5] For Flibe, this plot uses average thermophysical properties listed in Reference 40.

[6] For heat transfer oil, this plot uses average thermophysical properties of DOWTHERM™ A listed in APPENDIX B.

APPENDIX A. FRICTION FACTOR AND NUSSELT NUMBER CORRELATIONS FOR VARIOUS GEOMETRIES

A.1. Friction Factor Correlations

Laminar Friction Factor for Circular Pipes

$$f_{Darcy} = \frac{64}{Re_D} \qquad Re_D < 2{,}100 \tag{172}$$

Blasius Friction Factor Correlation for Circular Pipes

$$f_{Darcy} = \frac{0.316}{Re_D^{0.25}} \qquad 2{,}100 < Re_D < 10^5 \tag{173}$$

Petukhov Friction Factor Correlation for Circular Pipes

$$f_{Fanning} = \frac{1}{1.82 \log_{10} Re_D - 1.64^2} \qquad 2{,}300 \leq Re_D < 5 \times 10^6 \tag{174}$$

Note: $f_{Darcy} = 4 f_{Fanning}$.

A.2. Nusselt Number Correlation

Gnielinski Nusselt Number Correlation for Circular Pipes

$$Nu = \frac{(f/8) Re_D Pr}{1.07 + 12.7\sqrt{f/8}\,(Pr^{2/3} - 1)} \qquad \begin{gathered} 2{,}300 \leq Re_D < 5 \times 10^6 \\ 0.5 < Pr < 200 \\ 200 < Pr < 2{,}000 \end{gathered} \tag{175}$$

The Gnielinski Nusselt number is 6% accurate for the lower Prandtl range and 10% for the higher Prandtl range. The friction factor used in this correlation is the Fanning friction factor and it is recommended that Eq. (174) be used to calculate it.

APPENDIX B. THERMOPHYSICAL PROPERTIES OF FLUIDS

Thermophysical properties correlations for Flibe are listed in Reference 40. Thermophysical properties correlations for DOWTHERM™ A are listed in Table 13 between its freezing point (12°C) and boiling point (257°C).

Table 13. Thermophysical Properties of DOWTHERM™ A between 12°C and 257°C.

Property	Correlation[1]	Unit
Density	$\rho = 1306 - 0.837 \cdot T$	kg/m^3
Viscosity	$\mu = 4.85 \cdot 10^9 \cdot T^{-4.92}$	Pa-s
Heat capacity	$c_p = 748 + 2.82 \cdot T$	J/kg-K
Thermal conductivity	$k = 0.186 - 1.60 \cdot 10^{-4} \cdot T$	W/m-K

[1] T is in K

Enclosure 3

Kairos Power LLC Affidavit and Request for Withholding from Public Disclosure (10 CFR 2.390)

I, Peter Hastings, hereby state:

1. I am Vice President, Regulatory Affairs and Quality at Kairos Power LLC ("Kairos"), and as such I have been authorized by Kairos to review information sought to be withheld from public disclosure in connection with the development, testing, licensing, and deployment of the Kairos reactor and its associated structures, systems, and components, and to apply for its withholding from public disclosure on behalf of Kairos.
2. The information sought to be withheld, in its entirety, is contained in Kairos' Enclosure 1 to this letter.
3. I am making this request for withholding, and executing this affidavit in support thereof, pursuant to the provisions of 10 CFR 2.390(b)(1).
4. I have personal knowledge of the criteria and procedures utilized by Kairos in designating information as a trade secret, privileged, or as confidential commercial or financial information. Some examples of information Kairos considers proprietary and eligible for withholding under §2.390(a)(4) include:
    a. Information which discloses process, method, or apparatus, including supporting data and analyses, where prevention of its use by Kairos competitors without license or contract from Kairos constitutes a competitive economic advantage over other companies in the industry;
    b. Information, which if used by a competitor, would reduce his expenditure of resources or improve his competitive position in design, manufacture, shipment, installation, assurance of quality;
    c. Information which reveals cost or price information, production capacities, budget levels, or commercial strategies of Kairos, its customers, its partners, or its suppliers;
    d. Information which reveals aspects of past, present, or future Kairos or customer funded development plans or programs, of potential commercial value to Kairos;
    e. Information which discloses patentable subject matter for which it may be desirable to obtain patent protection; and/or
    f. Information obtained through Kairos actions which could reveal additional insights into reactor system development, testing, qualification processes, and/or regulatory proceedings, and which are not otherwise readily obtainable by a competitor.
5. Information contained in Enclosure 1 to this letter contains details of Kairos Power's design and testing information intended to support NRC staff review. This information includes details of Kairos Power's design and testing plans that could provide a competitor with a commercial advantage if the information were to be revealed publicly.

6. Pursuant to the provisions of §2.390(b)(4), the following is furnished for consideration by the Commission in determining whether the information sought to be withheld from public disclosure should be withheld:

   a. The information sought to be withheld from public disclosure is owned and has been held in confidence by Kairos.

   b. The information is of a type customarily held in confidence by Kairos and not customarily disclosed to the public. Kairos has a rational basis for determining the types of information customarily held in confidence by it and, in that connection, utilizes a system to determine when and whether to hold certain types of information in confidence. The application of that system and the substance of that system constitute Kairos policy and provide the rational basis required.

   c. The information is being transmitted to the Commission in confidence and, under the provisions of 10 CFR 2.390, it is to be received in confidence by the Commission.

   d. This information is not readily available in public sources.

   e. Public disclosure of this proprietary information is likely to cause substantial harm to the competitive position of Kairos, because it would enhance the ability of competitors to provide similar products and services by reducing their expenditure of resources using similar project methods, equipment, testing approach, contractors, or licensing approaches. This information is the result of considerable expense to Kairos and has great value in that it will assist Kairos in providing products and services to new, expanding markets not currently served by the company.

   f. The information could reveal or could be used to infer price information, cost information, budget levels, or commercial strategies of Kairos.

   g. Each component of proprietary information pertinent to a particular competitive advantage is potentially as valuable as the total competitive advantage. If competitors acquire components of proprietary information, any one component may be the key to the entire puzzle, thereby depriving Kairos of a competitive advantage.

   h. Unrestricted disclosure would jeopardize the position of Kairos in the world market, and thereby give a market advantage to the competition in those countries.

I declare under penalty of perjury that the foregoing is true and correct.

Executed on: March 6, 2019

Peter Hastings
Vice President, Regulatory Affairs and Quality